
Theses and Dissertations

Spring 2013

The use of surrounding lung parenchyma for the automated classification of pulmonary nodules

Samantha Kirsten Nowik Dilger
University of Iowa

Copyright 2013 Samantha Kirsten Nowik Dilger

This thesis is available at Iowa Research Online: <http://ir.uiowa.edu/etd/2475>

Recommended Citation

Dilger, Samantha Kirsten Nowik. "The use of surrounding lung parenchyma for the automated classification of pulmonary nodules." MS (Master of Science) thesis, University of Iowa, 2013. <http://ir.uiowa.edu/etd/2475>.

Follow this and additional works at: <http://ir.uiowa.edu/etd>



Part of the [Biomedical Engineering and Bioengineering Commons](#)

THE USE OF SURROUNDING LUNG PARENCHYMA FOR THE AUTOMATED
CLASSIFICATION OF PULMONARY NODULES

by

Samantha Kirsten Nowik Dilger

A thesis submitted in partial fulfillment
of the requirements for the Master of
Science degree in Biomedical Engineering
in the Graduate College of
The University of Iowa

May 2013

Thesis Supervisor: Assistant Professor Jessica C. Sieren

Graduate College
The University of Iowa
Iowa City, Iowa

CERTIFICATE OF APPROVAL

MASTER'S THESIS

This is to certify that the Master's thesis of

Samantha Kirsten Nowik Dilger

has been approved by the Examining Committee
for the thesis requirement for the Master of Science
degree in Biomedical Engineering at the May 2013 graduation.

Thesis Committee: _____
Jessica C. Sieren, Thesis Supervisor

Joseph M. Reinhardt

John D. Newell, Jr.

Eric A. Hoffman

Punam K. Saha

ACKNOWLEDGMENTS

This work would not be possible without the contributions of many. I would like to acknowledge my thesis advisor and mentor, Dr. Jessica Sieren. Without her guidance and support, I would not have had this wonderful opportunity to continue my education and to deepen my understanding of image processing and pattern recognition by developing this computer-aided diagnostic tool. I want to express my gratitude to my committee members, Dr. Joseph Reinhardt, Dr. Eric Hoffman, Dr. John Newell, and Dr. Punam Saha. Each of you have helped in the development of this project by providing me with different pieces to develop and extend in this project. I would also like to thank the Iowa-Comprehensive Lung Imaging Center (I-CLIC) members, including Krishna Iyer, Kizhakke Puliyakote, Sean Mobberly, and Emily Hammond for their feedback and input. I'd like to specifically thank Alex Judisch and Kristin Knudson for their contribution to this project. Their work on segmentation was invaluable. Finally, I would like to thank my family and husband for their support and encouragement.

ABSTRACT

Lung cancer is the leading cause of cancer-related death for both men and women in the United States, despite being the second-most frequent cancer diagnosis for both sexes. This high mortality rate is due to the majority of cases being diagnosed after the primary lung cancer has metastasized. In an effort to reduce mortality associated with lung cancer by diagnosing lung cancer at an earlier stage, screening of high-risk populations has been employed. One screening tool, computed tomography (CT), has been shown to reduce mortality by 20%, compared to screening for lung cancer by chest x-ray. This was achieved by earlier stage diagnosis of lung cancer in participants screened with CT. The use of chest CT in lung cancer screening has also led to increased numbers of false-positives – benign lung nodules that are marked as suspicious for lung cancer. These false-positives result in unnecessary invasive follow-up procedures and costs while incurring additional emotional stress on the patient.

In an effort to reduce the number of false-positives, a computer-aided diagnostic (CAD) tool can be designed to determine the probability of malignancy of a lung nodule based on objective measurements. While current CAD models characterize the pulmonary nodule's shape, density, and border, analyzing the parenchyma surrounding the nodule is an area that has been minimally explored. By quantifying characteristics, or features, of the surrounding tissue, this project explores the hypothesis that textural differences in both the nodule and surrounding parenchyma exist between malignant and benign cases. By incorporating these features, performance in the measures of sensitivity, specificity and accuracy can be improved over CAD tools that rely on nodule characteristics alone.

A CAD program was developed for the computation of features from a pulmonary nodule. A region of interest containing a nodule and surrounding parenchyma was extracted from a CT scan. Several novel feature extraction techniques were developed,

including a three-dimensional application of Laws' Texture Energy Measures to quantify the textures of the parenchyma surrounding the nodule and the nodule itself. In addition, the densities of the nodule and surrounding parenchyma were summarized through metrics such as mean, variance, and entropy of the intensities within each region. Finally, the margins of the nodule were characterized by analyzing mean and variance of border irregularity. A total of 299 features were extracted.

To illustrate proof of concept, the CAD program was applied to 27 regions of interest – 10 benign and 17 malignant. Through feature selection, 36 significant features were recognized (p -values < 0.05), including many textural and parenchymal features. These features were further reduced by forward feature selection to two features that summarized the dataset. A neural network was used to classify the cases in a leave-one-out method. Preliminary results yielded 92.6% accuracy in classification of test cases, with two benign nodules incorrectly classified as malignant.

The significance of texture and parenchymal features supports the hypothesis that features extracted from the parenchyma have the potential to improve classification of nodules, aiding in the reduction of false-positives identified through CT screening. As more cases are incorporated into the database, these textural features will play a larger role.

TABLE OF CONTENTS

LIST OF TABLES	vii
LIST OF FIGURES	viii
CHAPTER I INTRODUCTION.....	1
CHAPTER II BACKGROUND INFORMATION	3
2.1 Lung Cancer.....	3
2.2 Lung Cancer Detection and Diagnosis	5
2.3 Computer-Aided Diagnostic Tools.....	8
CHAPTER III METHODS	14
3.1 Data Preprocessing	15
3.2 Feature Extraction.....	17
3.2.1 Intensity Features.....	17
3.2.1.1 Intensity Histogram Features	18
3.2.1.2 Measures of Heterogeneity.....	18
3.2.1.2.1 Full width at half maximum (FWHM).....	18
3.2.1.2.2 Entropy	19
3.2.1.2.3 Kurtosis	20
3.2.1.2.4 Skewness.....	20
3.2.2 Shape Features.....	20
3.2.2.1 Maximum Diameter (RECIST).....	21
3.2.2.2 Sphericity	21
3.2.2.3 Differences in Spherical Shape	22
3.2.3 Border Features	23
3.2.4 Texture Features	26
3.3 Feature Selection	28
3.3.1 Testing for Significance	29
3.3.2 Rank Features	29
3.3.3 Forward Selection.....	31
3.4 Classification	32
CHAPTER IV RESULTS.....	34
4.1 Patient Database.....	34
4.2 Data Preprocessing – Segmentation Comparison.....	36
4.3 Feature Extraction.....	37
4.4 Feature Selection	37
4.4.1 Testing for Significance	38
4.4.2 Rank Feature Results.....	38
4.4.3 Forward Selection Results.....	39
4.5 Classification	39
CHAPTER V DISCUSSION	71
5.1 Feature Extraction and Segmentation.....	71
5.2 Feature Selection	71

5.3 Classification	72
5.4 Conclusion	73
CHAPTER VI FUTURE WORK	75
6.1 Introduction.....	75
6.2 Increasing Dataset Size.....	75
6.2.1 COPDGene Database	75
6.2.2 Clinical Cases	76
6.2.3 Variability of Cases	76
6.3 Feature Extraction.....	77
6.4 Classification	77
6.5 Segmentation	79
APPENDIX.....	80
REFERENCES	118

LIST OF TABLES

Table

1.	The Decision Matrix for a classifier	31
2.	Means and standard deviations (St. Dev.) for features computed using three users' manual segmentations from malignant nodules.....	40
3.	Means and standard deviations (St. Dev.) for features computed using three users' manual segmentations from benign nodules	49
4.	Means and standard deviations (St. Dev.) for features computed using one user's (K.K.) segmentation for both malignant and benign nodules	58
5.	The assignment of classes "Malignant" and "Benign", compared to actual diagnosis	70
A1.	The feature values computed during Feature Extraction for the 5 malignant regions of interest from NLST.....	80
A2.	The feature values computed during Feature Extraction for the 7 benign regions of interest from NLST.....	90
A3.	The feature values computed during Feature Extraction for the 5 malignant regions of interest from COPDGene.....	100
A4.	The feature values computed during Feature Extraction for the 10 benign regions of interest from COPDGene.....	109

LIST OF FIGURES

Figure

1.	Chest x-ray (left) and CT (right) from same patient. The nodule is difficult to locate in the chest x-ray but is readily apparent in CT	7
2.	Flowchart of a computer-aided diagnostic tool. The top row shows the training pathway, where the tool's classifier uses many nodules to learn which characteristics of a nodule are important in making a diagnosis. The bottom row shows the diagnosing pathway. In this stage, an individual nodule is run through the tool in order to obtain the diagnosis	9
3.	Diagram of framework for CAD program. The program is divided into four main stages – Region of Interest Segmentation, Feature Extraction, Feature Selection, and Classification. Each stage also has its key components outlined above.....	14
4.	Nodule Segmentation Interface. (a) shows the command prompt for the user, asking the user to manually segment the nodule. (b) shows a single slice of the segmentation process. The blue dots are placed by the user to outline the nodule.....	16
5.	Summary of features extracted from the regions of interest. Four categories of features (intensity, shape, border, and texture) were computed.	17
6.	Illustration of the FWHM computed from an intensity histogram. The FWHM (double arrow) is the distance between the points where the y-values are half of their maximum value.....	19
7.	Single slice of the binary mask of nodule, shown in white, which contains the centroid of the three-dimensional mask. The centroid is depicted by the small green circle located near the center of the image. The single slice of the sphere of equivalent volume, centered at the centroid, is outlined by the larger blue circle.....	22
8.	Illustration of the steps to generate the RBST. From an individual slice of the region of interest (top left), the border pixels are found (top middle). The lines normal to the tangent lines of each border pixel are computed (top right), and the intensity of each pixel in the RBST image (bottom) are interpolated by the pixels closest to the normal line radiating from the border pixels. In the RBST image, the pixels in the top row are those closest to the border, where the pixels in the bottom row are those farthest from the border.....	23
9.	Illustration of the RBST computed from the centroid. The slice containing the centroid of the nodule mask is selected (left). A line connecting the centroid (small circle in middle image) to the bounding box edge (diagonal line in middle image) is computed and the intensity values are interpolated for the straightened image (right). Each row of the straightened image (right) contains the same number of pixels as the distance shown by the white arrowed line in the middle image. The diagonal line (middle) corresponds to the horizontal line in the top row of the straightened image (right).	24

10.	Process for quantifying the border from the straightened image (far left). For each row of the straightened image, a plot of intensity vs. column position is generated (middle left). The minimum and maximum column of the border is found from the straightened mask (middle). A first-order polynomial was fit for each intensity plot over the column range in (middle right). The mean and variance of the slopes was computed for features.	25
11.	The original two-dimensional image (1) and the 24 normalized texture images (2-25), generated by applying different texture kernels to (1).....	27
12.	Example of a three-dimensional Laws' kernel stack. Each image (from left to right) is combined into a 5x5x5 kernel stack.....	28
13.	Flowchart for determining significance of each feature. Diamonds represent decisions and rectangles represent processes.....	30
14.	Examples of ROC curves (sensitivity vs. false positive rate). Curve (A) represents a perfect classification that has an area of 1, where (D) represents a random classifier with an area of 0.5.....	31
15.	Structure of an artificial neural network with two input nodes, a single hidden node, and two output nodes.	32
16.	Diagram illustrating the types and number of cases present in the COPDGene study. Nodules of size 6-10 (in yellow) were selected as cases for evaluating the CAD model.....	35
17.	Comparison of nodule and parenchyma masks between users. The original DICOM slice is on the left. Note the variation in segmentation between 1 (A.J.), 2 (K.K.), and 3 (S.D.), not only around the nodule (top) but also in the valid parenchymal tissue masks (bottom).....	37
18.	Results of measuring significance of intensity, shape, and border features. The thick vertical line denotes the significance level of 0.05. A total of 5 (4 intensity and 1 shape) features with p-values less than 0.05 are statistically significantly different between malignant and benign nodules.	67
19.	Results of measuring significance of texture features from the nodule. The thick vertical line denotes the significance level of 0.05. No features are statistically significantly different between malignant and benign nodules.	68
20.	Results of measuring significance of texture features from the parenchyma. The thick vertical line denotes the significance level of 0.05. A total of 31 variance features with p-values less than 0.05 are statistically significantly different between malignant and benign nodules..	69

CHAPTER I

INTRODUCTION

Lung cancer is the leading cause of cancer-related death for both men and women in the United States, despite being the second-most frequent cancer diagnosis for both sexes. According to the National Cancer Institute, the age-adjusted incidence rate of lung cancer was 62.6 per 100,000 people per year, resulting in an estimated 228,190 new cases of lung cancer in 2013 [3]. While the 5-year survival rate of lung cancer is low, the odds improve remarkably with early diagnosis [4]. These statistics demonstrate that lung cancer is a considerable public health problem for which early intervention is critical to improve survival. Historically, lung cancer has been non-invasively diagnosed with sputum tests and chest x-rays. With the development of computed tomography (CT), imaging gained a depth component that chest x-ray lacks, giving clinicians and researchers a three-dimensional view of human anatomy. The National Lung Screening Trial demonstrated that, in comparing chest x-ray and CT, high-risk individuals screened for lung cancer by CT had a 20% relative reduction in mortality rate due to lung cancer. This reduction was achieved because participants screened with CT were diagnosed with lung cancer at an earlier stage.

Given these results, it is not surprising that there has been increased utilization of CT for pulmonary nodule assessment. The high resolution achievable by CT has resulted in a significant increase in the number of small pulmonary nodules (4-30mm) detected, many of which are not cancerous. There is an increased need to process large amounts of data with sensitivity to subtle textures and effective monitoring of change over time, all through a time efficient process. Using computer computational power to automatically quantify and statistically compare features extracted from CT data may assist radiologists in identifying lung cancer at an earlier stage, improving the patient's chance of survival while improving the accuracy of classifying small nodules as likely malignant or benign.

Many researchers have worked to develop computer aided diagnosis (CAD) tools for lung nodules; however, these CAD tools focus on making a diagnosis based on the nodule properties alone. These studies neglected examination of the nodule's interaction with surrounding tissue, and this potentially valuable information is available in the CT images. By ignoring the information captured in the surrounding tissue and focusing solely on the nodule for diagnosis, other CAD tools may be missing half of the diagnostic picture. ***I hypothesize that textural and other properties of the nodule and the surrounding parenchyma differ between malignant and benign nodules.*** By incorporating these features, performance in the measures of sensitivity, specificity and accuracy can be improved over CAD tools that rely on nodule characteristics alone.

CHAPTER II

BACKGROUND INFORMATION

2.1 Lung Cancer

Cancer is the result of genetic mutations causing altered cellular differentiation and survival, culminating in the invasion of surrounding tissue and metastasis. More specifically, properties of cancerous cells include self-growth stimulation, ignoring growth-inhibiting signals, avoidance of apoptosis, angiogenesis, metastasis, uninhibited replication, and the ability to evade the immune system [5]. While the genetic mutations can occur spontaneously, the carcinogenic effects of cigarette smoke have increased the frequency of lung cancer in the world by inducing activating mutations in proto-oncogenes and inactivating mutations in tumor suppressor genes [6]. Approximately 90% of lung cancer cases are attributed to active smoking [7].

Lung cancer is the second-most common cancer diagnosis of men and women in the United States. In men, the age-adjusted incidence rate of lung cancer is 78.2 per 100,000, whereas the incidence of prostate cancer, the most common cancer in men, is 137.7 per 100,000. In women, the age-adjusted incidence rate of breast cancer, the most common cancer in women, is 123.1 per 100,000, and is more than twice as frequent as the incidence rate of lung cancer at 54.1 per 100,000 [8]. Despite the significant difference in incidence between the most common cancer (prostate or breast) and lung cancer, lung cancer is the leading cause of cancer death for both sexes. The World Health Organization states that, worldwide, lung cancer caused 1.37 million deaths in 2008. In men, lung cancer kills at an age-adjusted rate of 62 per 100,000. In women, that rate is 38.6 per 100,000 [8].

The high rate of death relative to incidence rate in lung cancer is strongly associated to the stage of cancer at diagnosis. Lung cancer can be divided into two histologic types, small cell and non-small cell lung cancers. Small cell lung cancers are

staged by treatment type [9]. With limited stage small cell lung cancer, the cancer is confined to an area that can easily be treated with radiation therapy. In extensive stage small cell lung cancer, cancer has metastasized and localized treatment is ineffective. Non-small cell lung cancers such as adenocarcinoma and squamous cell carcinoma are categorized into stages that are dependent on the size of the tumor (T), lymph node involvement (N), and distant metastases (M). These stages describe the severity of the cancer as well as guide therapy. While Stage I and II cancers are localized to the lungs alone or to the nearby lymph nodes, Stage III cancers describe more advanced disease in the chest as lymph nodes further from the initial tumor are affected. The size of the tumor is also important, with greater size leading to increasing stage. Stage IV describes the most advanced stage of lung cancer, where cancer has metastasized outside the lung. The stage at which lung cancer is diagnosed affects not only treatment, but it also plays a role in patient prognosis.

From the National Cancer Institute, only 15% of cases are diagnosed when the cancer is localized, in Stage I. These cases have a five-year relative survival rate of 52.2%. 22% of cases are diagnosed in Stages II and III, after cancer has spread to regional lymph nodes, and have a five-year survival rate of 25.1%. More than half of lung cancer cases (56%) are not diagnosed until after the primary tumor has metastasized (Stage IV disease), with a five-year survival rate of 3.7%. When averaged across all stages of lung cancer, the five-year relative survival rate is only 15.9% [4]. Because the majority of lung cancers are not diagnosed until after metastasis, improvements are needed to facilitate early diagnosis of lung cancer. *Identifying lung nodules (<3cm) and determining which are cancerous while at an early stage (Stage I) allows for early treatment and could significantly raise the overall lung cancer survival rate.*

2.2 Lung Cancer Detection and Diagnosis

Due to the often insidious progression of lung cancer, testing is frequently only implemented with the onset of symptoms. Because many symptoms of lung cancer (such as weight loss, fatigue, cough, and shortness of breath) are very nonspecific, lung cancer is often diagnosed at an advanced stage. Therefore, regular screening for lung cancer is indicated for asymptomatic high-risk populations, such as current or former smokers. Current screening tests include sputum testing, chest x-ray, and chest CT. In sputum testing, expectorated sputum is examined for cells with malignant characteristics. This test has the benefits of being low risk and noninvasive, but sensitivity of sputum cytology can be poor. This exam is dependent upon the sputum sample; if there are not cancerous cells in the sampled sputum, the diagnosis is missed. In a person with lung cancer symptoms, it can be used as a non-invasive and inexpensive way to determine the histological type of cancer, though absence of cancer cells in the sputum leads to the employment of other diagnostic tests such as biopsy or resection. Sputum testing has been used as a screening test in asymptomatic people, however, it has not led to reduced death rates [10].

Chest x-ray is another diagnostic test that has been implemented as a screening test. In this exam, ionizing radiation is generated by the acceleration of electrons toward an anode. The electrons collide at a focal point on the anode, producing characteristic and bremsstrahlung x-rays. The low energy photons are filtered, and the remaining x-rays are projected through the body from a single fixed source. These emitted photons interact with body matter in several ways. Compton scattering occurs when a portion of the photon's energy is transferred to an electron in the atoms within the body. The path of the photon is modified and its energy reduced. Therefore, this type of interaction contributes to noise in the image. The primary contrast-generating interaction, where the photon is absorbed by the atoms in the body, is called the photoelectric effect. The photon transfers

energy to an electron in an inner shell of an atom, causing the electron to leave its shell as a photoelectron. When an outer electron falls into the vacant position, it releases characteristic energy in the form of low-energy characteristic radiation which is absorbed by the tissue. The detector opposite the x-ray source counts the distribution of transmitted x-rays [11]. The denser the matter, the more photons are absorbed by the photoelectric effect. Consequently, fewer photons reach the detector, resulting in a brighter region in the image. This exam, like sputum testing, is noninvasive, but exposes the patient to low doses of ionizing radiation. Also like sputum cytology screening, chest x-ray screening has not led to a reduction of mortality rates by lung cancer [10, 12]. Lung cancer is often invasive by the time it is observed on chest x-ray. Chest x-ray is difficult to interpret because it is a projection – three-dimensional anatomy is imposed into a two-dimensional image. The lesions appear small and faint on x-ray and are often hidden by the superimposed anatomy.

Chest CT is similar to chest x-ray in that ionizing radiation is projected through the body. However, in chest CT, x-rays are projected in a cone-beam pattern through the body, while the x-ray source and detector move helically over the area to be imaged [11]. Because sequential images are obtained along a longitudinal axis, these images can be reconstructed into a high-resolution volumetric view of the body. This improvement in resolution over chest x-ray can be seen in Figure 1. The use of CT as a screening tool for lung cancer has been shown to be more effective than chest x-ray [13]. In the National Lung Screening Trial (NLST), over 53,000 former and current smokers were divided into lung cancer screening by either chest CT (cohort) or chest x-ray (control). Participants underwent three rounds of screening at one year intervals or until they were diagnosed with lung cancer. As expected, the first round of screening resulted in the most lung cancer positive screenings in both the CT and chest x-ray groups. For rounds two and three, however, fewer later stage cancers were seen in CT than in chest x-ray, indicating

that cancer was diagnosed at an earlier stage in the CT arm of the study. Additionally, more cancers were diagnosed at earlier stages of lung cancer for CT. Screening by chest CT resulted in a relative mortality reduction of 20% [13].

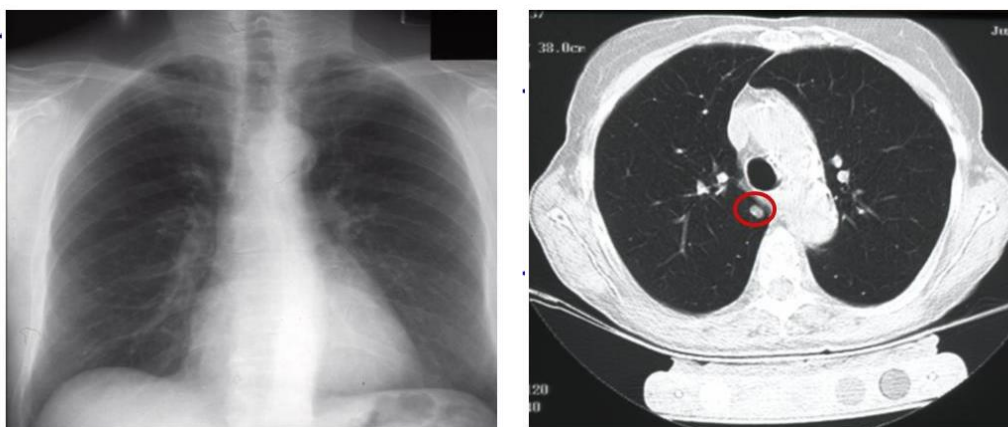


Figure 1: Chest x-ray (left) and CT (right) from same patient. The nodule is difficult to locate in the chest x-ray but is readily apparent in CT [1].

While chest CT has been shown to be effective in reducing lung cancer mortality as a screening test, there are some disadvantages to using chest CT for this purpose. Firstly, while still noninvasive, the test requires increased radiation exposure relative to chest x-ray. In the NLST protocol, the effective dose for a chest CT was approximately 2mSv, approximately one hundred times that of a chest x-ray (0.02mSv) [14]. Secondly, NLST found the CT cohort had a higher false-positive rate than the chest x-ray controls. False positives are especially common in smaller nodules – lung tumors with a diameter

smaller than 3 cm. Upon identification of a nodule in CT, a radiologist comments on the likelihood of cancer, affecting the clinician's recommended course of action. If the nodule cannot be determined to be benign, several diagnostic options are available for follow-up. These options include reimaging in three to six months if the likelihood of cancer is low, imaging with CT/positron emission tomography (PET) to look at metabolic activity of the tumor, or biopsy to determine the pathology of the nodule. Further testing on these false positive nodules causes increased emotional stress for the patient as well as unnecessary cost and risk caused by subsequent procedures. Using a computer-aided diagnostic (CAD) tool to assess CT data can help radiologists to identify likely benign and malignant nodules, thus reducing the false positive rate and resulting in a more appropriate course of action.

2.3 Computer-Aided Diagnostic Tools

CAD tools aim to increase the accuracy of diagnosis from an image set by serving as a second reader for radiologists [15]. They examine a particular region of interest in an image set by processing the information in the region to provide a diagnosis of the region. Some CAD tools also incorporate computer-aided detection to highlight suspicious cases, which a clinician can then focus on when they analyze the image set, however this is a secondary goal. The CAD tool and the clinician work in a complementary way to improve the diagnosis – for this study, the likelihood of cancer – by serving as a virtual second radiologist reader.

A CAD tool can be divided into two pathways– training and diagnosing. The flowchart for a CAD tool's workflow can be seen in Figure 2. Regardless of the pathway chosen, all datasets that are going to be processed through a CAD tool need to be reduced down to a region of interest. The process of isolating a region of interest can be accomplished by manual segmentation or through an automated method as a preprocessing step before either pathway is utilized. In cancer assessment, this region of

interest is typically a tumor or nodule. Once the datasets are reduced to the regions of interest, the pathway of the CAD program can be selected.

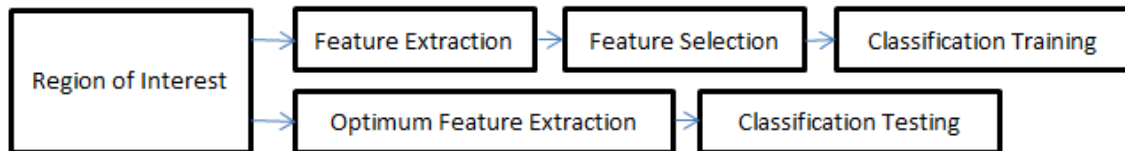


Figure 2. Flowchart of a computer-aided diagnostic tool. The top row shows the training pathway, where the tool's classifier uses many nodules to learn which characteristics of a nodule are important in making a diagnosis. The bottom row shows the diagnosing pathway. In this stage, an individual nodule is run through the tool in order to obtain the diagnosis.

The training pathway, as shown in Figure 2, involves feature extraction, selection, and classification training on a set of regions of interest. The training pathway requires a set of regions of interest for which the final diagnoses, i.e. malignant or benign, are known. Features are extracted from each region of interest. A feature is a characteristic quantified from the region of interest. Often, these features are related to a visual characteristic that radiologists use in determining their diagnosis. For example, small, condensed, spherical lung nodules with well-defined borders are usually benign [16]. By quantifying how spherical a nodule is, one has created a feature. Other examples of features include descriptions of intensity, uniformity, texture, and size.

Once all features are extracted from the regions of interest, the feature space needs to be reduced into a few features that best separate the diagnoses. The number of

features used depends on the number of regions of interest in the training dataset. On average, one feature for every 10 regions of interest can be used [17]. There are several analytical methods that can be utilized for feature selection. Basic statistical testing, such as Student's t-test or the nonparametric Wilcoxon Rank Sum test can determine which features independently separate the types of diagnoses. A feature selection method known as backward elimination then eliminates one feature at a time until the number of features used in classification results in the fewest features necessary to distinguish between the diagnoses. Another method, forward selection, adds one feature at a time to the classification until adding a feature no longer improves the separation of diagnoses.

After feature selection has reduced the number of features required to separate the diagnoses, the classifier can be trained with the selected features. Several different classifiers exist including logistic regression, decision trees, neural networks, and support vector machining. Though the structures of these classifiers differ, the overall process for training them is constant. Each classifier has parameters that require "training" – the values of the parameters are modified so the feature values from the regions of interest result in outcomes that match the known diagnoses.

The second pathway of a CAD tool uses the trained classifier described previously to predict the diagnosis of a new region of interest. The features selected in the training stage are computed from the region of interest. These feature values are then fed into the classifier, which computes the expected diagnosis. In this way, a CAD tool is able to provide a second opinion to a radiologist.

Developing a CAD tool to identify lung cancer is a topic that has been explored in many different ways. Current CAD approaches, however, have focused on the lung nodule itself. One of these CAD tools was implemented by McNitt-Gray et al. [18]. The regions of interest – the nodules – were extracted using a semi-automated contouring process where the user specifies threshold values the program then uses to determine the

boundary of the object. Features quantifying attenuation, size, shape, and texture were computed from the nodule. Texture features were found to be the best features for classification. Out of the 31 cases (14 benign and 17 malignant), 90.3% (28 cases) were correctly diagnosed.

In a comparison of the current literature, size, intensity, shape, texture, and location of the nodule have all been found to be significant features in determining diagnosis of lung nodules. Many of these features are extracted quantitatively from the regions of interest, such as average intensity, volume, and sphericity as utilized by Armato et al. in their dual nodule detection and classification program [19]. However, other features, such as those extracted by Chen Hui et al., have been specified based on user input. Examples of these subjective features include the presence of spiculation, how well-defined the nodule margins are, and presence of vessel or pleural attachment [20]. The majority of features used in classification have been derived only from the nodule, despite the fact that the nodule interacts with the surrounding parenchyma. Very few CAD programs have attempted to examine the parenchyma as well as the nodule, one of which is the CAD tool developed by Way et al. [21].

The Way et al. CAD program quantifies spiculation through the use of a rubber band straightening transform (RBST) [21]. Essentially, a two-dimensional slice of the nodule is taken and the border of the nodule is converted into a rectangular image. In addition to computing texture from this rectangular image, features characterizing surface smoothness and shape irregularity were computed from the original region of interest. When used for classification, the accuracy in primary lung cancer diagnosis was 90%. While the RBST helps to quantify spiculation and begins to examine the surrounding tissue, its reliance on consistent segmentation decreases its effectiveness.

Aoyama et al. have also examined the parenchyma surrounding the parenchyma, though they limit their examination to features extracted from two-dimensional slices of

the nodule [22]. In testing their CAD tool on 498 nodules, intensity histogram features from the nodule and the 5-pixel band surrounding the nodule were found to be significant predictors of malignancy, in addition to the nodule's effective diameter. Performance was measured by the area under the receiver operating characteristic (ROC) curve at 0.842.

In addition to the examination of intensities, Aoyama et al. began to examine texture based on the presence of ground glass [22]. Several CAD tools, including those developed by McNitt-Gray et al. and Way et al., quantitatively computed the texture of the nodule [18, 21]. While the texture of the nodule is shown to be an important predictor of lung cancer, lung parenchyma texture, especially in three dimensions, has been found to be a predictor of other lung diseases, such as emphysema and idiopathic pulmonary fibrosis. Xu et al. demonstrated that using 24 intensity and texture features, 1184 regions of interest were classified as one of five lung patterns (emphysema, ground-glass, honeycombing, normal nonsmoker, and nonsmoker) with an accuracy of 86.2% [23].

By improving and expanding these measures and implementing others, it should be possible to advance the current state of computer-aided diagnosis in lung cancer screening. Important data for classification may be found in texture as well as the parenchyma surrounding the nodule. Other CAD tools have only minimally examined quantification of texture as a possible measure of malignancy. Thus, there is room for current CAD tools to be improved upon to aid in the diagnostic process. In summary, while CT screening has been shown to reduce the mortality rate of lung cancer, it increases the number of false positives – nodules that cannot be ruled out for malignancy by visual assessment alone. In order to rectify this issue, CAD tools need to quantify features from both the nodule as well as from the surrounding parenchyma. Not only will these features add valuable data as to how the nodule interacts with its environment, using the parenchyma will increase the amount of data available. Small pulmonary nodules (4-10mm) identified through CT pose a challenging clinical management issue.

For these nodules there are a limited number of CT data voxels within the solid tumor, which makes them difficult to process through traditional CAD tools. Increasing feature extraction to include the surrounding parenchyma will expand the CT voxel set for analysis in these very small pulmonary nodule cases and likely increase diagnostic performance.

CHAPTER III

METHODS

Computer-aided diagnostic (CAD) tools are designed to extract pertinent features from a region of interest and apply decision making strategies to assign designated labels. When applied to assessing pulmonary lesions in computed tomography (CT) datasets, the typical CAD output is the distinction of new cases as benign or malignant. The CAD tool designed for this study was developed to incorporate features extracted from both the target pulmonary nodule as well as from the surrounding parenchyma, with the hypothesis that more data (from the surrounding parenchymal features) will improve classification performance. The system was developed using MATLAB (MathWorks, Natick, MA, USA).

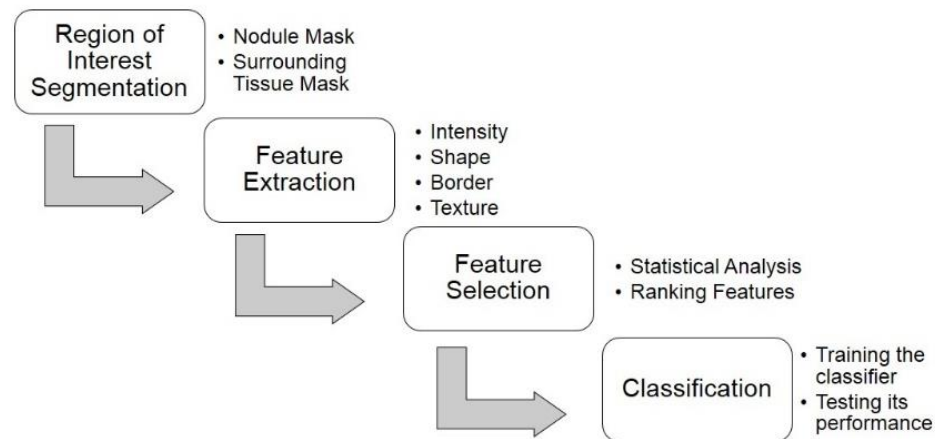


Figure 3. Diagram of framework for CAD program. The program is divided into four main stages – Region of Interest Segmentation, Feature Extraction, Feature Selection, and Classification. Each stage also has its key components outlined above.

As shown in Figure 3, the steps of a generic CAD program described in the previous section have been separated into modular functions of code. By implementing the CAD program this way, it is easy to quickly remove or insert feature extraction methods, as well as test portions independent of the entire program. Each of the sections shown in Figure 3 will now be described in more detail.

3. 1 Data Preprocessing

Chest CT scans incorporate data covering the complete anatomy of the thorax stored in Digital Imaging and Communications in Medicine (DICOM) format. The design of this CAD tool was specific for the analysis of individually identified pulmonary nodules. Therefore, a pre-processing step was required to isolate the nodule and surrounding parenchyma from the complete dataset. This preprocessing set serves to decrease the size of the dataset to a specific region of interest. First, the chest CT DICOM file was loaded into a pulmonary analysis software program, Apollo (Vida Diagnostics, Coralville, IA, USA) and the coordinates of the identified nodule were recorded in an Excel file along with the filename of the DICOM data.

Using this Excel file, the DICOM data was loaded into a segmentation module written in MATLAB. The coordinates encoded in the Excel file were used to create a bounding box surrounding the nodule, forming the region of interest. This region of interest was saved as a smaller DICOM file so as to expedite computation time. The solid nodule was then manually segmented with a point and click tracing tool built into the segmentation module to generate and save a binary nodule mask, shown in Figure 4. Next, the region of interest was manually segmented to exclude non-lung tissues including pleural wall and blood vessels. The resulting mask contained valid lung parenchyma as well as the nodule. The two masks generated by manual segmentation were then subtracted from each other to result in a nodule mask and a surrounding tissue mask.

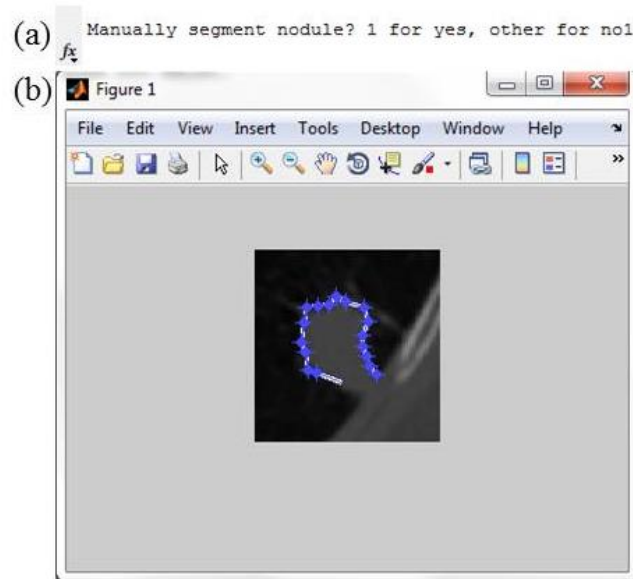


Figure 4. Nodule Segmentation Interface. (a) shows the command prompt for the user, asking the user to manually segment the nodule. (b) shows a single slice of the segmentation process. The blue dots are placed by the user to outline the nodule.

The identification and segmentation of the nodules is time consuming, hence the coordinates of the region of interest and the binary mask image sets for each region of interest are saved for future reference. These files can be loaded into the CAD program, which saves the user time in the training phase of the CAD program. Alternatively, if a new dataset is used for training, the segmentation module can easily be inserted into the CAD tool. Additional demographic information, such as age, sex, and smoking pack-years was also entered into the Excel file that stores the region of interest coordinates. Finally, the pathological diagnoses of the nodules were recorded in the file in binary where 0 represents a benign nodule and 1 represents malignancy. These diagnoses served as the class for the CAD tool.

3.2 Feature Extraction

Four classes of features were computed from the defined nodule and parenchymal areas of each region of interest (3.1 Data Preprocessing). These feature classes include: intensity, shape, border, and texture features. A summary of the features extracted can be seen in Figure 5.

Intensity	Shape	Border	Texture
<ul style="list-style-type: none"> • Histogram Features • Average • Median • Minimum • Maximum • Variance • Heterogeneity Measures • FWHM • Entropy • Kurtosis • Skewness 	<ul style="list-style-type: none"> • Recist • Sphericity • Effective Radius • Differences in Spherical Shape • Average • Variance • Kurtosis • Skewness • Range 	<ul style="list-style-type: none"> • Average rate of border change • Variance in rate of border change 	<ul style="list-style-type: none"> • Nodule Texture • Average • Variance • Kurtosis • Skewness • Parenchymal Texture • Average • Variance • Kurtosis • Skewness

Figure 5. Summary of features extracted from the regions of interest. Four categories of features (intensity, shape, border, and texture) were computed.

3.2.1 Intensity Features

The intensity of CT images describes radiodensity of the anatomy through Hounsfield units (HU). The voxels of the image contains are stored as 12-bit, therefore there are $2^{12} = 4096$ intensity values, typically ranging from -1000 HU to 3096 HU. Air measures at -1000 HU, the darkest voxel intensity, whereas soft tissue has a density of 100 to 300 HU [11]. By analyzing the distribution of intensities in each area of the

region of interest, the intensities for both the nodule and the parenchyma were reduced into a few features.

3.2.1.1 Intensity Histogram Features

The average, median, minimum, and maximum intensities in Hounsfield Units (HU) were determined for the nodule and parenchyma by using their respective masks. The variance of intensities was also computed for each region. The remaining intensity features were computed from the histogram of intensities for each region. These features examine the heterogeneity of the intensities of a region.

3.2.1.2 Measures of Heterogeneity

3.2.1.2.1 Full width at half maximum (FWHM): The FWHM is the width of a curve or function where the curve is at half its peak value. In systems analysis, the FWHM is one way to describe the spatial resolution of a system [11]. If the FWHM is less than the distance between input signals, the two signals are distinguishable in the output response. However, if the FWHM is greater than the distance between input signals, the output response appears to originate from a single signal. The FWHM can also be applied to curves to determine the width of a “bump” in a curve [24]. The determination of the FWHM is shown in Figure 6.

By applying the FWHM to a histogram of intensity values, the homogeneity of intensities was quantified. The larger the FWHM when compared to the range of intensities, the more heterogeneity exists within a region. Conversely, the smaller the FWHM, the more homogeneous the intensity distribution is within a region. By generating a histogram, the most frequent intensity was identified. The FWHM was computed by dividing the frequency of the mode intensity by two and summing the number of intensities with at least that number of counts. In order to compare FWHM

from one region to the FWHM from other regions, the FWHM was converted to a proportion of the range of intensities.

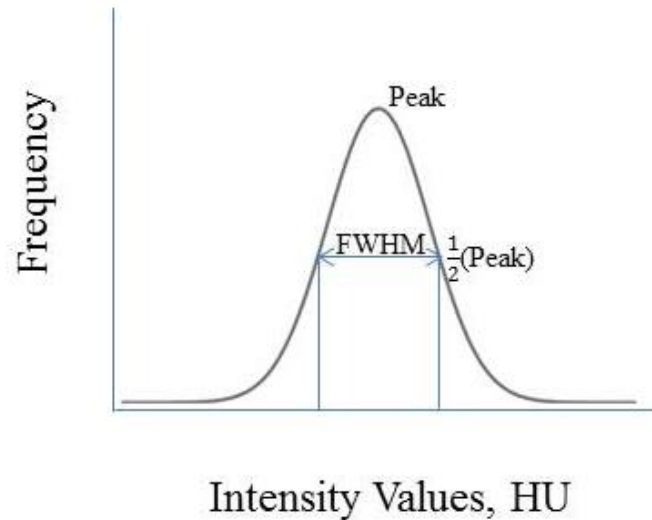


Figure 6. Illustration of the FWHM computed from an intensity histogram. The FWHM (double arrow) is the distance between the points where the y-values are half of their maximum value.

3.2.1.2.2 Entropy: The more disordered an image is, the larger the entropy. In the case of the nodule, the disorder arises in the form of variation in intensity. The equation for entropy [25] is:

Equation 1: The entropy equation.

$$H(X) = - \sum_{k=1}^n p(x_k) \log_2(p(x_k))$$

$p(x_k)$: probability of an outcome

In this application, $p(x_k)$ is the probability of each intensity value. These probabilities were estimated from the histogram by converting the frequency, in number of voxels, of each intensity value, into a proportion of the total number of voxels in the region.

3.2.1.2.3 Kurtosis: This measurement quantifies how similar the shape of the histogram is to a normal distribution, whether it has a steeper or flatter distribution.

Kurtosis is computed by the following equation [26]:

Equation 2: The kurtosis equation.

$$Kurtosis = \frac{\sum_{i=1}^N (Y_i - \bar{Y})^4}{(N-1)s^4}$$

Y: individual intensity value, HU

\bar{Y} : mean intensity value, HU

N is the number of pixels in the region

s is the standard deviation of intensity.

3.2.1.2.4 Skewness: This feature quantifies the normality of the intensity distribution. For example, a calcified nodule will have more intensity values at higher HU, and the distribution of intensities will be shifted to the right in the histogram. The equation for skewness is [26]:

Equation 3: The skewness equation.

$$Skewness = \frac{\sum_{i=1}^N (Y_i - \bar{Y})^3}{(N-1)s^3}$$

Y: individual intensity value, HU

\bar{Y} : mean intensity value, HU

N is the number of pixels in the region

s is the standard deviation of intensity.

3.2.2 Shape Features

The shape of a nodule is used by radiologists in evaluating the likelihood of malignancy, with a tendency for malignant lesions to have a less spherical shape than benign lesions [16]. Previous investigators have found sphericity to be an important measure of this observable tendency. In addition to nodule shape, radiologists examine

the maximum diameter of the nodule using the Response Evaluation Criteria In Solid Tumors (RECIST) criteria. By incorporating sphericity as well as other measures of nodule profile into the CAD tool, several shape features were extracted.

3.2.2.1 Maximum Diameter (RECIST)

The RECIST criteria were developed to evaluate cancer treatments by creating a standardized process to determine how tumors respond to treatment [27]. The primary measure is the maximum diameter. The largest diameter is measured from the two-dimensional slice containing the greatest area of the nodule.

3.2.2.2 Sphericity

The sphericity describes how similar a nodule is to a sphere and measures the compactness of an object [28]. The sphericity is computed by comparing the volume of an object, in this case the nodule, to its surface area. The formula for sphericity is:

Equation 4: The sphericity equation.

$$Sphericity = \frac{\pi^{\frac{1}{3}}(6V)^{\frac{2}{3}}}{SA}$$

V: volume of the nodule

SA: surface area of the nodule

The more spherical an object is, the closer the sphericity measure is to one. As benign nodules are typically well-defined and condensed [16], they should have a sphericity close to one. Malignant nodules, which tend to be spiculated and lobular in shape [16], should have a sphericity of less than one.

3.2.2.3 Differences in Spherical Shape

In order to analyze the shape of a nodule further, each nodule was compared to a sphere of an equivalent volume. The effective radius of the sphere was computed by rearranging the volume formula of a sphere. This derivation is as follows:

Equation 5: The effective radius equation.

$$V = \frac{4}{3}\pi r^3 \rightarrow r = \left(\frac{3V}{4\pi}\right)^{\frac{1}{3}}$$

r: radius of a sphere
V: volume of a sphere

The centroid of the nodule was computed from the nodule mask. The distance from each border pixel to the centroid of the nodule is compared to the effective radius by subtraction. A visualization of this comparison can be seen in Figure 7.



Figure 7. Single slice of the binary mask of nodule, shown in white, which contains the centroid of the three-dimensional mask. The centroid is depicted by the small green circle located near the center of the image. The single slice of the sphere of equivalent volume, centered at the centroid, is outlined by the larger blue circle.

The absolute differences between the nodule and a sphere of the same volume were summarized by the following features: mean difference, variance, kurtosis, skewness, and range of the differences. These differences were computed in physical dimensions of centimeters, allowing for comparison between regions of interest.

3.2.3 Border Features

While the comparison of the nodule to a sphere described in the Shape Features section began to examine the border, further analysis of the border to quantify spiculation was needed. In general, malignant lesions have spiculated borders, whereas benign cases tend to have smooth, well-defined boundaries [16]. Way's paper [29] introducing the RBST was the first CAD tool to examine the border alone. The process for computing the RBST is shown in Figure 8.

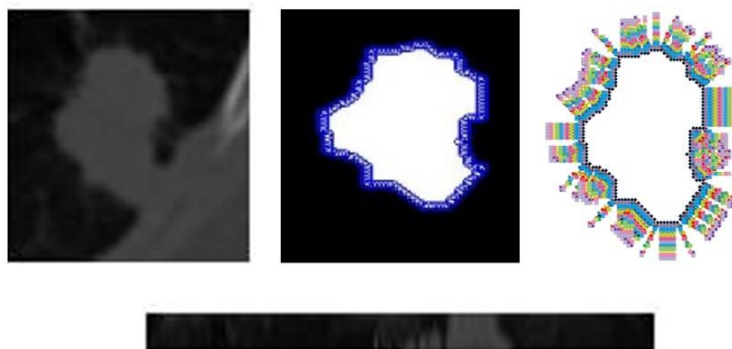


Figure 8. Illustration of the steps to generate the RBST. From an individual slice of the region of interest (top left), the border pixels are found (top middle). The lines normal to the tangent lines of each border pixel are computed (top right), and the intensity of each pixel in the RBST image (bottom) are interpolated by the pixels closest to the normal line radiating from the border pixels. In the RBST image, the pixels in the top row are those closest to the border, where the pixels in the bottom row are those farthest from the border.

In order to compute the RBST for a two dimensional image, the border pixels of the nodule were identified from a slice of the nodule mask. For every border pixel, the tangent line of the border at that point was computed. The line perpendicular to the tangent line was then computed. The two pixels nearest to the perpendicular line at various distances were used to interpolate the intensity of the pixel that would lie on the perpendicular line. This was repeated until the distance from the border intersects with the closest bounding box edge, generating the complete RBST image.

While groundbreaking, the RBST's reliance on the segmentation of the nodule hinders its versatility and robustness. By shifted the straightening from the border of the nodule to the nodule's centroid, the dependence on segmentation is reduced. While the identification of the boundary can vary greatly between users and segmentation methods, the centroid will be minimally affected. Instead of computing features from the RBST, a new approach was applied that quantifies the border based on straightening the nodule from the centroid.

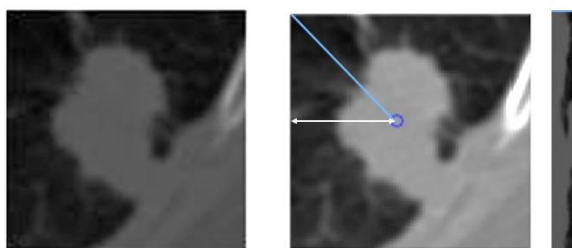


Figure 9. Illustration of the RBST computed from the centroid. The slice containing the centroid of the nodule mask is selected (left). A line connecting the centroid (small circle in middle image) to the bounding box edge (diagonal line in middle image) is computed and the intensity values are interpolated for the straightened image (right). Each row of the straightened image (right) contains the same number of pixels as the distance shown by the white arrowed line in the middle image. The diagonal line (middle) corresponds to the horizontal line in the top row of the straightened image (right).

To accomplish this task, illustrated in Figure 9, the slice of the region of interest containing the centroid was selected. For this slice, the line connecting the centroid and each bounding box coordinate was computed. Each of these lines represents a single row in the straightened image. The values along this line were interpolated for each distance (the columns of the straightened image) from one pixel to the distance between the centroid and the closest bounding box edge. By using this length as the maximum distance, the number of columns in the straightened image was ensured to be uniform for every row (every border pixel).

Once the straightened image was computed, the border was analyzed as described in Figure 10.

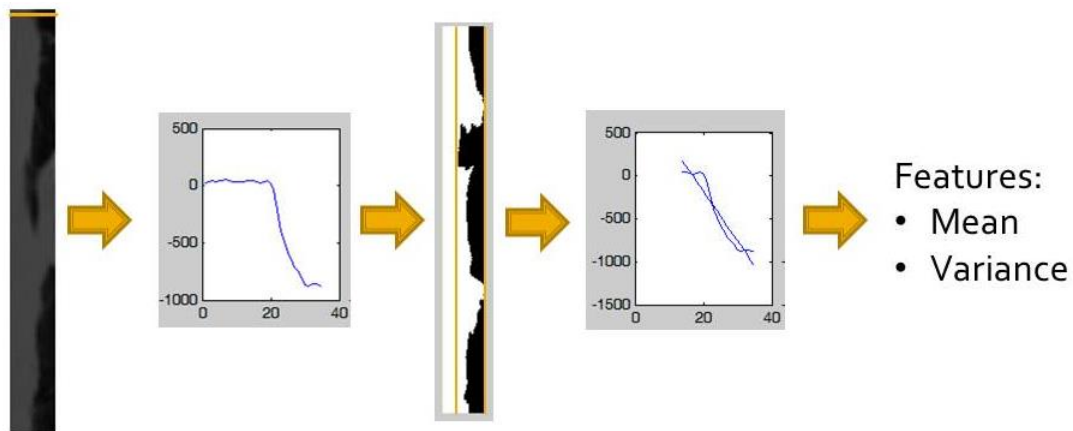


Figure 10. Process for quantifying the border from the straightened image (far left). For each row of the straightened image, a plot of intensity vs. column position is generated (middle left). The minimum and maximum column of the border is found from the straightened mask (middle). A first-order polynomial was fit for each intensity plot over the column range in (middle right). The mean and variance of the slopes was computed for features.

For each row of the straightened image, the intensities were plotted against the distance from the centroid (column values). The slope of each intensity plot was estimated over the range of the border, using the straightened nodule mask to identify the minimum and maximum distance where the border occurs. These slopes were averaged, and the variance computed. These features help to quantify the border transition based on intensities of both the nodule and the parenchyma. For benign nodules that have well-defined borders, the slope should be steeper, whereas a spiculated malignant nodule would have a shallower average change in intensity.

3.2.4 Texture Features

Finally, the texture for both the nodule and the parenchyma was quantified using Laws' texture energy measures (TEM) [30, 31]. These measures interrogate the greyscale images by looking for patterns in different gradients. In the two dimensional application, five 5-element vectors that describe levels, edges, spots, waves, and ripples are convolved with each other to form 25 five-by-five matrices called kernels. These kernels locate a different texture type in each direction, such as edges in the horizontal and spots in the vertical. These 25 kernels are then convolved with the two-dimensional image, creating 25 new images whose pixels contain information about the texture at that given point. 24 of these new images are convolved with an averaging filter to compute texture energy images. These 24 texture energy images are then normalized to the only image that was not averaged by convolution. These images can be seen in Figure 11. Finally, texture energy images are combined to achieve rotational invariance, resulting in 14 texture measure images for which the average, variance, kurtosis, and skewness for each region were computed.

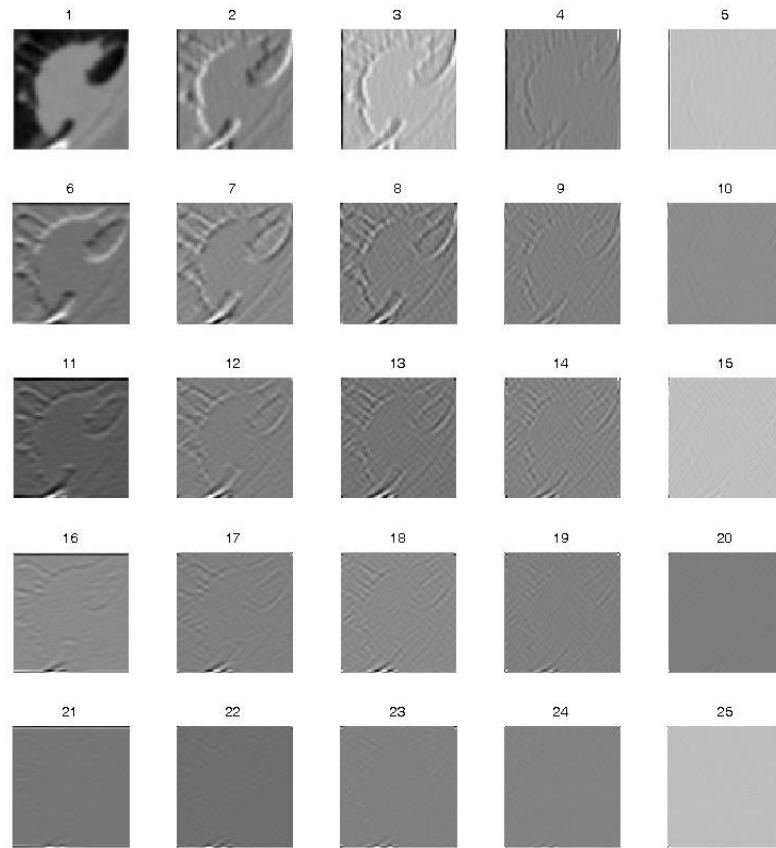


Figure 11. The original two-dimensional image (1) and the 24 normalized texture images (2-25), generated by applying different texture kernels to (1).

The regions of interest were presented in three dimensions; therefore features that quantified the three-dimensional textures in both the nodule and parenchyma were desired. By convolving the five five-element vectors with the 25 kernels, 125 kernel stacks in the form of five-by-five-by-five matrices were generated. One of these kernel stacks can be seen in Figure 12. These 125 kernels are convolved with the regions of interest, generating 125 texture stacks that, when combined and normalized as described above, simplifies into 34 rotationally-invariant texture energy image stacks. Using the

nodule and parenchyma binary masks to segment the texture energy image stacks, each stack was reduced into 8 features – the mean, variance, kurtosis, and skewness of the texture energies for both the nodule and the parenchyma. Therefore, 272 texture features are generated to quantify the texture of both the nodule and the parenchyma.

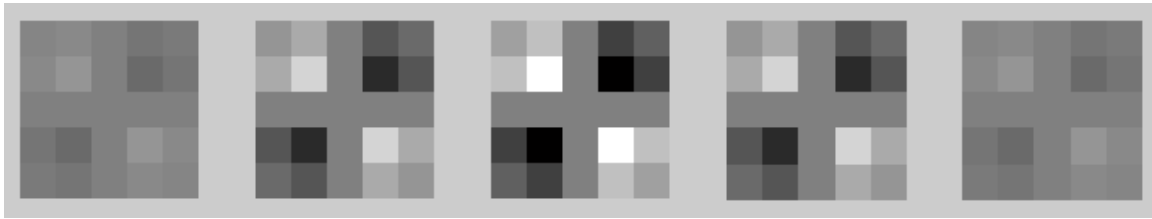


Figure 12. Example of a three-dimensional Laws' kernel stack. Each image (from left to right) is combined into a 5x5x5 kernel stack.

3.3 Feature Selection

After the extraction of the four feature types – intensity, shape, border, and texture – from the regions of interest, there were a total of 299 features that could potentially be used to differentiate between the classes of malignant and benign. In order to prevent overfitting of the classifier (where the classifier is so well tuned to correctly classify the training set that it loses generalizability), one feature for every 10 regions of interest can be used in the classifier [17]. Several methods were employed to determine which features best separated the two classes.

3.3.1 Testing for Significance

A statistical analysis module was created to determine which features were statistically significantly different between the malignant and benign cases. Each feature was tested for normality using the Jarque-Bera normality test. Additionally, the variances for each feature were tested for equivalence. If the feature followed a normal distribution and the variances for the malignant and benign groups were equal, a 2-sample t-test for equal variances was performed. If the feature followed a normal distribution but did not have equal variances between the two groups, a 2-sample unequal variances t-test was used. Finally, if the normality test showed the feature distribution was not normal, the nonparametric Wilcoxon Rank Sum test was used. A feature with a p-value less than 0.05 was determined to be statistically significant. This process is illustrated in Figure 13.

3.3.2 Rank Features

The features determined to be significant from the testing method above were then ranked according to how well they differentiated between the two classes. To determine how well a classifier performs, many criteria can be used, which are derived from the decision matrix, Table 1. The sensitivity is the ratio of true positive decisions (TP) to the number of actual positives (D+) and the specificity is the ratio of true negative decisions (TN) to the number of actual negatives (D-). The criterion used to determine the classifier's ability to separate classes with a particular feature was the area between the empirical receiver operator characteristic (ROC) curve and a random classifier. The ROC curve is a plot of the sensitivity of the classifier against 1- the specificity, or the false positive rate (FPR), of the classifier. Some examples of ROC curves can be seen in Figure 14.

A perfect classifier has an area under the ROC curve of 1. The significant features were ranked by subtracting 0.5, the area under the ROC curve of a random classifier, from the area under the ROC curve generated using each feature. When this method is

applied to a perfect classifier, the resulting value is $1 - 0.5 = 0.5$. Therefore, the closer this value is to 0.5, the better the feature performs in classifying the cases.

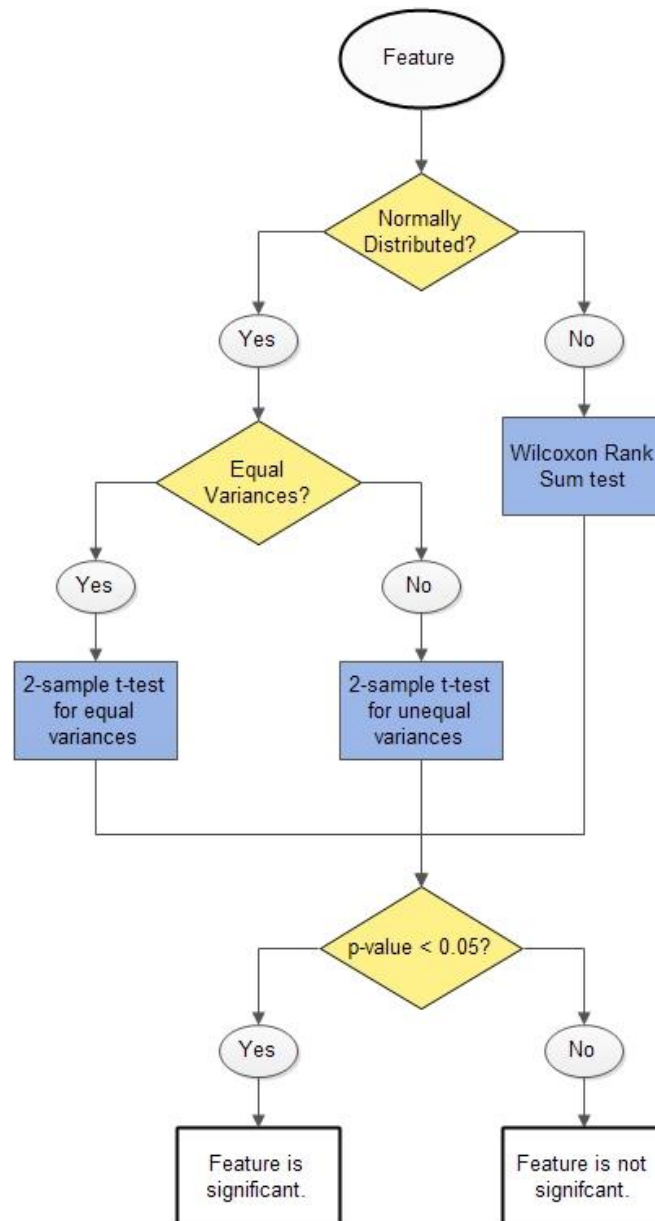


Figure 13. Flowchart for determining significance of each feature. Diamonds represent decisions and rectangles represent processes.

Table 1: The Decision Matrix for a classifier [2].

Test Result	True Condition Status		Total
	Positive	Negative	
Positive	TP	FP	T+
Negative	FN	TN	T-
Total	D+	D-	

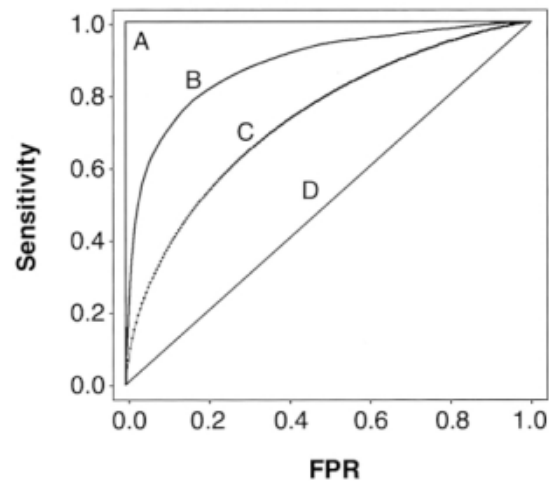


Figure 14. Examples of ROC curves (sensitivity vs. false positive rate) from [2]. Curve (A) represents a perfect classification that has an area of 1, where (D) represents a random classifier with an area of 0.5.

3.3.3 Forward Selection

As described in the Background, forward selection adds one feature at a time to the classification until adding a feature no longer improves the separation of diagnoses.

This algorithm was implemented to ensure that one feature was added for every ten regions of interest, in order to prevent overfitting [17].

3.4 Classification

As the last step in the CAD training pathway, a classifier was trained. An artificial neural network was selected as the classifier for several reasons. First of all, it is a nonlinear classifier that has a hidden layer, see Figure 15. Therefore, it is more robust to separating classes with non-linear separations. This enables the classifier to work well on many different datasets, regardless of whether the classes are linearly separable. Finally, when each class has its own output node, the classification results can be interpreted as the probability of belonging to each class.

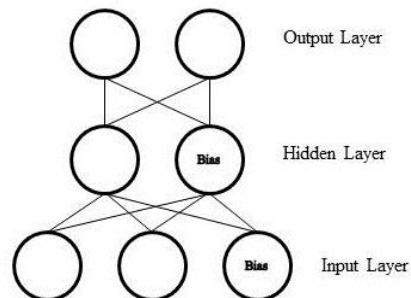


Figure 15. Structure of an artificial neural network with two input nodes, a single hidden node, and two output nodes.

In order to develop the artificial neural network, the weights of the formulas that connect the input and hidden nodes, as well as the weights to connect the hidden and output nodes, have to be trained. Because of its nonlinearity, neural network weights are

trained through iterative corrections, as opposed to deterministic linear classifiers. The artificial neural network was trained using batch back-propagation. Weights for the network were randomly selected. Then, every training case was classified by the neural network. Based on the accuracy of the classifier on all cases, the weights were adjusted until the change in classification error was very small.

Accuracy of classification is determined by how well the classification performs on test cases – regions of interest not used in training. To determine the accuracy of the neural network as a classifier, a leave-one-out approach was used. For n training cases total, $n-1$ cases were used for training. The remaining case was then used to test the classifier. This process was repeated n times, so every training case was used as a test case.

CHAPTER IV

RESULTS

4.1 Patient Database

The University of Iowa Hospitals and Clinics was a participating site in the National Lung Screening Trial (NLST). Hence, the Iowa cohort of NLST was the perfect starting place for developing a database of nodules with pathological diagnoses. Twelve subjects, 4 male and 8 female, imaged with CT at the University of Iowa were identified. These twelve also had only one nodule in their scans, and the diagnosis of the nodule was confirmed through pathology (five malignant and seven benign). These 12 subjects had a mean age of 61.6 years and an average of 31.25 pack-years of smoking. The CT images were acquired with a Philips Mx8000, Siemens Sensation 64, or Siemens Sensation 16. All scans were collected with a tube voltage of 120 kilovoltage peak (kVp), tube currents of 50 – 120 milliamperes (mA), and a tube current-time product of 40-80 milliamperes seconds (mAs). The three Philips scans had a slice thickness of 1.3 mm and were reconstructed with a B filter. The Siemens scans had slice thicknesses of 0.75 mm (2 scans) or 0.6 mm (7 scans) and were reconstructed with a B30f kernel.

The COPDGene study is one of the largest investigations into the factors of Chronic Obstructive Pulmonary Disease (COPD) [32], with twenty-one clinical study centers across the United States. 10,000 participants were, and continue to be, imaged with CT. As there is a strong association between COPD and lung cancer [33], this study was another suitable database for potential cases. A diagram illustrating the distribution of the presence and sizes of radiologist identified and measured nodules in the CT scans can be seen in Figure 16. In addition to providing quantitative information about the nodules, the radiologists also provided their opinion on likelihood of cancer. Through approval of an ancillary study, the participants of COPDGene were reduced into 136 participants with a single pulmonary nodule, size via CT of 6-10 mm. These participants

are shaded in yellow in Figure 16. The diagnoses of the nodules (cancer concern and no cancer concern) were determined by comparing the self-reported presence/absence of lung cancer by the participants and with the radiologists' opinions of the nodules.

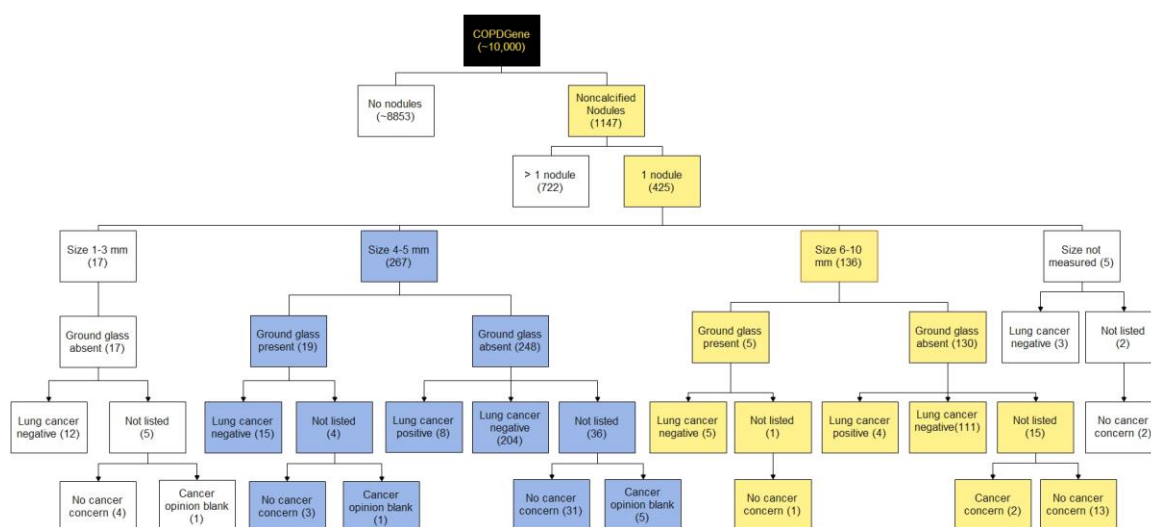


Figure 16. Diagram illustrating the types and number of cases present in the COPDGene study. Nodules of size 6-10mm (in yellow) were selected as cases for evaluating the CAD model.

The inspiratory scans were collected with a variety of CT scanners (Philips, Siemens, and GE). A tightly standardized and monitored CT protocol was utilized to minimize acquisition variation across scanners and scanner models. The protocol features a tube voltage of 120 kVp and a tube current-time product of 200 mAs. Reconstructions were performed with B, B31f, or Standard kernel for Philips, Siemens, and GE

respectively, and slice thicknesses between 0.6 – 0.9 mm [34]. The acquisition and reconstruction parameters are similar to those used for NLST, and will serve to increase the number of cases in the database. While growth of the database is an ongoing process, 15 COPDGene cases (5 malignant and 10 benign) were selected from the 136 participants. When added to the NLST cases, a total of 27 cases (10 malignant and 17 benign) were processed through the CAD tool.

4.2 Data Preprocessing – Segmentation Comparison

As manual segmentation is highly subjective, the segmentation of the 12 NLST cases was performed by three users (A.J., K.K., S.D.) to compare the repeatability of segmentation and the effect segmentation has on the feature values. From the same bounding box for each nodule, all three users created both a nodule mask as well as a surrounding parenchyma mask. Figure 17 shows a single slice of both masks created by the different users, as well as the slice in the original DICOM region of interest.

While the majority of the mask areas overlapped, there were significant differences in the boundaries of the nodules, as well as disagreement in what was valid parenchymal tissue. These masks were then used in the Feature Extraction method (Methods Section 3.2) of the CAD tool to quantify various characteristics of the nodule and parenchyma. The comparison of means and standard deviations for each feature across the three users can be seen in Table 2 for the malignant nodules and Table 3 for the benign nodules. One-way ANOVA tests were applied to each feature for each diagnosis (malignant and benign) to determine whether the feature value differed based on segmentation. The p-values from this test can also be found in Tables 2 and 3. *All ANOVA tests returned p-values greater than 0.05, indicating that user segmentation does not have a statistically significant impact on the computation of any of the features.*

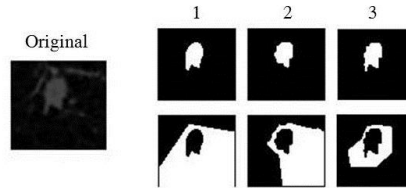


Figure 17. Comparison of nodule and parenchyma masks between users. The original DICOM slice is on the left. Note the variation in segmentation between 1 (A.J), 2 (K.K), and 3 (S.D.), not only around the nodule (top) but also in the valid parenchymal tissue masks (bottom).

4.3 Feature Extraction

Once the areas of nodule and parenchyma were identified in the regions of interest, the training pathway of the CAD tool could be conducted. This pathway is initiated with Feature Extraction from the regions of interest. Using one of the user's (K.K.) nodule and parenchyma masks, 299 features were extracted from the 27 cases. The means and standard deviations of these values for malignant and benign can be found in Table 4. Comparing means and standard deviations, apparent differences exist between malignant and benign. Statistical analysis to determine significance was performed with results presented in the Feature Selection method (Results Section 4.4). The computation time for feature extraction was approximately 10 minutes for this 27-case sample size.

4.4 Feature Selection

While many features were extracted, the use of all these features in classification is not feasible. Not all features contribute meaningful information in the separation of probable diagnoses, i.e. whether a nodule is likely malignant or benign in this CAD tool. Secondly, in classification, for every 10 regions of interest, one feature can be used in

classification [17]. This prevents overfitting of classifier in training, allowing for better prediction of new regions of interest. Based on this criterion, two features can be selected to classify the 27 cases used as a proof of concept. Finally, the computation time in extracting 299 features is significant at 25 seconds per case. By using feature selection in the training pathway, feature extraction in the testing pathway can be shortened without impairing the accuracy of the classifier.

4.4.1 Testing for Significance

The first step implemented in feature selection was to determine which features were statistically significantly different between the ten malignant and seventeen benign cases. Using the method outlined in Methods Section 3.3.1, the p-values were computed for each feature. The p-values of the intensity, shape, border, and texture features can be found in Table 4 and are displayed in Figures 18-20. 36 features (4 intensity, 1 shape, and 31 parenchymal texture) were found to be statistically significant with p-values less than 0.05. Testing for significance greatly reduced the feature set; however, further feature selection methods were required to determine which features were ideal for the training set.

4.4.2 Rank Feature Results

The 36 features determined to be significant in the previous section (4.4.1) were ranked using the process outlined in Methods 3.3.2. The area under the ROC curve (0.5) for a classifier that performs no better than random guessing was subtracted from the area under the ROC curve generated from a classifier with only one feature. The ten top-ranked features with the difference in ROC area from this method were as follows: Variance of the Nodule (0.42), Kurtosis of the Nodule (0.35), Sphericity (0.29), and seven texture variances of the parenchyma from Laws' TEM images (0.28 – 0.29).

4.4.3 Forward Selection Results

The rank feature algorithm further reduced the feature space of the 27 cases from 36 to 10 features. Two features could conservatively be selected to prevent overfitting of the classifier. Using forward selection as described in Methods Section 3.3.3, the features, variance and kurtosis of the nodule, were selected as adequate to separate the two classes of diagnoses.

4.5 Classification

Using the variance and kurtosis of the nodule as the selected features, the 27 cases were used to train a neural network for classification. To determine the accuracy of the classifier, a leave-one-out approach was used. 26 cases were used for training, while the last case was used to test the classifier. This was repeated, leaving out a different case, until all 27 cases were tested. Total run time was 20 minutes for the entire leave-one-out test. The resulting classification can be found in Table 5. *The overall accuracy of the neural network was 92.6%. Two benign cases were incorrectly classified as malignant, resulting in a sensitivity of 100% and a specificity of 88.2%.*

Table 2. Means and standard deviations (St. Dev.) for features computed using three users' manual segmentations from malignant nodules.

Features	Malignant Nodules						P-values
	User 1		User 2		User 3		
	Mean	St. Dev.	Mean	St. Dev.	Mean	St. Dev.	
Intensity							
<i>Nodule</i>							
Mean HU	-121.61	99.36	-121.49	84.26	-132.08	87.44	0.98
Variance	32485.39	14021.12	32134.17	10805.92	36187.27	10080.74	0.84
Maximum HU	336.60	402.30	336.60	402.30	336.60	402.30	1.00
Minimum HU	-847.40	135.57	-765.60	97.69	-859.00	110.96	0.41
Median HU	-82.80	119.60	-78.70	100.59	-85.20	108.87	1.00
FWHM	0.04	0.02	0.05	0.03	0.04	0.02	0.96
Entropy	8.59	0.65	8.62	0.65	8.68	0.60	0.97
Kurtosis	5.02	3.34	4.12	2.47	4.50	2.84	0.89
Skewness	-1.12	1.01	-0.99	0.89	-1.06	0.94	0.98
<i>Parenchyma</i>							
Mean HU	-811.69	48.56	-821.62	47.72	-812.35	42.53	0.93
Variance	21758.39	9590.68	17640.92	6435.95	19818.02	7259.47	0.72
Maximum HU	82.00	206.56	90.00	168.05	34.60	134.25	0.86
Minimum HU	-1014.40	13.15	-1014.40	13.15	-1014.40	13.15	1.00
Median HU	-845.80	46.58	-849.60	46.59	-844.00	44.36	0.98
FWHM	0.07	0.07	0.07	0.06	0.08	0.07	0.98
Entropy	8.72	0.36	8.62	0.29	8.70	0.29	0.89
Kurtosis	8.30	2.52	8.86	2.63	7.66	1.66	0.72
Skewness	1.92	0.50	1.93	0.59	1.80	0.43	0.91
Shape							
Recist Diameter	18.28	11.91	18.63	13.02	18.19	12.52	1.00
Sphericity	0.84	0.14	0.83	0.19	0.84	0.16	1.00
Effective Radius	7.63	4.32	7.73	4.54	7.73	4.42	1.00
<i>Differences</i>							
Mean	0.22	0.04	0.20	0.07	0.21	0.05	0.79
Variance	0.04	0.02	0.02	0.01	0.03	0.01	0.37
Kurtosis	4.21	1.25	3.63	1.04	3.56	1.25	0.65
Skewness	1.13	0.45	0.89	0.27	0.95	0.50	0.66
Range	0.95	0.29	0.73	0.23	0.73	0.18	0.28
Border							
Mean of Slopes	-110.86	40.39	-111.29	48.94	-88.20	48.52	0.67
St. Dev. of Slopes	13.69	6.97	19.76	12.25	12.29	9.02	0.45

Note: P-values from a one-way ANOVA test are also shown with significance at $p < 0.05$, highlighted with ***bolded italics***. Features not computed from segmentation, such as demographic features, have been removed.

Table 2. Continued

Features	Malignant Nodules						P-values
	User 1		User 2		User 3		
Texture	Mean	St. Dev.	Mean	St. Dev.	Mean	St. Dev.	
<i>Mean of Nodule</i>							
TEM 1	3.47	1.12	3.47	1.12	3.47	1.12	1.00
TEM 2	3.40	0.99	3.40	1.00	3.40	1.00	1.00
TEM 3	3.49	1.12	3.49	1.12	3.49	1.12	1.00
TEM 4	3.59	1.23	3.59	1.23	3.59	1.23	1.00
TEM 5	3.44	1.05	3.44	1.05	3.44	1.05	1.00
TEM 6	3.42	1.13	3.42	1.13	3.42	1.13	1.00
TEM 7	3.46	1.25	3.46	1.25	3.46	1.25	1.00
TEM 8	3.39	1.12	3.39	1.12	3.39	1.12	1.00
TEM 9	3.41	1.19	3.41	1.19	3.41	1.19	1.00
TEM 10	3.39	1.15	3.39	1.15	3.39	1.15	1.00
TEM 11	3.36	1.16	3.36	1.16	3.36	1.16	1.00
TEM 12	3.36	1.20	3.36	1.20	3.36	1.20	1.00
TEM 13	3.41	1.25	3.40	1.25	3.41	1.25	1.00
TEM 14	3.36	1.24	3.36	1.24	3.36	1.24	1.00
TEM 15	3.47	0.97	3.47	0.97	3.47	0.97	1.00
TEM 16	3.43	1.11	3.42	1.11	3.43	1.11	1.00
TEM 17	3.38	1.13	3.38	1.13	3.38	1.13	1.00
TEM 18	3.33	1.16	3.33	1.16	3.33	1.16	1.00
TEM 19	3.31	0.93	3.31	0.93	3.31	0.93	1.00
TEM 20	3.35	1.07	3.35	1.07	3.35	1.07	1.00
TEM 21	3.34	1.23	3.34	1.23	3.34	1.23	1.00
TEM 22	3.33	1.06	3.33	1.06	3.33	1.06	1.00
TEM 23	3.37	1.30	3.37	1.30	3.37	1.30	1.00
TEM 24	3.41	1.29	3.41	1.29	3.41	1.29	1.00
TEM 25	3.41	1.31	3.41	1.31	3.41	1.31	1.00
TEM 26	3.38	1.17	3.38	1.17	3.38	1.17	1.00
TEM 27	3.45	1.18	3.45	1.18	3.45	1.18	1.00
TEM 28	3.36	1.24	3.36	1.24	3.36	1.24	1.00
TEM 29	3.37	1.26	3.37	1.26	3.37	1.26	1.00
TEM 30	3.34	1.21	3.34	1.21	3.34	1.21	1.00
TEM 31	3.32	0.76	3.32	0.77	3.32	0.76	1.00
TEM 32	3.35	1.24	3.34	1.24	3.35	1.24	1.00
TEM 33	3.50	1.25	3.50	1.25	3.50	1.25	1.00
TEM 34	3.29	1.27	3.29	1.27	3.29	1.27	1.00

Table 2. Continued

Features	Malignant Nodules						
	User 1		User 2		User 3		P-values
Texture	Mean	St. Dev.	Mean	St. Dev.	Mean	St. Dev.	
<i>Variance of Nodule</i>							
TEM 1	0.01	0.02	0.01	0.02	0.01	0.02	0.98
TEM 2	0.01	0.02	0.01	0.02	0.01	0.02	0.98
TEM 3	0.01	0.02	0.01	0.02	0.01	0.02	0.97
TEM 4	0.01	0.02	0.01	0.02	0.01	0.02	0.97
TEM 5	0.01	0.02	0.01	0.02	0.01	0.02	0.98
TEM 6	0.01	0.02	0.01	0.02	0.01	0.02	0.97
TEM 7	0.01	0.02	0.01	0.02	0.01	0.02	0.97
TEM 8	0.01	0.02	0.01	0.02	0.01	0.02	0.97
TEM 9	0.01	0.02	0.01	0.02	0.01	0.02	0.97
TEM 10	0.01	0.02	0.01	0.02	0.01	0.02	0.97
TEM 11	0.01	0.02	0.01	0.02	0.01	0.02	0.97
TEM 12	0.01	0.02	0.01	0.02	0.01	0.02	0.97
TEM 13	0.01	0.02	0.01	0.02	0.01	0.02	0.97
TEM 14	0.01	0.02	0.01	0.02	0.01	0.02	0.97
TEM 15	0.01	0.02	0.01	0.02	0.01	0.02	0.98
TEM 16	0.01	0.02	0.01	0.02	0.01	0.02	0.97
TEM 17	0.01	0.02	0.01	0.02	0.01	0.02	0.97
TEM 18	0.01	0.02	0.01	0.02	0.01	0.02	0.97
TEM 19	0.01	0.02	0.01	0.02	0.01	0.02	0.98
TEM 20	0.01	0.02	0.01	0.02	0.01	0.02	0.97
TEM 21	0.01	0.02	0.01	0.02	0.01	0.02	0.97
TEM 22	0.01	0.02	0.01	0.02	0.01	0.02	0.97
TEM 23	0.01	0.02	0.01	0.02	0.01	0.02	0.97
TEM 24	0.01	0.02	0.01	0.02	0.01	0.02	0.97
TEM 25	0.01	0.02	0.01	0.02	0.01	0.02	0.97
TEM 26	0.01	0.02	0.01	0.02	0.01	0.02	0.97
TEM 27	0.01	0.02	0.01	0.02	0.01	0.02	0.97
TEM 28	0.01	0.02	0.01	0.02	0.01	0.02	0.97
TEM 29	0.01	0.02	0.01	0.02	0.01	0.02	0.97
TEM 30	0.01	0.02	0.01	0.02	0.01	0.02	0.97
TEM 31	0.01	0.01	0.02	0.02	0.01	0.02	0.98
TEM 32	0.01	0.02	0.01	0.02	0.01	0.02	0.97
TEM 33	0.01	0.02	0.01	0.02	0.01	0.02	0.97
TEM 34	0.01	0.02	0.01	0.02	0.01	0.02	0.97

Table 2. Continued

Features	Malignant Nodules						P-values
	User 1		User 2		User 3		
Texture	Mean	St. Dev.	Mean	St. Dev.	Mean	St. Dev.	
<i>Kurtosis of Nodule</i>							
TEM 1	6554.49	13002.23	7054.95	14072.45	6844.90	13571.32	1.00
TEM 2	6493.46	12965.39	6995.12	14036.25	6783.71	13536.84	1.00
TEM 3	6536.48	13041.58	7061.68	14154.17	6843.05	13649.81	1.00
TEM 4	6746.47	13382.23	7298.00	14556.11	7072.74	14032.33	1.00
TEM 5	6503.50	13028.55	6992.92	14077.62	6784.98	13588.64	1.00
TEM 6	6751.21	13507.57	7286.03	14651.53	7063.12	14133.13	1.00
TEM 7	6873.36	13670.00	7427.93	14857.93	7200.86	14326.86	1.00
TEM 8	6644.94	13201.42	7150.65	14277.71	6934.75	13774.75	1.00
TEM 9	6706.11	13297.91	7232.57	14425.80	7015.17	13913.60	1.00
TEM 10	6487.62	12805.77	6993.85	13891.03	6787.65	13401.03	1.00
TEM 11	6790.66	13608.22	7319.72	14745.85	7099.31	14228.99	1.00
TEM 12	6596.50	13124.91	7119.22	14248.96	6908.10	13749.38	1.00
TEM 13	6787.04	13585.52	7340.30	14780.57	7119.95	14259.31	1.00
TEM 14	6796.45	13564.64	7334.86	14724.36	7114.40	14204.37	1.00
TEM 15	6349.72	12757.68	6811.76	13754.13	6616.41	13286.19	1.00
TEM 16	6596.95	13120.95	7095.34	14180.63	6882.71	13685.69	1.00
TEM 17	6545.25	12979.05	7035.88	14027.61	6825.62	13532.73	1.00
TEM 18	6295.43	12366.51	6805.38	13452.30	6605.13	12980.68	1.00
TEM 19	6604.07	13308.79	7107.69	14395.23	6899.57	13904.51	1.00
TEM 20	6816.58	13706.07	7355.31	14864.52	7132.45	14343.98	1.00
TEM 21	6892.57	13765.32	7444.47	14954.43	7219.30	14424.30	1.00
TEM 22	6682.93	13390.58	7192.33	14485.13	6979.49	13985.31	1.00
TEM 23	6977.65	13988.52	7529.91	15182.98	7302.61	14645.76	1.00
TEM 24	6878.88	13753.96	7431.40	14946.12	7207.44	14417.30	1.00
TEM 25	7011.98	14079.92	7576.14	15301.99	7346.82	14759.24	1.00
TEM 26	6757.67	13543.13	7285.00	14678.72	7065.78	14162.95	1.00
TEM 27	6737.04	13533.04	7295.47	14741.36	7076.18	14222.58	1.00
TEM 28	6301.64	12468.69	6808.85	13555.24	6610.18	13084.81	1.00
TEM 29	6507.41	12981.11	7040.59	14133.77	6833.20	13639.17	1.00
TEM 30	6259.67	12440.17	6775.06	13553.19	6577.12	13080.10	1.00
TEM 31	6423.30	13016.16	6907.91	14067.67	6711.31	13598.09	1.00
TEM 32	6905.05	13806.36	7438.41	14955.24	7215.72	14430.78	1.00
TEM 33	7038.80	14208.91	7619.48	15467.76	7386.84	14919.11	1.00
TEM 34	5506.45	10657.26	5951.44	11617.01	5785.94	11210.30	1.00

Table 2. Continued

Features	Malignant Nodules						P-values
	User 1		User 2		User 3		
Texture	Mean	St. Dev.	Mean	St. Dev.	Mean	St. Dev.	
<i>Skewness of Nodule</i>							
TEM 1	-28.98	75.63	-30.47	78.14	-29.58	77.05	1.00
TEM 2	-28.32	75.59	-29.59	78.27	-28.87	77.05	1.00
TEM 3	-27.75	76.34	-29.02	79.24	-28.38	77.95	1.00
TEM 4	-27.20	78.55	-28.54	81.65	-27.86	80.32	1.00
TEM 5	-28.48	75.61	-29.68	78.20	-29.02	77.00	1.00
TEM 6	-28.09	78.46	-29.33	81.42	-28.70	80.10	1.00
TEM 7	-27.23	79.93	-28.52	83.05	-27.86	81.70	1.00
TEM 8	-26.85	77.55	-27.95	80.30	-27.34	79.01	1.00
TEM 9	-26.59	78.25	-27.78	81.21	-27.14	79.90	1.00
TEM 10	-25.28	76.39	-26.41	79.26	-25.80	78.01	1.00
TEM 11	-27.60	79.08	-28.82	82.00	-28.17	80.70	1.00
TEM 12	-26.28	77.35	-27.48	80.31	-26.86	79.05	1.00
TEM 13	-27.36	79.13	-28.68	82.27	-28.02	80.98	1.00
TEM 14	-27.00	79.30	-28.26	82.31	-27.60	81.01	1.00
TEM 15	-30.51	73.04	-31.83	75.33	-31.10	74.27	1.00
TEM 16	-27.21	76.93	-28.34	79.60	-27.71	78.36	1.00
TEM 17	-26.15	76.66	-27.20	79.33	-26.60	78.07	1.00
TEM 18	-24.22	74.72	-25.38	77.69	-24.80	76.48	1.00
TEM 19	-28.68	76.80	-29.88	79.51	-29.25	78.32	1.00
TEM 20	-28.39	79.16	-29.63	82.15	-28.99	80.84	1.00
TEM 21	-27.08	80.38	-28.38	83.47	-27.71	82.15	1.00
TEM 22	-27.45	78.00	-28.63	80.75	-27.99	79.52	1.00
TEM 23	-27.92	80.92	-29.26	83.95	-28.55	82.64	1.00
TEM 24	-27.61	79.93	-28.92	83.03	-28.25	81.71	1.00
TEM 25	-28.29	81.16	-29.66	84.30	-28.95	82.97	1.00
TEM 26	-27.54	78.75	-28.73	81.68	-28.10	80.38	1.00
TEM 27	-27.76	78.51	-29.13	81.71	-28.46	80.43	1.00
TEM 28	-25.50	74.26	-26.70	77.18	-26.11	75.99	1.00
TEM 29	-26.28	76.44	-27.59	79.51	-26.94	78.29	1.00
TEM 30	-24.98	73.88	-26.28	76.85	-25.64	75.70	1.00
TEM 31	-30.23	74.34	-31.47	76.92	-30.84	75.81	1.00
TEM 32	-27.15	80.45	-28.43	83.33	-27.72	82.06	1.00
TEM 33	-29.33	81.19	-30.73	84.48	-30.05	83.11	1.00
TEM 34	-20.46	65.32	-21.66	67.89	-21.04	66.92	1.00

Table 2. Continued

Features	Malignant Nodules						P-values
	User 1		User 2		User 3		
Texture	Mean	St. Dev.	Mean	St. Dev.	Mean	St. Dev.	
<i>Mean of Parenchyma</i>							
TEM 1	3.47	1.12	3.47	1.12	3.47	1.12	1.00
TEM 2	3.40	0.99	3.40	0.99	3.40	0.99	1.00
TEM 3	3.49	1.12	3.49	1.12	3.49	1.12	1.00
TEM 4	3.59	1.23	3.59	1.23	3.59	1.23	1.00
TEM 5	3.45	1.05	3.45	1.05	3.45	1.05	1.00
TEM 6	3.43	1.13	3.43	1.13	3.43	1.13	1.00
TEM 7	3.46	1.25	3.46	1.25	3.46	1.25	1.00
TEM 8	3.40	1.12	3.40	1.12	3.40	1.12	1.00
TEM 9	3.41	1.19	3.41	1.19	3.41	1.19	1.00
TEM 10	3.40	1.15	3.40	1.15	3.40	1.15	1.00
TEM 11	3.36	1.15	3.36	1.15	3.36	1.15	1.00
TEM 12	3.37	1.20	3.37	1.20	3.37	1.20	1.00
TEM 13	3.41	1.25	3.41	1.25	3.41	1.25	1.00
TEM 14	3.36	1.23	3.36	1.23	3.36	1.23	1.00
TEM 15	3.47	0.97	3.47	0.97	3.47	0.97	1.00
TEM 16	3.43	1.10	3.43	1.10	3.43	1.10	1.00
TEM 17	3.38	1.13	3.38	1.13	3.38	1.13	1.00
TEM 18	3.33	1.16	3.33	1.16	3.33	1.16	1.00
TEM 19	3.31	0.92	3.31	0.92	3.31	0.92	1.00
TEM 20	3.35	1.07	3.35	1.07	3.35	1.07	1.00
TEM 21	3.34	1.23	3.34	1.23	3.34	1.23	1.00
TEM 22	3.34	1.06	3.34	1.06	3.34	1.06	1.00
TEM 23	3.38	1.30	3.38	1.30	3.38	1.30	1.00
TEM 24	3.42	1.29	3.42	1.29	3.42	1.29	1.00
TEM 25	3.41	1.30	3.41	1.30	3.41	1.30	1.00
TEM 26	3.38	1.17	3.38	1.17	3.38	1.17	1.00
TEM 27	3.46	1.18	3.46	1.18	3.46	1.18	1.00
TEM 28	3.36	1.24	3.36	1.24	3.36	1.24	1.00
TEM 29	3.37	1.26	3.37	1.26	3.37	1.26	1.00
TEM 30	3.35	1.21	3.35	1.21	3.35	1.21	1.00
TEM 31	3.32	0.76	3.32	0.76	3.32	0.76	1.00
TEM 32	3.35	1.24	3.35	1.24	3.35	1.24	1.00
TEM 33	3.50	1.25	3.50	1.25	3.50	1.25	1.00
TEM 34	3.29	1.27	3.29	1.27	3.29	1.27	1.00

Table 2. Continued

Features	Malignant Nodules						
	User 1		User 2		User 3		P-values
Texture	Mean	St. Dev.	Mean	St. Dev.	Mean	St. Dev.	
<i>Variance of Parenchyma</i>							
TEM 1	4.6E-07	9.8E-07	1.4E-07	2.6E-07	5.9E-07	1.3E-06	0.74
TEM 2	5.3E-07	1.0E-06	2.1E-07	3.5E-07	6.3E-07	1.3E-06	0.77
TEM 3	9.4E-07	1.4E-06	4.8E-07	6.5E-07	1.1E-06	1.7E-06	0.74
TEM 4	4.0E-06	6.7E-06	3.1E-06	6.2E-06	4.7E-06	8.1E-06	0.94
TEM 5	5.1E-07	1.1E-06	1.8E-07	3.3E-07	6.0E-07	1.3E-06	0.78
TEM 6	7.1E-07	1.5E-06	2.3E-07	4.4E-07	8.6E-07	1.8E-06	0.76
TEM 7	9.6E-07	1.9E-06	3.3E-07	5.3E-07	1.1E-06	2.1E-06	0.74
TEM 8	5.7E-07	1.2E-06	1.9E-07	3.6E-07	6.9E-07	1.5E-06	0.77
TEM 9	6.8E-07	1.2E-06	2.6E-07	3.7E-07	8.1E-07	1.5E-06	0.72
TEM 10	7.2E-07	1.0E-06	3.3E-07	4.7E-07	8.8E-07	1.3E-06	0.68
TEM 11	6.3E-07	1.3E-06	2.3E-07	4.1E-07	7.4E-07	1.6E-06	0.78
TEM 12	5.3E-07	1.1E-06	1.8E-07	3.2E-07	6.4E-07	1.3E-06	0.76
TEM 13	6.1E-07	1.2E-06	2.0E-07	3.4E-07	7.4E-07	1.5E-06	0.74
TEM 14	6.2E-07	1.3E-06	2.0E-07	3.7E-07	7.4E-07	1.6E-06	0.76
TEM 15	6.1E-07	1.3E-06	2.1E-07	3.9E-07	7.6E-07	1.6E-06	0.77
TEM 16	4.3E-07	9.1E-07	1.5E-07	2.8E-07	5.2E-07	1.1E-06	0.78
TEM 17	5.0E-07	9.8E-07	1.8E-07	3.1E-07	6.1E-07	1.2E-06	0.76
TEM 18	1.7E-06	2.6E-06	1.0E-06	1.9E-06	2.1E-06	3.2E-06	0.80
TEM 19	6.1E-07	1.2E-06	2.5E-07	4.1E-07	7.1E-07	1.4E-06	0.79
TEM 20	6.9E-07	1.4E-06	2.5E-07	4.6E-07	8.3E-07	1.7E-06	0.78
TEM 21	7.1E-07	1.5E-06	2.4E-07	4.5E-07	8.4E-07	1.8E-06	0.77
TEM 22	6.0E-07	1.2E-06	2.4E-07	4.0E-07	6.9E-07	1.4E-06	0.79
TEM 23	6.6E-07	1.4E-06	2.3E-07	4.1E-07	7.8E-07	1.6E-06	0.77
TEM 24	6.5E-07	1.4E-06	2.0E-07	3.7E-07	7.8E-07	1.6E-06	0.75
TEM 25	5.6E-07	1.2E-06	1.9E-07	3.4E-07	6.7E-07	1.4E-06	0.76
TEM 26	5.2E-07	1.1E-06	1.9E-07	3.5E-07	6.2E-07	1.3E-06	0.78
TEM 27	6.2E-07	1.2E-06	2.2E-07	3.1E-07	7.8E-07	1.5E-06	0.71
TEM 28	6.4E-07	1.1E-06	2.3E-07	3.3E-07	7.7E-07	1.4E-06	0.71
TEM 29	7.3E-07	1.4E-06	2.5E-07	3.6E-07	9.1E-07	1.7E-06	0.70
TEM 30	8.3E-07	1.4E-06	3.0E-07	4.1E-07	1.1E-06	1.8E-06	0.67
TEM 31	8.3E-07	1.7E-06	3.2E-07	5.3E-07	1.0E-06	2.1E-06	0.77
TEM 32	6.8E-07	1.4E-06	2.5E-07	4.3E-07	7.7E-07	1.6E-06	0.79
TEM 33	5.1E-07	1.0E-06	1.8E-07	3.0E-07	6.3E-07	1.3E-06	0.75
TEM 34	1.1E-06	1.6E-06	4.3E-07	6.8E-07	1.3E-06	2.0E-06	0.64

Table 2. Continued

Features	Malignant Nodules						
	User 1		User 2		User 3		P-values
Texture	Mean	St. Dev.	Mean	St. Dev.	Mean	St. Dev.	
<i>Kurtosis of Parenchyma</i>							
TEM 1	237.41	469.86	137.68	203.47	184.95	379.00	0.91
TEM 2	189.34	381.65	117.75	184.91	160.33	346.12	0.94
TEM 3	189.00	414.61	90.02	187.70	170.28	373.96	0.89
TEM 4	157.14	344.22	71.30	152.34	152.49	333.81	0.87
TEM 5	207.24	409.18	140.79	203.64	176.67	373.93	0.95
TEM 6	220.40	438.84	138.20	206.96	184.58	396.56	0.94
TEM 7	183.76	389.22	95.04	174.71	174.85	379.80	0.90
TEM 8	225.43	441.51	137.51	209.33	185.90	398.82	0.93
TEM 9	199.78	419.37	103.65	189.30	180.17	389.26	0.90
TEM 10	205.45	436.80	99.15	193.16	180.48	382.85	0.88
TEM 11	216.88	413.96	156.80	228.40	179.89	380.95	0.96
TEM 12	221.65	424.64	134.76	202.97	178.53	383.25	0.93
TEM 13	235.99	454.59	139.50	210.73	187.99	403.88	0.92
TEM 14	221.15	429.53	140.64	205.83	184.75	397.85	0.94
TEM 15	215.49	431.23	138.23	198.89	176.01	367.80	0.94
TEM 16	210.86	410.04	139.00	205.28	177.82	375.48	0.95
TEM 17	214.51	425.85	129.81	207.26	173.97	374.99	0.93
TEM 18	210.63	451.80	95.69	192.60	184.02	391.39	0.87
TEM 19	196.83	392.96	160.59	225.31	169.51	362.92	0.98
TEM 20	210.46	413.49	153.72	221.05	175.28	375.05	0.97
TEM 21	203.20	398.86	132.91	193.18	172.07	371.81	0.95
TEM 22	198.42	385.67	163.58	231.28	171.53	364.59	0.99
TEM 23	222.31	411.94	156.08	226.00	182.12	380.13	0.96
TEM 24	233.91	451.65	144.02	214.00	191.74	412.25	0.93
TEM 25	228.54	415.75	153.21	223.69	179.54	372.94	0.94
TEM 26	222.70	414.42	150.18	221.51	175.78	370.17	0.95
TEM 27	246.57	483.48	138.54	213.71	192.72	415.73	0.91
TEM 28	214.13	427.51	120.07	193.24	178.68	384.73	0.91
TEM 29	233.06	469.60	120.51	196.20	188.75	408.04	0.89
TEM 30	244.75	516.57	116.97	206.30	198.50	432.82	0.88
TEM 31	219.63	450.41	161.17	225.91	184.45	396.46	0.97
TEM 32	203.00	380.23	157.03	222.10	174.05	365.39	0.98
TEM 33	239.49	430.03	153.66	224.56	180.47	376.28	0.93
TEM 34	243.87	533.16	98.37	201.51	202.49	443.01	0.85

Table 2. Continued

Features	Malignant Nodules						
	User 1		User 2		User 3		P-values
Texture	Mean	St. Dev.	Mean	St. Dev.	Mean	St. Dev.	
<i>Skewness of Parenchyma</i>							
TEM 1	3.82	14.83	0.48	10.59	3.79	13.06	0.90
TEM 2	3.71	12.84	0.83	9.26	4.18	11.70	0.88
TEM 3	4.84	12.52	2.44	7.69	4.62	11.94	0.93
TEM 4	4.24	11.54	1.97	6.50	4.10	11.26	0.92
TEM 5	3.44	13.72	0.23	10.60	3.94	12.55	0.88
TEM 6	3.79	14.03	0.63	10.49	4.39	12.70	0.88
TEM 7	4.10	12.73	1.54	8.08	4.26	12.29	0.91
TEM 8	3.78	14.18	0.82	10.51	4.50	12.71	0.89
TEM 9	4.19	13.27	1.62	8.67	4.31	12.59	0.92
TEM 10	4.24	13.52	1.73	8.52	3.96	12.79	0.93
TEM 11	3.36	14.03	0.52	11.36	4.18	12.55	0.89
TEM 12	3.55	14.12	0.82	10.30	4.40	12.49	0.89
TEM 13	3.80	14.63	0.90	10.60	4.59	12.91	0.89
TEM 14	3.72	14.08	0.69	10.56	4.63	12.62	0.87
TEM 15	3.57	13.99	0.15	10.48	3.72	12.62	0.88
TEM 16	3.44	13.84	0.43	10.59	4.05	12.57	0.89
TEM 17	3.83	13.80	1.13	10.08	4.33	12.36	0.91
TEM 18	4.35	13.80	1.78	8.39	3.99	13.05	0.94
TEM 19	3.52	13.27	0.22	11.27	4.06	12.14	0.87
TEM 20	3.58	13.70	0.47	11.08	4.25	12.31	0.88
TEM 21	3.68	13.41	0.63	10.08	4.50	12.09	0.87
TEM 22	3.29	13.42	0.24	11.46	4.00	12.25	0.88
TEM 23	3.23	14.34	0.50	11.48	4.17	12.71	0.90
TEM 24	3.87	14.54	0.89	10.82	4.77	12.95	0.88
TEM 25	3.25	14.55	0.65	11.40	4.23	12.62	0.90
TEM 26	3.30	14.19	0.68	11.16	4.22	12.36	0.90
TEM 27	4.02	15.01	0.98	10.57	4.66	13.19	0.89
TEM 28	3.74	13.93	1.01	9.53	4.29	12.66	0.90
TEM 29	4.13	14.54	1.13	9.56	4.60	13.06	0.90
TEM 30	4.91	14.88	1.70	9.39	4.99	13.44	0.90
TEM 31	3.95	13.99	0.21	11.35	4.24	12.77	0.86
TEM 32	3.06	13.72	0.19	11.34	3.94	12.42	0.89
TEM 33	3.23	14.92	0.65	11.43	4.25	12.72	0.91
TEM 34	5.48	15.01	2.33	8.48	5.08	13.82	0.91

Table 3. Means and standard deviations (St. Dev.) for features computed using three users' manual segmentations from benign nodules.

Features	Benign Nodules						
	User 1		User 2		User 3		P-values
	Mean	St. Dev.	Mean	St. Dev.	Mean	St. Dev.	
Intensity							
<i>Nodule</i>							
Mean HU	-106.17	324.30	-162.05	360.29	-111.82	362.64	0.95
Variance	160988.8	287654.9	167735.1	273606.6	158104.3	267994.4	1.00
Maximum HU	496.57	870.65	496.57	870.65	496.57	870.65	1.00
Minimum HU	-788.71	102.09	-827.86	83.73	-757.29	59.21	0.31
Median HU	-133.50	237.67	-205.21	279.93	-133.29	279.81	0.85
FWHM	0.02	0.01	0.02	0.01	0.02	0.01	0.87
Entropy	8.08	0.67	8.31	0.55	8.13	0.63	0.76
Kurtosis	2.05	0.21	1.88	0.11	1.97	0.13	0.16
Skewness	-0.10	0.35	0.11	0.27	-0.07	0.33	0.44
<i>Parenchyma</i>							
Mean HU	-894.42	26.41	-901.36	24.15	-892.21	22.88	0.77
Variance	9429.77	6315.45	6580.69	4317.94	9943.43	6868.90	0.53
Maximum HU	-160.43	394.97	-298.43	206.60	-164.29	386.82	0.69
Minimum HU	-1020.57	9.07	-1020.57	9.07	-1020.57	9.07	1.00
Median HU	-914.14	21.38	-916.00	21.10	-913.57	20.68	0.97
FWHM	0.08	0.05	0.08	0.06	0.07	0.05	0.88
Entropy	7.97	0.39	7.87	0.39	7.98	0.32	0.81
Kurtosis	12.41	4.77	8.92	1.44	10.46	2.25	0.14
Skewness	2.42	0.56	1.84	0.27	2.20	0.41	0.06
Shape							
Recist Diameter	5.51	0.78	6.14	0.93	6.00	0.76	0.35
Sphericity	1.21	0.07	1.22	0.07	1.24	0.04	0.70
Effective Radius	2.78	0.50	2.95	0.46	2.81	0.43	0.77
<i>Differences</i>							
Mean	0.15	0.05	0.14	0.05	0.14	0.02	0.78
Variance	0.02	0.01	0.02	0.02	0.01	0.00	0.53
Kurtosis	3.72	0.93	4.63	2.47	2.91	0.77	0.16
Skewness	0.96	0.36	1.19	0.70	0.69	0.31	0.19
Range	0.57	0.25	0.60	0.36	0.43	0.09	0.42
Border							
Mean of Slopes	-319.99	124.11	-238.55	114.49	-286.50	114.81	0.45
Variance of Slopes	15.92	9.72	19.22	10.33	14.15	11.64	0.67

P-values from a one-way ANOVA test are also shown with significance at $p < 0.05$, highlighted with bolded italics. Features not computed from segmentation, such as demographic features, have been removed.

Table 3. Continued

Features	Benign Nodules						
	User 1		User 2		User 3		P-values
Texture	Mean	St. Dev.	Mean	St. Dev.	Mean	St. Dev.	
<i>Mean of Nodule</i>							
TEM 1	4.71	1.45	4.72	1.46	4.71	1.45	1.00
TEM 2	4.70	1.45	4.71	1.45	4.70	1.45	1.00
TEM 3	4.67	1.48	4.68	1.49	4.68	1.48	1.00
TEM 4	4.68	1.50	4.69	1.51	4.68	1.50	1.00
TEM 5	4.77	1.41	4.78	1.42	4.77	1.41	1.00
TEM 6	4.77	1.42	4.78	1.43	4.77	1.42	1.00
TEM 7	4.74	1.46	4.75	1.46	4.74	1.46	1.00
TEM 8	4.75	1.42	4.76	1.43	4.75	1.42	1.00
TEM 9	4.72	1.45	4.74	1.46	4.72	1.45	1.00
TEM 10	4.73	1.43	4.74	1.44	4.73	1.43	1.00
TEM 11	4.77	1.43	4.78	1.43	4.77	1.43	1.00
TEM 12	4.75	1.45	4.76	1.46	4.75	1.45	1.00
TEM 13	4.75	1.44	4.77	1.45	4.75	1.44	1.00
TEM 14	4.75	1.46	4.76	1.47	4.75	1.46	1.00
TEM 15	4.74	1.43	4.75	1.44	4.74	1.43	1.00
TEM 16	4.75	1.42	4.77	1.43	4.76	1.42	1.00
TEM 17	4.74	1.43	4.75	1.43	4.74	1.42	1.00
TEM 18	4.73	1.43	4.74	1.44	4.73	1.43	1.00
TEM 19	4.78	1.42	4.79	1.43	4.78	1.42	1.00
TEM 20	4.79	1.41	4.80	1.42	4.79	1.41	1.00
TEM 21	4.75	1.46	4.76	1.46	4.75	1.46	1.00
TEM 22	4.76	1.44	4.77	1.45	4.76	1.44	1.00
TEM 23	4.77	1.43	4.78	1.43	4.77	1.43	1.00
TEM 24	4.75	1.45	4.76	1.46	4.75	1.45	1.00
TEM 25	4.77	1.42	4.79	1.43	4.78	1.42	1.00
TEM 26	4.77	1.43	4.78	1.43	4.77	1.43	1.00
TEM 27	4.77	1.42	4.78	1.42	4.77	1.41	1.00
TEM 28	4.73	1.45	4.74	1.46	4.73	1.45	1.00
TEM 29	4.74	1.44	4.75	1.45	4.74	1.44	1.00
TEM 30	4.76	1.40	4.78	1.41	4.77	1.40	1.00
TEM 31	4.80	1.40	4.81	1.40	4.80	1.40	1.00
TEM 32	4.76	1.44	4.77	1.45	4.76	1.44	1.00
TEM 33	4.78	1.40	4.79	1.41	4.78	1.40	1.00
TEM 34	4.77	1.38	4.78	1.39	4.77	1.38	1.00

Table 3. Continued

Features	Benign Nodules						
	User 1		User 2		User 3		P-values
Texture <i>Variance of Nodule</i>	Mean	St. Dev.	Mean	St. Dev.	Mean	St. Dev.	
TEM 1	0.13	0.07	0.11	0.05	0.13	0.07	0.75
TEM 2	0.13	0.07	0.11	0.05	0.13	0.08	0.76
TEM 3	0.13	0.07	0.11	0.05	0.13	0.07	0.75
TEM 4	0.13	0.07	0.11	0.05	0.13	0.07	0.76
TEM 5	0.13	0.07	0.11	0.05	0.13	0.07	0.75
TEM 6	0.13	0.07	0.11	0.05	0.13	0.08	0.76
TEM 7	0.13	0.07	0.11	0.05	0.13	0.07	0.75
TEM 8	0.14	0.07	0.11	0.05	0.13	0.08	0.76
TEM 9	0.13	0.07	0.11	0.05	0.13	0.07	0.75
TEM 10	0.14	0.07	0.11	0.05	0.14	0.07	0.75
TEM 11	0.13	0.07	0.11	0.05	0.13	0.07	0.75
TEM 12	0.14	0.07	0.11	0.05	0.14	0.07	0.75
TEM 13	0.14	0.07	0.11	0.05	0.14	0.07	0.74
TEM 14	0.14	0.07	0.11	0.05	0.13	0.07	0.75
TEM 15	0.13	0.07	0.11	0.05	0.13	0.07	0.75
TEM 16	0.14	0.07	0.11	0.05	0.13	0.07	0.75
TEM 17	0.14	0.07	0.11	0.05	0.13	0.08	0.76
TEM 18	0.14	0.07	0.11	0.05	0.14	0.07	0.75
TEM 19	0.13	0.07	0.11	0.05	0.13	0.07	0.75
TEM 20	0.13	0.07	0.11	0.05	0.13	0.07	0.75
TEM 21	0.13	0.07	0.11	0.05	0.13	0.07	0.74
TEM 22	0.14	0.07	0.11	0.05	0.13	0.08	0.75
TEM 23	0.14	0.07	0.11	0.05	0.14	0.07	0.75
TEM 24	0.14	0.07	0.11	0.05	0.14	0.07	0.74
TEM 25	0.14	0.07	0.11	0.05	0.14	0.07	0.74
TEM 26	0.13	0.07	0.11	0.05	0.13	0.07	0.75
TEM 27	0.14	0.07	0.11	0.05	0.14	0.07	0.74
TEM 28	0.14	0.07	0.11	0.05	0.14	0.07	0.74
TEM 29	0.14	0.07	0.11	0.05	0.14	0.07	0.74
TEM 30	0.14	0.07	0.11	0.05	0.14	0.07	0.74
TEM 31	0.13	0.07	0.11	0.05	0.13	0.07	0.75
TEM 32	0.14	0.07	0.11	0.05	0.14	0.08	0.75
TEM 33	0.14	0.07	0.11	0.05	0.14	0.08	0.75
TEM 34	0.14	0.07	0.11	0.05	0.14	0.08	0.75

Table 3. Continued

Features	Benign Nodules						
	User 1		User 2		User 3		P-values
Texture <i>Kurtosis of Nodule</i>	Mean	St. Dev.	Mean	St. Dev.	Mean	St. Dev.	
TEM 1	176.82	97.08	208.04	119.35	186.37	123.35	0.87
TEM 2	177.00	96.11	207.27	117.44	185.68	121.38	0.87
TEM 3	183.02	97.58	214.20	119.23	192.49	125.16	0.87
TEM 4	182.45	101.30	214.47	125.68	192.87	132.18	0.88
TEM 5	179.62	94.52	209.45	113.99	187.71	118.37	0.87
TEM 6	181.18	94.98	211.35	115.01	189.78	120.16	0.87
TEM 7	179.94	98.71	211.04	122.00	189.68	127.81	0.88
TEM 8	177.51	95.46	207.56	116.32	186.08	120.50	0.87
TEM 9	175.32	98.22	206.24	121.37	185.01	126.06	0.88
TEM 10	171.91	97.35	202.36	119.83	181.27	123.33	0.88
TEM 11	180.15	96.09	211.05	117.57	189.33	122.51	0.87
TEM 12	176.56	100.10	208.47	123.88	187.19	129.22	0.88
TEM 13	174.15	99.30	205.68	122.96	184.47	127.77	0.88
TEM 14	178.30	100.19	210.30	124.31	189.04	130.22	0.88
TEM 15	176.85	95.37	207.77	116.98	186.13	121.45	0.87
TEM 16	178.67	95.27	208.24	114.97	186.56	119.16	0.87
TEM 17	174.71	96.49	204.81	117.99	183.56	121.43	0.88
TEM 18	171.04	97.27	201.86	120.02	180.79	123.68	0.88
TEM 19	183.92	95.22	214.44	114.69	192.42	120.06	0.87
TEM 20	183.51	94.47	214.19	114.29	192.04	119.33	0.87
TEM 21	179.96	99.77	211.78	123.61	190.35	129.59	0.88
TEM 22	181.32	96.98	212.09	118.14	190.47	123.59	0.87
TEM 23	176.89	96.79	207.72	119.15	186.28	123.72	0.87
TEM 24	175.49	100.45	207.19	124.68	186.11	129.98	0.88
TEM 25	175.65	96.67	206.71	119.02	185.25	123.47	0.87
TEM 26	179.14	96.62	210.31	118.40	188.60	123.15	0.87
TEM 27	172.10	97.48	203.33	119.93	181.97	123.68	0.87
TEM 28	172.67	100.44	204.40	124.23	183.17	128.56	0.88
TEM 29	172.31	98.89	203.57	122.44	182.36	126.69	0.88
TEM 30	170.39	95.45	201.09	117.15	179.65	119.87	0.87
TEM 31	184.30	91.63	214.99	110.56	192.69	116.13	0.86
TEM 32	178.98	98.11	209.97	120.68	188.57	126.00	0.88
TEM 33	172.86	96.30	203.95	117.99	182.54	121.62	0.87
TEM 34	168.54	93.86	198.73	114.72	177.38	116.23	0.87

Table 3. Continued

Features	Benign Nodules						
	User 1		User 2		User 3		P-values
Texture <i>Skewness of Nodule</i>	Mean	St. Dev.	Mean	St. Dev.	Mean	St. Dev.	
TEM 1	-7.24	9.74	-7.59	10.75	-6.63	10.39	0.98
TEM 2	-7.28	9.64	-7.61	10.62	-6.65	10.25	0.98
TEM 3	-7.22	10.00	-7.56	11.04	-6.59	10.69	0.98
TEM 4	-7.01	10.28	-7.33	11.38	-6.36	11.04	0.99
TEM 5	-7.42	9.62	-7.75	10.57	-6.79	10.22	0.98
TEM 6	-7.44	9.74	-7.76	10.71	-6.80	10.37	0.98
TEM 7	-7.21	10.05	-7.51	11.09	-6.54	10.75	0.99
TEM 8	-7.34	9.64	-7.65	10.61	-6.70	10.25	0.98
TEM 9	-7.11	9.83	-7.42	10.86	-6.46	10.51	0.98
TEM 10	-7.08	9.61	-7.41	10.61	-6.46	10.24	0.98
TEM 11	-7.37	9.81	-7.70	10.81	-6.74	10.47	0.98
TEM 12	-7.12	10.01	-7.46	11.06	-6.49	10.72	0.99
TEM 13	-7.10	9.89	-7.43	10.93	-6.47	10.58	0.99
TEM 14	-7.14	10.09	-7.47	11.16	-6.50	10.83	0.99
TEM 15	-7.23	9.66	-7.59	10.67	-6.63	10.31	0.98
TEM 16	-7.36	9.63	-7.67	10.57	-6.71	10.21	0.98
TEM 17	-7.23	9.59	-7.56	10.57	-6.61	10.20	0.98
TEM 18	-7.04	9.63	-7.39	10.64	-6.44	10.27	0.98
TEM 19	-7.52	9.80	-7.85	10.77	-6.88	10.43	0.98
TEM 20	-7.57	9.76	-7.91	10.73	-6.93	10.38	0.98
TEM 21	-7.21	10.11	-7.52	11.17	-6.55	10.84	0.99
TEM 22	-7.33	9.90	-7.66	10.90	-6.69	10.57	0.98
TEM 23	-7.24	9.79	-7.57	10.80	-6.61	10.45	0.98
TEM 24	-7.06	10.01	-7.39	11.07	-6.43	10.73	0.99
TEM 25	-7.23	9.75	-7.56	10.76	-6.60	10.40	0.98
TEM 26	-7.35	9.81	-7.69	10.82	-6.72	10.47	0.98
TEM 27	-7.20	9.63	-7.54	10.63	-6.59	10.27	0.98
TEM 28	-7.02	9.88	-7.36	10.93	-6.40	10.57	0.98
TEM 29	-7.06	9.80	-7.40	10.83	-6.44	10.47	0.98
TEM 30	-7.23	9.42	-7.58	10.39	-6.63	10.01	0.98
TEM 31	-7.66	9.61	-8.02	10.57	-7.05	10.23	0.98
TEM 32	-7.22	9.96	-7.54	10.98	-6.57	10.64	0.98
TEM 33	-7.26	9.56	-7.61	10.54	-6.65	10.18	0.98
TEM 34	-7.30	9.15	-7.66	10.08	-6.72	9.68	0.98

Table 3. Continued

Features	Benign Nodules						
	User 1		User 2		User 3		P-values
Texture <i>Mean of Parenchyma</i>	Mean	St. Dev.	Mean	St. Dev.	Mean	St. Dev.	
TEM 1	4.78	1.50	4.78	1.50	4.78	1.50	1.00
TEM 2	4.76	1.49	4.76	1.49	4.76	1.49	1.00
TEM 3	4.72	1.52	4.72	1.52	4.73	1.52	1.00
TEM 4	4.70	1.52	4.70	1.52	4.71	1.52	1.00
TEM 5	4.84	1.47	4.84	1.47	4.84	1.47	1.00
TEM 6	4.84	1.47	4.84	1.47	4.84	1.47	1.00
TEM 7	4.81	1.50	4.81	1.50	4.81	1.50	1.00
TEM 8	4.82	1.47	4.82	1.47	4.82	1.47	1.00
TEM 9	4.79	1.50	4.79	1.50	4.79	1.50	1.00
TEM 10	4.80	1.48	4.80	1.48	4.80	1.48	1.00
TEM 11	4.84	1.48	4.84	1.48	4.84	1.48	1.00
TEM 12	4.82	1.50	4.82	1.50	4.82	1.50	1.00
TEM 13	4.83	1.49	4.83	1.49	4.83	1.49	1.00
TEM 14	4.82	1.51	4.82	1.51	4.82	1.51	1.00
TEM 15	4.82	1.48	4.82	1.48	4.82	1.48	1.00
TEM 16	4.83	1.47	4.83	1.47	4.83	1.47	1.00
TEM 17	4.81	1.48	4.81	1.48	4.81	1.48	1.00
TEM 18	4.79	1.48	4.79	1.48	4.79	1.48	1.00
TEM 19	4.85	1.47	4.85	1.47	4.85	1.47	1.00
TEM 20	4.86	1.46	4.86	1.46	4.86	1.46	1.00
TEM 21	4.83	1.51	4.83	1.51	4.83	1.51	1.00
TEM 22	4.83	1.49	4.83	1.49	4.83	1.49	1.00
TEM 23	4.84	1.48	4.84	1.48	4.84	1.48	1.00
TEM 24	4.82	1.50	4.82	1.50	4.82	1.50	1.00
TEM 25	4.85	1.47	4.85	1.47	4.85	1.47	1.00
TEM 26	4.84	1.48	4.84	1.48	4.84	1.48	1.00
TEM 27	4.84	1.47	4.84	1.47	4.84	1.47	1.00
TEM 28	4.80	1.50	4.80	1.50	4.80	1.50	1.00
TEM 29	4.81	1.49	4.81	1.49	4.81	1.49	1.00
TEM 30	4.84	1.45	4.84	1.45	4.84	1.45	1.00
TEM 31	4.87	1.45	4.87	1.45	4.87	1.45	1.00
TEM 32	4.84	1.49	4.84	1.49	4.84	1.49	1.00
TEM 33	4.85	1.45	4.85	1.45	4.85	1.45	1.00
TEM 34	4.84	1.43	4.84	1.43	4.84	1.43	1.00

Table 3. Continued

Features	Benign Nodules						
	User 1		User 2		User 3		P-values
Texture <i>Variance of Parenchyma</i>	Mean	St. Dev.	Mean	St. Dev.	Mean	St. Dev.	
TEM 1	2.4E-05	5.3E-05	3.0E-05	6.9E-05	2.6E-05	6.0E-05	0.98
TEM 2	6.9E-05	1.5E-04	8.6E-05	1.9E-04	7.5E-05	1.7E-04	0.98
TEM 3	2.2E-04	3.5E-04	2.6E-04	4.6E-04	2.2E-04	4.0E-04	0.98
TEM 4	9.9E-04	1.0E-03	1.0E-03	1.0E-03	8.2E-04	7.4E-04	0.91
TEM 5	7.7E-05	1.9E-04	9.7E-05	2.4E-04	8.5E-05	2.1E-04	0.98
TEM 6	9.3E-05	2.2E-04	1.2E-04	2.8E-04	1.0E-04	2.5E-04	0.98
TEM 7	1.6E-04	3.0E-04	1.9E-04	3.9E-04	1.7E-04	3.4E-04	0.98
TEM 8	1.0E-04	2.3E-04	1.3E-04	3.0E-04	1.1E-04	2.6E-04	0.98
TEM 9	1.6E-04	3.0E-04	1.9E-04	3.9E-04	1.6E-04	3.4E-04	0.98
TEM 10	1.9E-04	2.6E-04	2.1E-04	3.1E-04	1.5E-04	2.7E-04	0.93
TEM 11	5.9E-05	1.3E-04	7.3E-05	1.7E-04	6.5E-05	1.5E-04	0.98
TEM 12	7.0E-05	1.5E-04	8.7E-05	2.0E-04	7.5E-05	1.8E-04	0.98
TEM 13	6.1E-05	1.3E-04	7.6E-05	1.7E-04	6.6E-05	1.5E-04	0.98
TEM 14	7.5E-05	1.7E-04	9.4E-05	2.2E-04	8.2E-05	1.9E-04	0.98
TEM 15	5.3E-05	1.3E-04	6.7E-05	1.7E-04	5.9E-05	1.5E-04	0.98
TEM 16	9.6E-05	2.3E-04	1.2E-04	3.0E-04	1.1E-04	2.6E-04	0.98
TEM 17	1.0E-04	2.1E-04	1.3E-04	2.8E-04	1.1E-04	2.4E-04	0.98
TEM 18	3.0E-04	3.1E-04	3.0E-04	3.2E-04	2.1E-04	2.3E-04	0.80
TEM 19	6.9E-05	1.6E-04	8.7E-05	2.1E-04	7.7E-05	1.8E-04	0.98
TEM 20	6.4E-05	1.5E-04	8.1E-05	1.9E-04	7.1E-05	1.6E-04	0.98
TEM 21	8.6E-05	2.0E-04	1.1E-04	2.6E-04	9.4E-05	2.2E-04	0.98
TEM 22	6.6E-05	1.5E-04	8.2E-05	1.9E-04	7.3E-05	1.6E-04	0.98
TEM 23	6.1E-05	1.3E-04	7.5E-05	1.7E-04	6.7E-05	1.5E-04	0.98
TEM 24	6.8E-05	1.5E-04	8.5E-05	2.0E-04	7.4E-05	1.7E-04	0.98
TEM 25	5.3E-05	1.1E-04	6.5E-05	1.4E-04	5.8E-05	1.3E-04	0.98
TEM 26	5.3E-05	1.1E-04	6.5E-05	1.5E-04	5.8E-05	1.3E-04	0.98
TEM 27	5.6E-05	1.1E-04	6.8E-05	1.4E-04	5.8E-05	1.2E-04	0.98
TEM 28	9.0E-05	1.9E-04	1.1E-04	2.5E-04	9.4E-05	2.2E-04	0.98
TEM 29	7.6E-05	1.5E-04	9.3E-05	2.0E-04	7.8E-05	1.7E-04	0.98
TEM 30	6.3E-05	1.2E-04	7.7E-05	1.6E-04	6.4E-05	1.4E-04	0.98
TEM 31	6.7E-05	1.6E-04	8.5E-05	2.0E-04	7.5E-05	1.8E-04	0.98
TEM 32	6.6E-05	1.4E-04	8.1E-05	1.8E-04	7.2E-05	1.6E-04	0.98
TEM 33	4.8E-05	9.3E-05	5.7E-05	1.2E-04	5.2E-05	1.0E-04	0.99
TEM 34	7.0E-05	1.2E-04	8.3E-05	1.6E-04	7.3E-05	1.4E-04	0.98

Table 3. Continued

Features	Benign Nodules						
	User 1		User 2		User 3		P-values
Texture <i>Kurtosis of Parenchyma</i>	Mean	St. Dev.	Mean	St. Dev.	Mean	St. Dev.	
TEM 1	50.30	124.35	39.50	96.03	45.06	110.51	0.98
TEM 2	50.32	125.42	39.61	96.86	45.19	111.47	0.98
TEM 3	50.12	125.35	39.33	96.69	45.01	111.33	0.98
TEM 4	50.69	127.61	39.77	98.52	45.68	113.46	0.98
TEM 5	48.58	119.85	38.36	92.99	43.37	106.78	0.98
TEM 6	48.71	118.98	38.43	92.17	43.76	105.78	0.98
TEM 7	49.34	119.98	38.95	92.89	45.07	106.37	0.98
TEM 8	49.48	119.66	39.05	92.68	44.70	106.32	0.98
TEM 9	50.95	122.88	40.19	95.02	47.28	108.70	0.98
TEM 10	51.02	122.03	40.32	94.26	48.35	107.66	0.98
TEM 11	49.34	122.71	38.86	94.96	44.20	109.18	0.98
TEM 12	51.47	122.90	40.62	94.84	48.47	108.45	0.98
TEM 13	53.26	129.21	41.97	99.56	49.19	114.30	0.98
TEM 14	51.28	123.09	40.43	95.07	47.18	108.98	0.98
TEM 15	49.00	120.60	38.78	93.47	43.85	107.36	0.98
TEM 16	49.25	120.44	38.99	93.45	43.94	107.35	0.98
TEM 17	50.06	120.63	39.41	93.27	45.88	106.87	0.98
TEM 18	52.67	124.97	41.52	96.66	49.77	110.53	0.98
TEM 19	49.06	120.90	38.79	93.76	43.90	107.71	0.98
TEM 20	49.30	121.85	38.96	94.34	44.22	108.42	0.98
TEM 21	50.04	120.02	39.65	92.78	45.47	106.47	0.98
TEM 22	49.06	121.55	38.73	94.22	43.94	108.23	0.98
TEM 23	50.49	125.55	39.64	97.08	45.19	111.73	0.98
TEM 24	53.17	129.13	41.94	99.54	48.86	114.32	0.98
TEM 25	51.14	125.84	40.11	97.24	45.54	112.08	0.98
TEM 26	49.56	122.15	38.98	94.45	44.09	108.78	0.98
TEM 27	52.56	127.59	41.40	98.32	47.76	113.13	0.98
TEM 28	53.09	125.39	41.93	96.66	50.39	110.58	0.98
TEM 29	54.58	132.28	43.10	101.76	49.79	117.18	0.98
TEM 30	53.95	130.77	42.49	100.67	48.75	116.01	0.98
TEM 31	49.72	122.11	39.37	94.69	44.44	108.82	0.98
TEM 32	49.65	123.44	39.10	95.60	44.50	109.85	0.98
TEM 33	50.57	123.40	39.65	95.36	45.30	109.80	0.98
TEM 34	55.69	134.91	43.40	104.02	50.06	119.84	0.98

Table 3. Continued

Features	Benign Nodules						
	User 1		User 2		User 3		P-values
Texture <i>Skewness of Parenchyma</i>	Mean	St. Dev.	Mean	St. Dev.	Mean	St. Dev.	
TEM 1	1.71	6.37	1.44	5.64	1.54	6.04	1.00
TEM 2	1.89	6.33	1.57	5.62	1.66	6.03	0.99
TEM 3	2.02	6.27	1.70	5.56	1.78	5.97	0.99
TEM 4	2.21	6.29	1.91	5.56	1.94	6.02	0.99
TEM 5	1.57	6.19	1.35	5.50	1.53	5.83	1.00
TEM 6	1.44	6.23	1.21	5.54	1.38	5.88	1.00
TEM 7	1.33	6.33	1.10	5.63	1.12	6.06	1.00
TEM 8	1.27	6.35	1.05	5.64	1.20	5.99	1.00
TEM 9	1.19	6.54	0.97	5.82	0.94	6.31	1.00
TEM 10	1.05	6.59	0.82	5.87	0.69	6.44	0.99
TEM 11	1.92	6.20	1.67	5.49	1.78	5.87	1.00
TEM 12	1.47	6.51	1.19	5.79	1.15	6.31	0.99
TEM 13	1.70	6.68	1.42	5.93	1.47	6.40	1.00
TEM 14	1.58	6.45	1.30	5.73	1.36	6.15	1.00
TEM 15	1.46	6.27	1.22	5.58	1.37	5.93	1.00
TEM 16	1.45	6.28	1.20	5.60	1.48	5.89	1.00
TEM 17	1.19	6.45	0.98	5.72	1.01	6.16	1.00
TEM 18	0.92	6.78	0.72	6.03	0.61	6.60	1.00
TEM 19	1.55	6.27	1.31	5.58	1.47	5.92	1.00
TEM 20	1.72	6.25	1.46	5.55	1.59	5.92	1.00
TEM 21	1.48	6.33	1.18	5.64	1.33	5.99	1.00
TEM 22	1.73	6.22	1.50	5.53	1.61	5.89	1.00
TEM 23	2.02	6.29	1.77	5.56	1.90	5.94	1.00
TEM 24	1.75	6.65	1.46	5.91	1.52	6.35	1.00
TEM 25	1.96	6.37	1.70	5.64	1.94	5.96	1.00
TEM 26	1.92	6.22	1.67	5.50	1.87	5.83	1.00
TEM 27	1.72	6.60	1.45	5.86	1.57	6.25	1.00
TEM 28	1.18	6.72	0.96	5.97	0.91	6.52	1.00
TEM 29	1.55	6.85	1.28	6.08	1.44	6.48	1.00
TEM 30	1.56	6.80	1.31	6.02	1.50	6.39	1.00
TEM 31	1.46	6.36	1.21	5.67	1.43	5.99	1.00
TEM 32	1.91	6.24	1.67	5.53	1.76	5.91	1.00
TEM 33	1.87	6.35	1.63	5.61	1.83	5.94	1.00
TEM 34	1.65	6.94	1.49	6.09	1.64	6.50	1.00

Table 4. Means and standard deviations (St. Dev.) for features computed using one user's (K.K.) segmentation for both malignant and benign nodules.

Regions of Interest	Malignant		Benign		P-values
	Mean	St. Dev.	Mean	St. Dev.	
Intensity Features					
<i>Nodule</i>					
Mean HU	-239.99	161.50	-240.97	242.45	0.353
Variance	34638.42	11176.04	100382.82	177546.53	3.3E-04
Maximum HU	194.50	315.31	261.88	571.31	0.861
Minimum HU	-784.20	76.50	-836.35	75.32	0.160
Median HU	-212.80	199.01	-247.94	207.57	0.407
FWHM	0.04	0.03	0.04	0.04	0.238
Entropy	8.49	0.63	8.70	0.62	0.414
Kurtosis	3.24	1.90	2.01	0.22	0.003
Skewness	-0.48	0.88	-0.08	0.42	0.127
<i>Parenchyma</i>					
Mean HU	-838.89	43.44	-876.24	33.69	0.019
Variance	12604.14	8075.81	6920.25	3956.16	0.083
Maximum HU	-90.30	246.21	-228.12	208.69	0.133
Minimum HU	-1003.60	29.24	-1011.18	19.63	0.729
Median HU	-860.50	44.01	-894.24	30.19	0.026
FWHM	0.09	0.06	0.09	0.05	0.889
Entropy	8.23	0.55	7.87	0.36	0.052
Kurtosis	9.89	5.09	11.72	7.78	0.744
Skewness	2.01	0.93	2.14	0.77	0.782
Shape					
Recist	14.06	10.41	9.01	3.74	0.167
Sphericity	0.96	0.20	1.12	0.18	0.044
Effective Radius	5.98	3.76	4.24	1.60	0.238
<i>Differences</i>					
Mean	0.21	0.07	0.19	0.11	0.380
Variance	0.03	0.03	0.03	0.05	0.467
Kurtosis	4.36	2.20	4.28	2.09	0.353
Skewness	1.16	0.55	1.12	0.58	0.633
Range	0.81	0.25	0.74	0.42	0.280
Border					
Mean of Slopes	-119.30	59.64	-181.17	119.73	0.141
Variance of Slopes	13.33	10.94	14.44	9.02	0.530

P-values computed through appropriate statistical test are also shown, with significance at $p < 0.05$, highlighted by ***bolded italics***.

Table 4. Continued

Regions of Interest	Malignant		Benign		P-values
	Mean	St. Dev.	Mean	St. Dev.	
Texture Features					
<i>Mean of Nodule</i>					
TEM 1	3.04	1.50	3.38	2.03	0.651
TEM 2	2.93	1.55	3.34	2.05	0.589
TEM 3	2.90	1.59	3.39	2.01	0.514
TEM 4	3.02	1.62	3.46	1.97	0.560
TEM 5	2.92	1.56	3.40	2.03	0.531
TEM 6	2.91	1.58	3.46	2.01	0.469
TEM 7	2.96	1.59	3.48	1.99	0.486
TEM 8	2.88	1.61	3.48	2.01	0.434
TEM 9	2.90	1.59	3.48	2.00	0.441
TEM 10	2.89	1.60	3.48	2.01	0.438
TEM 11	2.84	1.65	3.46	2.01	0.418
TEM 12	2.85	1.63	3.47	2.01	0.414
TEM 13	2.86	1.68	3.48	2.00	0.413
TEM 14	2.84	1.63	3.48	2.00	0.402
TEM 15	2.98	1.49	3.34	2.05	0.632
TEM 16	2.90	1.59	3.45	2.02	0.473
TEM 17	2.87	1.64	3.48	2.01	0.427
TEM 18	2.85	1.58	3.47	2.01	0.418
TEM 19	2.84	1.53	3.40	2.04	0.461
TEM 20	2.86	1.58	3.46	2.02	0.429
TEM 21	2.86	1.60	3.48	2.00	0.414
TEM 22	2.83	1.59	3.42	2.02	0.438
TEM 23	2.83	1.73	3.47	1.99	0.405
TEM 24	2.86	1.68	3.48	1.99	0.414
TEM 25	2.84	1.75	3.49	1.99	0.405
TEM 26	2.84	1.67	3.47	2.01	0.414
TEM 27	2.89	1.69	3.50	1.99	0.421
TEM 28	2.86	1.61	3.49	2.01	0.407
TEM 29	2.84	1.65	3.51	2.00	0.382
TEM 30	2.84	1.66	3.53	2.00	0.367
TEM 31	2.85	1.49	3.36	2.07	0.505
TEM 32	2.82	1.68	3.44	2.00	0.419
TEM 33	2.89	1.76	3.51	1.98	0.420
TEM 34	2.80	1.66	3.53	1.99	0.335

Table 4. Continued

Regions of Interest	Malignant		Benign		P-values
	Mean	St. Dev.	Mean	St. Dev.	
Features					
<i>Variance Texture of Nodule</i>					
TEM 1	0.06	0.15	0.07	0.08	0.053
TEM 2	0.06	0.15	0.06	0.08	0.067
TEM 3	0.05	0.15	0.07	0.08	0.060
TEM 4	0.05	0.12	0.06	0.07	0.083
TEM 5	0.06	0.15	0.07	0.08	0.075
TEM 6	0.06	0.16	0.06	0.08	0.067
TEM 7	0.05	0.15	0.06	0.08	0.093
TEM 8	0.06	0.16	0.07	0.08	0.075
TEM 9	0.06	0.15	0.06	0.08	0.093
TEM 10	0.06	0.15	0.06	0.08	0.103
TEM 11	0.06	0.16	0.06	0.08	0.093
TEM 12	0.06	0.15	0.06	0.08	0.103
TEM 13	0.06	0.15	0.07	0.08	0.103
TEM 14	0.06	0.16	0.07	0.08	0.093
TEM 15	0.06	0.17	0.07	0.08	0.103
TEM 16	0.05	0.15	0.07	0.08	0.075
TEM 17	0.06	0.16	0.06	0.08	0.103
TEM 18	0.05	0.15	0.06	0.07	0.103
TEM 19	0.06	0.15	0.06	0.08	0.093
TEM 20	0.06	0.16	0.06	0.07	0.093
TEM 21	0.06	0.15	0.06	0.08	0.093
TEM 22	0.06	0.16	0.07	0.08	0.093
TEM 23	0.06	0.16	0.07	0.08	0.093
TEM 24	0.06	0.16	0.07	0.08	0.103
TEM 25	0.06	0.15	0.06	0.08	0.093
TEM 26	0.06	0.15	0.06	0.07	0.093
TEM 27	0.06	0.15	0.07	0.07	0.103
TEM 28	0.06	0.16	0.07	0.08	0.103
TEM 29	0.06	0.16	0.06	0.07	0.103
TEM 30	0.06	0.16	0.06	0.07	0.103
TEM 31	0.06	0.16	0.07	0.08	0.126
TEM 32	0.06	0.17	0.07	0.08	0.093
TEM 33	0.06	0.15	0.07	0.08	0.093
TEM 34	0.06	0.18	0.06	0.07	0.103

Table 4. Continued

Regions of Interest	Malignant		Benign		P-values
	Mean	St. Dev.	Mean	St. Dev.	
Features					
<i>Kurtosis Texture of Nodule</i>					
TEM 1	4053.03	10021.53	458.15	419.50	0.940
TEM 2	4013.54	9987.89	472.95	447.71	0.900
TEM 3	3987.15	10067.37	480.08	470.57	0.861
TEM 4	4110.97	10359.03	481.07	457.58	0.900
TEM 5	3982.61	10010.17	460.20	425.77	0.940
TEM 6	4111.96	10416.94	468.15	435.12	0.940
TEM 7	4188.79	10570.28	479.33	455.52	0.940
TEM 8	4038.92	10160.06	487.76	459.75	0.900
TEM 9	4089.56	10267.01	481.66	455.91	0.980
TEM 10	3986.20	9894.02	479.61	451.66	0.980
TEM 11	4138.64	10482.15	462.06	420.89	0.980
TEM 12	4037.94	10137.72	461.77	425.46	0.980
TEM 13	4147.02	10507.22	461.28	424.31	0.940
TEM 14	4136.93	10470.74	461.03	424.18	0.980
TEM 15	3900.09	9778.65	456.64	424.45	0.940
TEM 16	4011.97	10090.12	476.36	450.29	0.940
TEM 17	4010.72	9986.69	499.41	476.07	0.900
TEM 18	3887.24	9587.93	469.17	436.08	0.980
TEM 19	4011.92	10225.92	462.54	421.91	0.940
TEM 20	4148.62	10561.85	458.35	415.43	0.940
TEM 21	4196.00	10633.32	465.58	431.35	0.980
TEM 22	4057.62	10296.65	465.58	426.38	0.940
TEM 23	4249.69	10791.26	459.68	420.73	0.980
TEM 24	4190.44	10626.06	459.53	424.72	0.980
TEM 25	4277.75	10873.75	459.17	420.54	0.980
TEM 26	4135.99	10435.36	464.31	424.32	0.980
TEM 27	4127.61	10475.35	463.86	424.30	0.940
TEM 28	3880.52	9652.01	459.31	424.55	0.940
TEM 29	3995.21	10052.31	464.85	426.88	0.940
TEM 30	3865.43	9645.30	465.27	423.85	0.940
TEM 31	3921.61	9988.15	475.76	432.02	0.861
TEM 32	4194.46	10632.92	467.19	428.47	0.980
TEM 33	4295.69	10984.59	454.21	412.67	0.940
TEM 34	3472.88	8303.98	450.96	409.36	0.980

Table 4. Continued

Regions of Interest	Malignant		Benign		P-values
	Mean	St. Dev.	Mean	St. Dev.	
Features					
<i>Skewness Texture of Nodule</i>					
TEM 1	-23.20	56.42	-3.34	16.06	0.861
TEM 2	-22.61	56.38	-3.41	16.82	0.821
TEM 3	-21.74	56.46	-3.47	17.03	0.821
TEM 4	-21.60	57.97	-2.97	17.32	0.861
TEM 5	-22.40	56.08	-2.70	16.83	0.980
TEM 6	-22.08	57.93	-2.93	16.91	0.861
TEM 7	-21.76	58.93	-2.99	17.13	0.821
TEM 8	-21.35	57.09	-2.77	17.59	0.861
TEM 9	-21.38	57.70	-2.68	17.41	0.861
TEM 10	-20.85	56.54	-2.54	17.46	0.861
TEM 11	-21.93	58.32	-2.41	17.12	0.900
TEM 12	-21.27	57.17	-2.58	16.94	0.861
TEM 13	-21.85	58.47	-2.68	16.94	0.861
TEM 14	-21.57	58.40	-2.70	16.87	0.821
TEM 15	-23.56	54.54	-2.18	16.68	0.980
TEM 16	-21.53	56.69	-2.80	17.33	0.900
TEM 17	-21.27	56.67	-2.53	17.98	0.900
TEM 18	-20.31	55.46	-2.46	17.26	0.821
TEM 19	-22.24	56.70	-2.18	17.27	0.980
TEM 20	-22.27	58.41	-2.57	16.98	0.900
TEM 21	-21.68	59.17	-2.90	16.92	0.821
TEM 22	-21.65	57.41	-2.19	17.44	0.900
TEM 23	-22.23	59.61	-2.39	17.04	0.861
TEM 24	-21.94	58.94	-2.68	16.86	0.861
TEM 25	-22.48	59.89	-2.55	16.96	0.861
TEM 26	-22.03	58.23	-2.53	17.08	0.900
TEM 27	-22.10	58.17	-2.85	17.03	0.940
TEM 28	-20.86	55.16	-2.66	16.82	0.900
TEM 29	-21.28	56.66	-2.79	16.97	0.861
TEM 30	-20.64	54.96	-3.10	16.90	0.900
TEM 31	-23.12	55.28	-1.92	17.52	0.980
TEM 32	-21.71	59.10	-2.22	17.47	0.821
TEM 33	-22.97	60.05	-2.71	16.76	0.900
TEM 34	-18.52	49.39	-3.33	16.28	0.706

Table 4. Continued

Regions of Interest	Malignant		Benign		P-values
	Mean	St. Dev.	Mean	St. Dev.	
Features					
<i>Mean Texture of Parenchyma</i>					
TEM 1	3.10	1.60	3.43	2.09	0.673
TEM 2	2.97	1.62	3.37	2.09	0.604
TEM 3	2.90	1.59	3.42	2.04	0.497
TEM 4	2.94	1.51	3.47	1.98	0.482
TEM 5	2.99	1.68	3.45	2.09	0.564
TEM 6	2.97	1.69	3.50	2.06	0.503
TEM 7	3.02	1.68	3.52	2.04	0.513
TEM 8	2.94	1.71	3.52	2.06	0.465
TEM 9	2.96	1.69	3.52	2.04	0.468
TEM 10	2.94	1.69	3.52	2.05	0.463
TEM 11	2.91	1.76	3.50	2.06	0.453
TEM 12	2.92	1.74	3.52	2.06	0.447
TEM 13	2.92	1.79	3.53	2.05	0.445
TEM 14	2.91	1.75	3.52	2.05	0.436
TEM 15	3.05	1.62	3.39	2.11	0.671
TEM 16	2.97	1.70	3.49	2.07	0.504
TEM 17	2.93	1.74	3.52	2.06	0.457
TEM 18	2.90	1.66	3.50	2.06	0.438
TEM 19	2.91	1.65	3.44	2.09	0.496
TEM 20	2.93	1.70	3.50	2.07	0.465
TEM 21	2.93	1.71	3.52	2.05	0.448
TEM 22	2.90	1.72	3.47	2.07	0.474
TEM 23	2.90	1.84	3.51	2.05	0.439
TEM 24	2.92	1.79	3.53	2.04	0.447
TEM 25	2.91	1.85	3.53	2.04	0.437
TEM 26	2.91	1.79	3.51	2.06	0.448
TEM 27	2.95	1.79	3.54	2.04	0.451
TEM 28	2.92	1.72	3.53	2.06	0.440
TEM 29	2.90	1.76	3.55	2.05	0.414
TEM 30	2.90	1.76	3.57	2.05	0.397
TEM 31	2.93	1.62	3.41	2.13	0.542
TEM 32	2.89	1.79	3.49	2.05	0.455
TEM 33	2.95	1.86	3.55	2.03	0.451
TEM 34	2.87	1.77	3.57	2.03	0.369

Table 4. Continued

Regions of Interest	Malignant		Benign		P-values
	Mean	St. Dev.	Mean	St. Dev.	
Features					
<i>Variance Texture of Parenchyma</i>					
TEM 1	7.2E-05	2.3E-04	6.1E-04	2.4E-03	0.060
TEM 2	2.3E-04	7.4E-04	3.0E-04	1.0E-03	0.053
TEM 3	1.7E-03	5.3E-03	3.3E-04	7.2E-04	0.022
TEM 4	7.8E-03	2.5E-02	7.7E-04	1.2E-03	0.037
TEM 5	1.6E-04	5.1E-04	3.5E-04	1.2E-03	0.022
TEM 6	4.2E-04	1.3E-03	2.8E-04	8.0E-04	0.020
TEM 7	1.3E-03	4.0E-03	2.5E-04	5.1E-04	0.017
TEM 8	4.3E-04	1.4E-03	2.3E-04	6.6E-04	0.029
TEM 9	1.1E-03	3.6E-03	1.9E-04	4.1E-04	0.029
TEM 10	1.7E-03	5.3E-03	1.8E-04	3.4E-04	0.033
TEM 11	9.3E-05	2.9E-04	1.6E-04	4.7E-04	0.020
TEM 12	1.1E-04	3.6E-04	1.3E-04	3.5E-04	0.015
TEM 13	1.1E-04	3.5E-04	1.4E-04	3.7E-04	0.020
TEM 14	1.1E-04	3.4E-04	1.5E-04	4.1E-04	0.017
TEM 15	9.7E-05	3.1E-04	4.9E-04	1.8E-03	0.029
TEM 16	2.2E-04	6.8E-04	3.0E-04	9.4E-04	0.020
TEM 17	7.3E-04	2.3E-03	1.8E-04	4.8E-04	0.025
TEM 18	3.3E-03	1.0E-02	2.3E-04	3.3E-04	0.042
TEM 19	7.0E-05	2.2E-04	2.3E-04	7.0E-04	0.022
TEM 20	9.4E-05	3.0E-04	1.8E-04	5.4E-04	0.020
TEM 21	1.2E-04	3.7E-04	1.6E-04	4.2E-04	0.017
TEM 22	8.1E-05	2.6E-04	1.8E-04	5.2E-04	0.022
TEM 23	1.0E-04	3.2E-04	1.5E-04	4.2E-04	0.020
TEM 24	1.2E-04	3.8E-04	1.5E-04	4.0E-04	0.020
TEM 25	1.0E-04	3.3E-04	1.5E-04	4.1E-04	0.022
TEM 26	9.6E-05	3.0E-04	1.5E-04	4.3E-04	0.020
TEM 27	1.2E-04	3.9E-04	1.5E-04	4.1E-04	0.033
TEM 28	1.5E-04	4.6E-04	1.4E-04	3.4E-04	0.029
TEM 29	1.3E-04	4.1E-04	1.4E-04	3.6E-04	0.033
TEM 30	1.2E-04	3.7E-04	1.5E-04	4.3E-04	0.042
TEM 31	6.4E-05	2.0E-04	3.2E-04	1.1E-03	0.025
TEM 32	9.7E-05	3.1E-04	1.6E-04	4.2E-04	0.025
TEM 33	1.2E-04	3.8E-04	1.5E-04	4.4E-04	0.020
TEM 34	1.8E-04	5.8E-04	1.6E-04	4.2E-04	0.053

Table 4. Continued

Regions of Interest	Malignant		Benign		P-values
	Mean	St. Dev.	Mean	St. Dev.	
Features					
<i>Kurtosis Texture of Parenchyma</i>					
TEM 1	80.28	151.25	52.21	88.80	0.900
TEM 2	70.67	136.50	44.05	73.29	0.980
TEM 3	53.82	132.71	41.03	71.75	0.598
TEM 4	47.36	109.17	37.81	70.21	0.670
TEM 5	76.51	152.10	43.08	71.48	0.940
TEM 6	76.77	153.38	41.48	70.02	0.861
TEM 7	60.76	126.82	39.44	66.14	0.530
TEM 8	74.90	154.94	41.73	69.36	0.633
TEM 9	63.85	136.61	41.10	67.40	0.407
TEM 10	61.00	138.04	40.65	67.13	0.353
TEM 11	83.03	171.09	41.27	68.89	0.670
TEM 12	77.05	150.03	42.08	67.95	0.821
TEM 13	78.61	155.90	43.44	71.09	0.706
TEM 14	79.30	152.93	42.31	68.12	0.900
TEM 15	75.21	148.69	46.08	74.30	0.940
TEM 16	74.39	153.06	43.38	72.22	0.782
TEM 17	72.66	151.85	41.06	68.36	0.436
TEM 18	59.01	136.94	41.74	69.44	0.280
TEM 19	83.58	170.76	42.38	69.41	0.744
TEM 20	81.22	166.09	41.22	68.63	0.940
TEM 21	74.88	143.56	41.91	66.20	0.633
TEM 22	85.26	174.92	42.13	69.42	0.782
TEM 23	82.58	169.56	42.22	70.48	0.782
TEM 24	80.48	158.80	43.44	70.79	0.744
TEM 25	82.66	167.07	42.16	70.44	1.000
TEM 26	81.51	164.93	40.91	68.23	0.861
TEM 27	77.96	157.50	43.48	71.14	0.900
TEM 28	74.24	141.99	43.54	69.34	0.980
TEM 29	71.90	143.44	44.03	72.19	0.900
TEM 30	68.68	148.75	43.62	72.13	0.861
TEM 31	83.52	171.43	43.94	70.52	0.782
TEM 32	81.84	167.98	42.59	70.07	0.900
TEM 33	83.36	167.64	42.11	69.83	1.000
TEM 34	61.92	143.44	43.96	74.11	0.670

Table 4. Continued

Regions of Interest	Malignant		Benign		P-values
	Mean	St. Dev.	Mean	St. Dev.	
Features					
<i>Skewness Texture of Parenchyma</i>					
TEM 1	-0.83	7.47	-0.67	5.62	0.706
TEM 2	-0.55	6.68	-0.03	4.91	0.598
TEM 3	0.28	5.82	0.18	4.56	0.380
TEM 4	-0.11	5.22	0.47	4.19	0.126
TEM 5	-0.83	7.22	-0.33	4.74	0.353
TEM 6	-0.67	7.24	-0.32	4.54	0.498
TEM 7	-0.46	6.17	-0.24	4.23	0.706
TEM 8	-0.44	7.21	-0.34	4.66	0.940
TEM 9	-0.31	6.43	-0.29	4.46	0.940
TEM 10	-0.22	6.30	-0.32	4.44	0.861
TEM 11	-0.50	7.68	-0.09	4.49	0.353
TEM 12	-0.56	7.18	-0.23	4.39	0.782
TEM 13	-0.41	7.34	-0.06	4.60	0.744
TEM 14	-0.64	7.29	-0.31	4.45	0.782
TEM 15	-0.84	7.13	-0.50	5.03	0.564
TEM 16	-0.62	7.18	-0.40	4.85	0.530
TEM 17	-0.35	7.02	-0.27	4.56	0.821
TEM 18	-0.25	6.23	-0.23	4.35	0.821
TEM 19	-0.59	7.58	-0.39	4.62	0.782
TEM 20	-0.52	7.49	-0.26	4.48	0.670
TEM 21	-0.70	6.97	-0.42	4.34	0.940
TEM 22	-0.60	7.71	-0.31	4.63	0.530
TEM 23	-0.46	7.74	0.03	4.59	0.380
TEM 24	-0.43	7.46	-0.14	4.62	0.706
TEM 25	-0.40	7.73	0.05	4.58	0.633
TEM 26	-0.47	7.60	0.01	4.42	0.564
TEM 27	-0.35	7.33	0.02	4.60	0.706
TEM 28	-0.72	6.94	-0.25	4.44	0.564
TEM 29	-0.45	6.85	-0.08	4.62	0.633
TEM 30	-0.06	6.76	0.00	4.63	0.706
TEM 31	-0.55	7.63	-0.44	4.81	0.744
TEM 32	-0.58	7.61	-0.11	4.66	0.436
TEM 33	-0.36	7.76	0.11	4.56	0.670
TEM 34	0.15	6.46	0.24	4.71	0.530

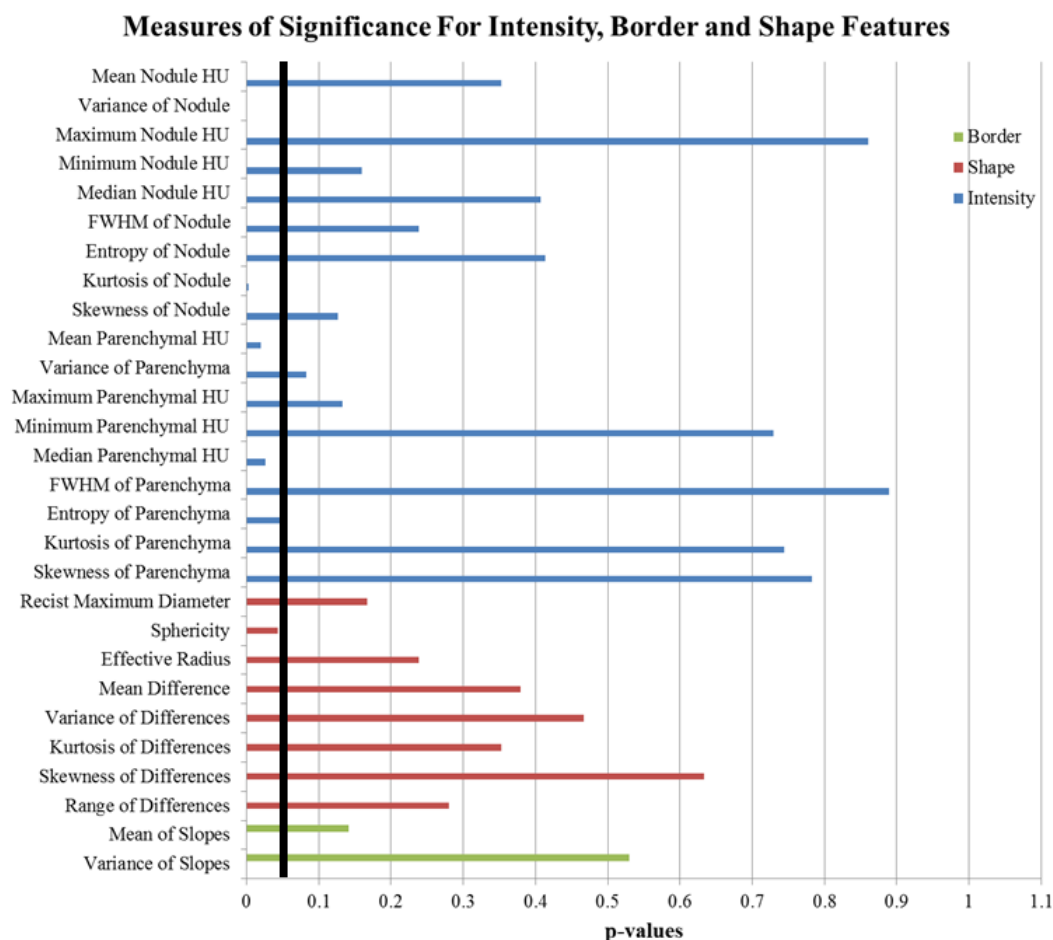


Figure 18. Results of measuring significance of intensity, shape, and border features. The thick vertical line denotes the significance level of 0.05. A total of 5 (4 intensity and 1 shape) features with p-values less than 0.05 are statistically significantly different between malignant and benign nodules.

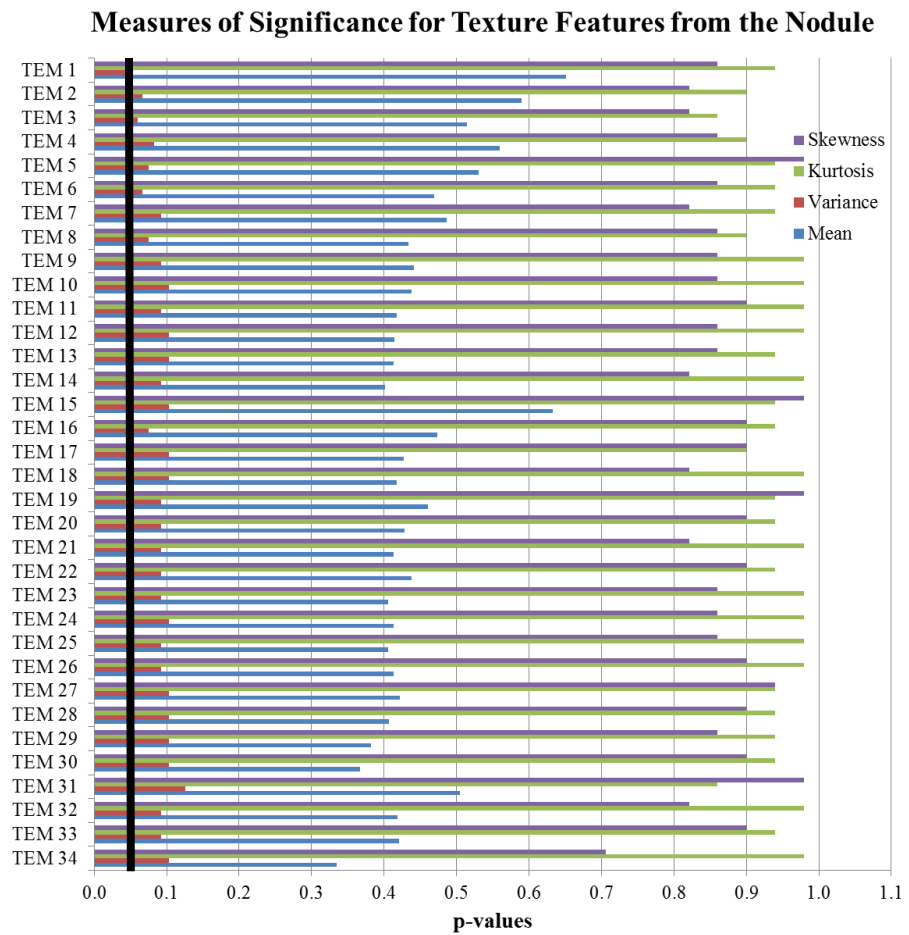


Figure 19. Results of measuring significance of texture features from the nodule. The thick vertical line denotes the significance level of 0.05. No features are statistically significantly different between malignant and benign nodules.

Measures of Significance for Texture Features from the Parenchyma

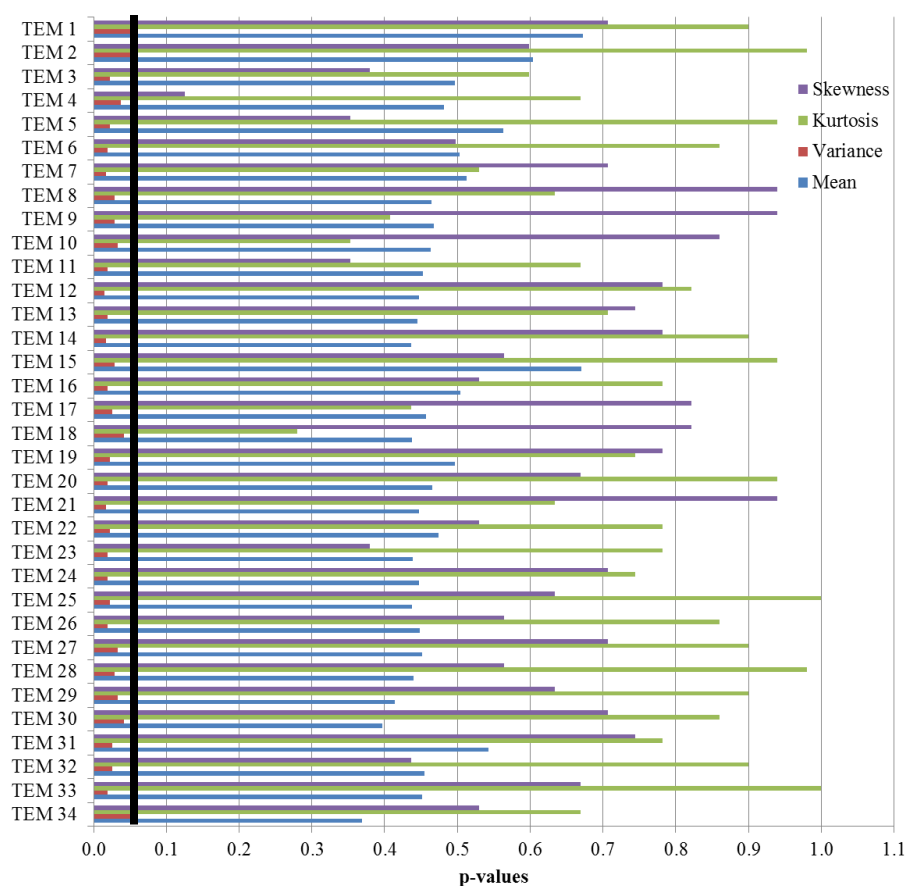


Figure 20. Results of measuring significance of texture features from the parenchyma. The thick vertical line denotes the significance level of 0.05. A total of 31 variance features with p-values less than 0.05 are statistically significantly different between malignant and benign nodules.

Table 5. The assignment of classes “Malignant” and “Benign”, compared to actual diagnosis.

		Predicted Class	
		Malignant	Benign
Actual Class	Malignant	10	0
	Benign	2	15

Note: All ten malignant nodules were correctly classified. Two benign nodules were misclassified as malignant.

CHAPTER V

DISCUSSION

In developing this CAD tool, the key objective was to incorporate parenchymal and texture features into the Feature Extraction process, with the hypothesis that these areas, having been minimally explored, would improve the accuracy of the predicted diagnosis of lung nodules. In order to determine the usefulness of the developed CAD tool, a set of 27 cases were processed through the CAD tool as a proof of concept.

5.1 Feature Extraction and Segmentation

The regions of interest were manually segmented to identify the nodule and the surrounding parenchyma. The effects of this manual segmentation were analyzed by comparing the feature values across three different segmentations. Based on the results of the one-way ANOVA test, none of the features varied significantly from the others when segmented by a different user. The features that were most affected were those pertaining to the intensity histogram, the kurtosis and skewness of the histogram, as well as the minimum intensity of the nodule. The shape features computed through Differences in Spherical Shape (Methods Section 3.2.2) were also affected by manual segmentation. These variations were expected, as they are directly influenced by the nodule mask, however, none of the features were affected at a 0.05 level of significance. Though significant difference was not achieved, a transition from manual segmentation to semi-automated or automated segmentation is desirable to reduce the variation in segmentation observed.

5.2 Feature Selection

From the feature selection process, many interesting characteristics stand out. First of all, the texture features of the parenchyma were key components in separating diagnoses. 31 of the 36 significant features were texture features derived from the

parenchyma. Other parenchymal features were also found to be important during statistical testing, including the variance in intensity and the median intensity of the parenchyma. *These observations support the hypothesis that inclusion of features from the surrounding parenchyma can aid in the classification of malignant and benign nodules.*

The fact that parenchymal features may influence classification is also important in regards to the size of lung tumor for which the CAD tool was developed. The CAD tool was developed to aid in the classification of nodules, lesions detected in CT with a maximum diameter of 4-30 mm. For small pulmonary nodules (4-10mm), the number of voxels from which nodule features can be computed via CT data is limited. By showing that parenchymal features contribute to a probable diagnosis, the number of voxels that can be used in feature extraction is increased. Additionally, inclusion of the parenchymal features quantifies the reaction of the nodule to its surroundings. The significance of these features further shows that by examining the nodule alone, valuable classification data is being ignored.

5.3 Classification

The 27 regions of interest from NLST and COPDGene had some interesting properties that highlight the CAD tool's robustness. There were five malignant and five benign cases near the pleural wall, and the sizes of the nodules, as measured by radiologists varied from 0.6 – 2.2 cm for benign nodules and 0.6 – 3 cm for malignant. There was also great diversity in the scanner parameters. While the tube voltage was consistent at 120 kVp, the NLST scans were acquired with low-dose CT (tube current-time products between 25 – 50 mAs) and the COPDGene cases were acquired with a higher-dose protocol (tube current-time products of 200 mAs). Slice thicknesses ranged from 0.6 – 1.3 mm and were acquired using several different models of CT machines.

In the leave-one-out testing of the neural network classifier, 25 of the 27 test nodules (92.6%) were correctly classified. The two missed cases were from the COPDGene database. COPDGene's primary goal is to study COPD; the identification and determination of lung cancer is a secondary purpose that relies heavily on participant reporting. Therefore, there is a chance that these nodules are not truly benign. In any case, classification occurred so that no malignant nodules were missed, which is an important point.

Classification was based on two features, variance and kurtosis of the nodule intensity. The accuracy of classification in this preliminary database is promising. Given the degree of variety in the sample set, the CAD tool is robust to variation in collection of the images, and the feature set is diverse enough to identify key characteristics that differ in nodules with similar sizes but differing outcomes. While features from the nodule were selected for classification, with the addition of more cases it is expected that textural and parenchymal features will play a larger role in the classification of lung nodules. The textures in the parenchyma were highly significant in differentiating classes; testing on a dataset of 300 nodules (100 malignant and 200 benign) would allow for 30 significant features, including these texture features, to be incorporated into the neural network.

5.4 Conclusion

In an effort to diagnose lung cancer before metastasis, thus improving the five-year survival, screening of high-risk populations such as current and past smokers has gained popularity. While sputum testing and chest x-ray did not have a significant effect in improving the mortality rate [10, 12], screening with CT has been shown to reduce mortality by 20% [13]. With the utilization of CT as a screening tool for lung cancer, the number of benign nodules for which malignancy cannot be ruled out through imaging has increased drastically. In an effort to reduce the number of false positives indicated on CT, several CAD tools have been developed. This CAD tool was developed to incorporate the

significant features of prior CAD tools and expand them to include areas that have previously received little to no attention. Several novel approaches to interrogate the parenchyma, including quantifying spiculation through the straightening of the nodule's border from the centroid and quantifying texture in three dimensions by expanding Laws' TEM, were incorporated into the CAD tool. By quantifying parenchymal features from the database, it has been shown that the parenchyma can provide useful information in the separation of diagnoses. The modular framework of the CAD tool allows individual processes of the CAD tool pathways to be easily tested, further developed, or applied to additional classification problems. Preliminary results revealed an accuracy of 92.6% in determining likelihood of cancer in lung nodules, indicating the CAD tool to be fully functional and very promising.

CHAPTER VI

FUTURE WORK

6.1 Introduction

Several projects are planned in expanding this CAD tool. They vary in range from expanding datasets, further feature extraction, improving classification, and incorporating an automated segmentation method.

6.2 Increasing Dataset Size

As a proof-of-concept, 27 nodules were used to test the CAD tool. While this sample size shows the functionality of the CAD tool and displays promising classification ability, the limited number of cases restricts the number of features that can be selected for classification. To highlight the value of the extended feature set, which includes parenchymal and textural features, two databases are being investigated as sources for more nodule cases.

6.2.1 COPDGene Database

As mentioned earlier, nodules from the COPDGene study were incorporated into the proof of concept database. There are still 286 nodules, size 4 – 10 mm (the cases highlighted in blue and yellow in Figure 16) left to add to the database. Additionally, COPDGene will also be starting its second round of screening. In the five years since the first visit, new nodules are likely to have developed, providing a larger database for advancing the CAD tool. Additional framework for collecting cancer information from the participants and their primary care physicians has also been established, which will aid in verifying the diagnosis of the lung nodules identified through CT.

In addition to providing more nodule cases, the continued tracking of participants opens the doors to the possibility of extending the CAD tool to incorporate longitudinal datasets. By examining the future location of a nodule, it is likely that textural differences

can be identified to indicate the region as a potential area to watch for nodule development.

6.2.2 Clinical Cases

Currently, clinical cases are being identified through EPIC to determine the effectiveness of this CAD tool on CT scans obtained with clinical settings. These scans tend to have a larger slice thickness (~3mm), which reduces resolution. The differences between clinical and high-resolution slice thickness on feature values and classification can then be determined by using this dataset. While non-contrast scans will be tested initially, the application to contrast-CT scans is another potential avenue to explore.

6.2.3 Variability of Cases

The current dataset contains primarily solid nodules. In the future, an increased percentage of sub-solid nodules will be added to the training and testing datasets. Ground glass nodules (GGN) are defined as localized regions of increased attenuation through which it is possible to visualize normal pulmonary structures (parenchyma, airways and vessels). The category of sub-solid nodules encompasses purely GGN and partially solid GGN. This class of nodules present challenges in the areas of quantification due to some ambiguity in defining the nodule boundary. It is likely that the expanded parenchymal feature sets described in this thesis will be highly suited to the analysis of sub-solid nodules.

Additional variations include the effects of reconstruction slice thickness (clinical versus high resolution) and reconstruction kernels on the feature values extracted. For high resolution imaging used for pulmonary CT quantification (research studies such as NLST and COPDGene), the slice thickness is targeted at 0.6-2 mm. Clinical CT images have slice thicknesses on the order of 1 – 10 mm to reduce the volume of data radiologists need to analyze. The optimal CAD tool has the ability to perform effectively

on both high resolution and clinical data. In the future, exploration of the impact of both high and clinical resolution CT scans on individual features will be performed by using the clinical database. After determining how the features are affected by slice thickness, its effect on the performance of the CAD tool can be assessed. From this study we will determine if the expanded feature set presented in this thesis is largely unaffected by imaging protocol such that clinical and high resolution CT data may be analyzed together via the same CAD tool. Alternatively, we will present two CAD tools - one optimized for high resolution CT data for application in large multi-center clinical trials, and a secondary CAD tool optimized for processing clinical CT cases.

6.3 Feature Extraction

While many features derived from the region of interest have been incorporated into this CAD tool, there is the potential to include other features. These include, and are in no way limited to, other demographic risk factors such as personal and/or family history of cancer and lifestyle habits. As genetic testing becomes more prevalent, the presence of genetic risk factors could also serve as features [35].

Until now, the focus of the CAD program has been on features extracted from the regions of interest. Gierada et al. found that quantitative CT measurements of emphysema were weakly associated with lung cancer [36]. As COPD and lung cancer are strongly associated [33], including quantitative measurements of emphysema, such as percentage of lobar or lung volume CT voxels less than -950 HU, may serve as useful features in cases from patients with COPD.

6.4 Classification

This CAD program was developed specifically to serve as a second reader for radiologists by quantitatively developing a prediction of diagnosis of lung nodules. Due

to the modularity of the implementation of the program, the classification process can easily be modified to become more specialized.

A neural network was selected for a classifier due to its ability to fit both linearly and non-linearly separated datasets. While a neural network works well for most datasets, including the current subset of nodules, specific classifiers may work better once a priori knowledge of the dataset is known. As the database size increases, other classifiers can be explored to determine which best classify the nodules.

An additional project involving classification would be to return a probability of being malignant or benign instead of a direct diagnosis. By returning a probability, the CAD program would further imitate a second reader as the radiologist labels nodules as likely malignant or likely benign. Using a neural network, this process is straightforward; however, it could be more challenging to implement with other classifiers.

Further expansion of classification includes incorporating sub-categories into the classification options. For example, instead of malignant or benign diagnoses, options for diagnosis could include adenocarcinoma, squamous cell carcinoma, small- or large- cell carcinoma, carcinoid tumor or benign. Classification by histological subtype, if achievable, would lead to a more specific diagnosis and tailored treatment approach by noninvasive assessment.

In addition to classification by histological subtype, incorporating CT features to return presence or absence of genetic mutations would provide information to personalize treatment plans without undergoing further genetic testing. Lee et al. found that an increased percentage of ground glass volume was correlated with Exon 21 missense mutation, an epidermal growth factor receptor (EGFR) mutation [37]. In a retrospective clinical study, comparison features extracted from CT with the results of genetic testing could be performed to identify additional quantitative CT markers of specific genetic mutations.

Not only could this CAD tool aid in reducing false-positives, but it could also be modified to predict how a nodule will respond to different treatments. By comparing feature values of easily-treated nodules to those that did not respond to treatment, it could be possible to identify radiological markers of treatment response.

In another effort to improve patient treatment response, a retrospective study could be designed to determine the effect different follow-up procedures had on patient outcome. By incorporating quantitative CT features from the nodule before treatment with the clinical information available from follow-up treatment, the CAD program could be modified to predict treatment outcome.

6.5 Segmentation

The results of the presented study reflect that the variations in boundary segmentation did not significantly affect feature extraction. This is supportive of future incorporation of automated or semi-automated segmentation approaches. By automating the process, subjectivity would be reduced and valuable preprocessing time saved. From the methods developed for feature extraction, several possibilities for segmentation of lung nodules could be adapted.

The first possibility would be to adapt the RBST straightening from the centroid to three dimensional and determining the threshold from the straightened image stack. The second technique uses the image stacks generated from the three dimensional application of Laws' TEM. The voxels in these image stacks could be interrogated to determine the boundaries of the nodule and the presence of pleural wall or vessels.

APPENDIX

Table A1. The feature values computed during Feature Extraction for the 5 malignant regions of interest from NLST

Regions of Interest	Malignant				
	1	2	3	4	5
Features					
Demographics					
Age	56	71	61	68	64
Race	2	2	2	2	2
Ethnicity	5	5	5	5	5
Gender	2	1	2	1	2
Years Smoked	35	56	43	55	42
Pack Years	20	35	40	20	30
Intensity					
<i>Nodule</i>					
Mean HU	-24.43	-181.48	-38.52	-156.11	-206.92
Variance	19623.88	34495.17	23398.59	36558.62	46594.59
Maximum HU	135.00	109.00	178.00	1053.00	208.00
Minimum HU	-808.00	-605.00	-755.00	-797.00	-863.00
Median HU	33.00	-148.00	25.00	-122.00	-181.50
FWHM	0.04	0.02	0.07	0.08	0.02
Entropy	7.84	8.09	8.66	9.34	9.14
Kurtosis	8.00	1.95	4.76	3.78	2.11
Skewness	-2.31	-0.41	-1.51	-0.33	-0.38
<i>Parenchyma</i>					
Mean HU	-763.40	-836.64	-892.96	-805.38	-809.71
Variance	25982.28	10656.88	16456.42	22345.79	12763.24
Maximum HU	275.00	-163.00	156.00	163.00	19.00
Minimum HU	-1000.00	-1000.00	-1024.00	-1024.00	-1024.00
Median HU	-809.00	-857.00	-927.00	-825.00	-830.00
FWHM	0.10	0.11	0.00	0.00	0.13
Entropy	8.78	8.30	8.40	9.02	8.61
Kurtosis	10.42	9.14	11.85	4.93	7.96
Skewness	2.43	2.00	2.50	1.09	1.62

Table A1. Continued

Regions of Interest	Malignant				
	1	2	3	4	5
Features					
Shape					
Recist	40.98	8.51	15.24	17.80	10.63
Sphericity	0.68	1.12	0.72	0.72	0.93
Effective Radius	15.14	3.87	7.36	8.08	4.22
<i>Differences</i>					
Mean	0.16	0.11	0.28	0.25	0.21
Variance	0.01	0.01	0.04	0.04	0.03
Kurtosis	2.79	5.26	2.65	3.82	3.60
Skewness	0.62	1.24	0.62	0.99	1.00
Range	0.46	0.53	0.93	0.96	0.78
Border					
Mean of Slopes	-48.81	-153.82	-141.01	-68.11	-144.73
Variance of Slopes	7.02	9.71	19.66	37.32	25.11

Table A1. Continued

Regions of Interest	Malignant				
	1	2	3	4	5
Features					
<i>Mean Texture of Nodule</i>					
TEM 1	5.12	2.44	2.70	2.97	4.12
TEM 2	4.89	2.50	3.16	2.58	3.86
TEM 3	4.77	2.43	3.57	2.28	4.38
TEM 4	4.83	2.46	3.48	2.31	4.87
TEM 5	4.75	2.54	2.92	2.60	4.41
TEM 6	4.70	2.53	2.98	2.33	4.57
TEM 7	4.74	2.50	2.97	2.22	4.85
TEM 8	4.55	2.58	2.84	2.34	4.66
TEM 9	4.55	2.61	2.78	2.29	4.83
TEM 10	4.47	2.63	2.72	2.33	4.81
TEM 11	4.56	2.58	2.67	2.32	4.67
TEM 12	4.44	2.60	2.56	2.33	4.88
TEM 13	4.50	2.55	2.62	2.35	5.00
TEM 14	4.53	2.55	2.57	2.28	4.87
TEM 15	4.80	2.46	2.93	3.00	4.16
TEM 16	4.65	2.57	2.87	2.43	4.59
TEM 17	4.49	2.61	2.78	2.31	4.70
TEM 18	4.35	2.64	2.66	2.19	4.79
TEM 19	4.42	2.58	2.88	2.48	4.20
TEM 20	4.54	2.57	2.83	2.34	4.47
TEM 21	4.56	2.52	2.57	2.24	4.79
TEM 22	4.49	2.57	2.75	2.37	4.49
TEM 23	4.85	2.50	2.47	2.31	4.75
TEM 24	4.65	2.56	2.57	2.30	4.98
TEM 25	4.87	2.50	2.56	2.31	4.80
TEM 26	4.54	2.59	2.68	2.32	4.76
TEM 27	4.38	2.54	2.82	2.48	5.06
TEM 28	4.34	2.62	2.51	2.30	5.03
TEM 29	4.15	2.54	2.55	2.37	5.21
TEM 30	3.92	2.47	2.62	2.48	5.22
TEM 31	4.45	2.62	2.95	2.82	3.74
TEM 32	4.76	2.50	2.53	2.30	4.64
TEM 33	4.86	2.53	2.90	2.36	4.84
TEM 34	3.77	2.37	2.44	2.55	5.31

Table A1. Continued

Regions of Interest	Malignant				
	1	2	3	4	5
Features					
<i>Variance Texture of Nodule</i>					
TEM 1	6.4E-04	5.4E-02	2.6E-03	5.0E-03	8.4E-03
TEM 2	6.0E-04	5.3E-02	2.8E-03	5.4E-03	9.5E-03
TEM 3	6.3E-04	5.3E-02	2.7E-03	5.5E-03	5.1E-03
TEM 4	6.4E-04	5.3E-02	2.4E-03	5.4E-03	2.7E-03
TEM 5	5.3E-04	5.3E-02	3.5E-03	5.4E-03	6.3E-03
TEM 6	5.7E-04	5.3E-02	3.7E-03	5.6E-03	4.6E-03
TEM 7	6.1E-04	5.3E-02	3.4E-03	5.6E-03	3.0E-03
TEM 8	5.4E-04	5.2E-02	3.9E-03	5.5E-03	3.7E-03
TEM 9	5.7E-04	5.3E-02	3.6E-03	5.9E-03	2.7E-03
TEM 10	5.6E-04	5.3E-02	3.5E-03	6.1E-03	2.7E-03
TEM 11	5.7E-04	5.3E-02	4.6E-03	6.1E-03	3.7E-03
TEM 12	5.5E-04	5.3E-02	4.3E-03	6.2E-03	2.4E-03
TEM 13	5.5E-04	5.3E-02	4.2E-03	6.5E-03	1.9E-03
TEM 14	5.6E-04	5.3E-02	4.2E-03	6.3E-03	2.7E-03
TEM 15	5.1E-04	5.3E-02	3.2E-03	5.6E-03	8.3E-03
TEM 16	5.0E-04	5.3E-02	3.5E-03	5.3E-03	4.6E-03
TEM 17	5.6E-04	5.2E-02	3.7E-03	6.0E-03	3.3E-03
TEM 18	5.4E-04	5.3E-02	3.9E-03	6.2E-03	2.9E-03
TEM 19	5.4E-04	5.3E-02	4.8E-03	6.1E-03	7.3E-03
TEM 20	5.6E-04	5.2E-02	4.5E-03	5.9E-03	5.0E-03
TEM 21	5.6E-04	5.3E-02	4.2E-03	6.2E-03	3.2E-03
TEM 22	5.5E-04	5.3E-02	4.6E-03	6.0E-03	5.0E-03
TEM 23	6.3E-04	5.3E-02	4.6E-03	6.4E-03	3.1E-03
TEM 24	5.9E-04	5.3E-02	4.2E-03	6.3E-03	2.2E-03
TEM 25	6.4E-04	5.3E-02	4.3E-03	6.6E-03	2.8E-03
TEM 26	5.6E-04	5.3E-02	4.3E-03	6.3E-03	3.0E-03
TEM 27	5.2E-04	5.3E-02	4.0E-03	6.6E-03	1.6E-03
TEM 28	5.4E-04	5.3E-02	4.6E-03	6.2E-03	1.9E-03
TEM 29	4.8E-04	5.3E-02	4.5E-03	6.6E-03	1.2E-03
TEM 30	4.4E-04	5.4E-02	4.4E-03	6.5E-03	1.1E-03
TEM 31	5.5E-04	5.2E-02	5.3E-03	6.3E-03	1.1E-02
TEM 32	6.1E-04	5.2E-02	4.7E-03	6.1E-03	3.8E-03
TEM 33	6.3E-04	5.3E-02	3.8E-03	6.8E-03	2.5E-03
TEM 34	4.4E-04	5.5E-02	4.2E-03	6.5E-03	8.6E-04

Table A1. Continued

Regions of Interest	Malignant				
	1	2	3	4	5
Features					
<i>Kurtosis Texture of Nodule</i>					
TEM 1	32211.80	180.22	1300.31	1249.97	332.44
TEM 2	32089.52	174.53	1149.68	1235.99	325.87
TEM 3	32366.21	183.61	1028.64	1384.02	345.92
TEM 4	33318.55	178.52	1258.84	1405.62	328.48
TEM 5	32161.19	174.31	1147.65	1207.60	273.86
TEM 6	33479.63	176.46	1181.05	1306.38	286.65
TEM 7	33988.00	175.21	1348.29	1335.98	292.18
TEM 8	32673.54	173.47	1272.83	1329.87	303.55
TEM 9	33019.42	168.70	1410.77	1251.86	312.09
TEM 10	31823.31	167.27	1455.17	1199.73	323.76
TEM 11	33683.05	172.50	1260.63	1181.05	301.39
TEM 12	32592.01	169.77	1355.07	1157.93	321.32
TEM 13	33765.73	172.54	1324.83	1117.68	320.74
TEM 14	33658.10	173.65	1351.04	1188.92	302.61
TEM 15	31404.04	181.75	1111.84	1064.98	296.18
TEM 16	32444.55	172.76	1224.42	1349.59	285.38
TEM 17	32111.37	171.56	1352.59	1231.41	312.46
TEM 18	30849.51	164.89	1387.08	1291.91	333.51
TEM 19	32846.36	172.32	1150.42	1079.71	289.62
TEM 20	33931.91	173.53	1187.26	1190.99	292.84
TEM 21	34178.95	175.84	1351.47	1223.60	292.47
TEM 22	33089.51	173.17	1233.34	1170.40	295.24
TEM 23	34675.03	179.14	1354.77	1124.65	315.98
TEM 24	34151.85	173.35	1356.09	1166.75	308.97
TEM 25	34934.61	177.18	1354.30	1094.51	320.10
TEM 26	33528.52	170.95	1278.04	1138.09	309.38
TEM 27	33652.54	171.15	1268.63	1051.99	333.02
TEM 28	31040.11	167.71	1325.27	1182.57	328.56
TEM 29	32308.76	171.81	1321.67	1081.45	319.27
TEM 30	31004.92	174.97	1303.40	1056.82	335.20
TEM 31	32063.28	171.57	1073.66	931.22	299.83
TEM 32	34175.55	180.27	1341.98	1176.64	317.60
TEM 33	35276.43	171.05	1276.30	1048.03	325.59
TEM 34	26711.15	180.80	1483.44	1040.52	341.28

Table A1. Continued

Regions of Interest	Malignant				
	1	2	3	4	5
Features					
<i>Skewness Texture of Nodule</i>					
TEM 1	-169.79	6.41	13.72	-3.08	0.37
TEM 2	-169.58	5.66	5.44	6.98	3.56
TEM 3	-170.43	6.58	0.23	14.84	3.70
TEM 4	-174.32	6.15	5.47	16.60	3.42
TEM 5	-169.55	5.31	4.85	7.17	3.82
TEM 6	-174.81	5.44	3.78	13.96	4.97
TEM 7	-176.84	5.68	6.98	16.80	4.77
TEM 8	-171.41	4.90	6.27	14.91	5.58
TEM 9	-172.86	4.51	9.09	14.92	5.47
TEM 10	-168.00	4.18	11.09	14.65	6.01
TEM 11	-175.38	4.88	7.91	13.16	5.35
TEM 12	-171.01	4.64	9.36	13.48	6.13
TEM 13	-175.78	5.17	8.59	12.36	6.24
TEM 14	-175.32	5.22	9.36	14.81	4.61
TEM 15	-166.42	6.25	3.12	-3.93	1.84
TEM 16	-170.61	4.95	6.94	12.47	4.54
TEM 17	-168.96	4.52	7.90	14.35	6.19
TEM 18	-164.03	4.01	11.23	17.24	4.63
TEM 19	-172.10	4.89	5.12	7.75	4.96
TEM 20	-176.46	5.01	5.09	12.77	5.45
TEM 21	-177.50	5.55	9.44	15.78	4.80
TEM 22	-173.00	5.00	8.26	11.68	4.90
TEM 23	-179.34	5.84	9.95	12.44	4.80
TEM 24	-177.29	5.09	9.00	13.93	4.67
TEM 25	-180.40	5.77	8.72	11.77	5.85
TEM 26	-174.75	4.72	7.39	12.51	6.47
TEM 27	-175.26	5.19	7.58	10.01	6.84
TEM 28	-164.61	4.36	8.22	13.63	4.91
TEM 29	-169.74	5.19	9.15	11.68	5.76
TEM 30	-163.72	5.90	9.32	10.21	6.88
TEM 31	-169.00	4.47	3.01	-0.92	5.09
TEM 32	-177.33	5.88	11.70	13.41	4.20
TEM 33	-181.80	5.28	5.56	10.95	6.36
TEM 34	-143.04	6.95	11.64	9.93	6.23

Table A1. Continued

Regions of Interest	Malignant				
	1	2	3	4	5
Features					
<i>Mean Texture of Parenchyma</i>					
TEM 1	5.12	2.45	2.70	2.97	4.12
TEM 2	4.89	2.52	3.16	2.58	3.86
TEM 3	4.77	2.44	3.57	2.28	4.38
TEM 4	4.83	2.47	3.48	2.31	4.87
TEM 5	4.75	2.55	2.92	2.60	4.41
TEM 6	4.70	2.55	2.98	2.33	4.57
TEM 7	4.74	2.52	2.97	2.22	4.85
TEM 8	4.55	2.59	2.84	2.34	4.66
TEM 9	4.55	2.62	2.78	2.29	4.83
TEM 10	4.47	2.65	2.72	2.33	4.81
TEM 11	4.56	2.59	2.67	2.32	4.67
TEM 12	4.44	2.61	2.56	2.33	4.88
TEM 13	4.50	2.56	2.62	2.35	5.00
TEM 14	4.53	2.56	2.56	2.28	4.87
TEM 15	4.80	2.48	2.93	3.00	4.16
TEM 16	4.65	2.59	2.87	2.44	4.59
TEM 17	4.49	2.63	2.78	2.31	4.70
TEM 18	4.35	2.66	2.66	2.19	4.79
TEM 19	4.42	2.59	2.88	2.48	4.20
TEM 20	4.54	2.58	2.83	2.35	4.47
TEM 21	4.56	2.53	2.57	2.24	4.79
TEM 22	4.49	2.58	2.75	2.37	4.49
TEM 23	4.85	2.51	2.47	2.31	4.75
TEM 24	4.65	2.57	2.57	2.30	4.98
TEM 25	4.87	2.51	2.56	2.31	4.80
TEM 26	4.54	2.60	2.68	2.32	4.76
TEM 27	4.38	2.56	2.81	2.48	5.06
TEM 28	4.34	2.63	2.51	2.30	5.03
TEM 29	4.15	2.56	2.55	2.37	5.21
TEM 30	3.92	2.49	2.62	2.48	5.22
TEM 31	4.45	2.63	2.95	2.82	3.74
TEM 32	4.76	2.51	2.53	2.30	4.64
TEM 33	4.86	2.55	2.89	2.37	4.84
TEM 34	3.77	2.38	2.43	2.55	5.31

Table A1. Continued

Regions of Interest	Malignant				
	1	2	3	4	5
Features					
<i>Variance Texture of Parenchyma</i>					
TEM 1	4.7E-10	7.9E-08	6.0E-07	1.3E-09	7.0E-09
TEM 2	3.6E-10	2.3E-07	8.1E-07	2.2E-09	1.8E-08
TEM 3	7.5E-10	1.4E-06	9.9E-07	4.1E-09	2.8E-08
TEM 4	5.7E-09	1.4E-05	1.3E-06	9.6E-09	8.4E-08
TEM 5	3.3E-10	1.2E-07	7.6E-07	1.4E-09	9.7E-09
TEM 6	2.3E-10	1.1E-07	1.0E-06	1.5E-09	7.5E-09
TEM 7	2.9E-10	4.1E-07	1.2E-06	1.9E-09	6.8E-09
TEM 8	2.2E-10	1.1E-07	8.3E-07	1.9E-09	3.1E-09
TEM 9	2.5E-10	4.6E-07	8.2E-07	2.2E-09	4.1E-09
TEM 10	2.5E-10	1.0E-06	6.6E-07	2.3E-09	4.3E-09
TEM 11	2.1E-10	1.9E-07	9.5E-07	2.2E-09	4.0E-09
TEM 12	1.0E-10	1.6E-07	7.4E-07	1.7E-09	2.0E-09
TEM 13	9.1E-11	2.1E-07	7.9E-07	1.7E-09	1.5E-09
TEM 14	1.4E-10	1.4E-07	8.6E-07	1.8E-09	3.1E-09
TEM 15	4.3E-10	1.2E-07	9.0E-07	1.6E-09	1.3E-08
TEM 16	2.8E-10	1.1E-07	6.4E-07	1.6E-09	4.6E-09
TEM 17	2.0E-10	2.0E-07	7.1E-07	2.2E-09	2.8E-09
TEM 18	2.8E-10	4.3E-06	6.6E-07	2.2E-09	6.3E-09
TEM 19	2.9E-10	2.8E-07	9.4E-07	2.2E-09	1.2E-08
TEM 20	2.0E-10	1.9E-07	1.1E-06	1.9E-09	7.3E-09
TEM 21	1.4E-10	1.4E-07	1.0E-06	2.0E-09	5.2E-09
TEM 22	3.0E-10	2.6E-07	9.3E-07	2.5E-09	6.4E-09
TEM 23	2.2E-10	2.0E-07	9.5E-07	2.8E-09	3.4E-09
TEM 24	1.4E-10	1.6E-07	8.6E-07	1.9E-09	2.3E-09
TEM 25	1.6E-10	1.7E-07	7.9E-07	2.8E-09	2.5E-09
TEM 26	1.6E-10	1.5E-07	8.0E-07	2.3E-09	2.6E-09
TEM 27	5.7E-11	3.9E-07	6.9E-07	1.8E-09	1.0E-09
TEM 28	7.4E-11	4.3E-07	7.1E-07	1.5E-09	1.8E-09
TEM 29	5.2E-11	4.7E-07	7.8E-07	1.7E-09	1.3E-09
TEM 30	3.3E-11	7.9E-07	7.0E-07	1.8E-09	1.1E-09
TEM 31	3.3E-10	3.2E-07	1.2E-06	2.2E-09	1.9E-08
TEM 32	3.0E-10	2.6E-07	1.0E-06	3.2E-09	4.7E-09
TEM 33	1.2E-10	2.3E-07	6.8E-07	2.8E-09	1.8E-09
TEM 34	5.4E-11	1.6E-06	5.6E-07	2.4E-09	1.6E-09

Table A1. Continued

Regions of Interest	Malignant				
	1	2	3	4	5
Features					
<i>Kurtosis Texture of Parenchyma</i>					
TEM 1	205.89	2.64	466.78	4.94	8.15
TEM 2	143.26	2.90	430.68	4.14	7.78
TEM 3	15.67	2.31	425.64	3.95	2.55
TEM 4	3.47	1.90	343.81	5.01	2.34
TEM 5	229.29	3.19	460.80	4.05	6.60
TEM 6	204.35	3.21	474.36	3.60	5.50
TEM 7	59.82	4.08	404.51	2.73	4.03
TEM 8	193.63	3.42	481.95	3.68	4.86
TEM 9	68.51	3.89	438.55	2.89	4.40
TEM 10	39.47	5.03	443.61	2.79	4.85
TEM 11	249.47	3.40	518.91	3.43	8.79
TEM 12	192.35	2.86	467.46	3.98	7.16
TEM 13	199.27	3.07	484.92	3.48	6.78
TEM 14	222.03	3.06	467.98	3.28	6.87
TEM 15	226.24	2.83	449.99	5.64	6.45
TEM 16	211.53	3.73	469.41	3.95	6.36
TEM 17	156.40	3.24	481.21	3.46	4.73
TEM 18	24.45	7.21	439.88	3.03	3.90
TEM 19	293.52	3.11	495.76	3.06	7.50
TEM 20	258.39	3.17	496.75	3.58	6.69
TEM 21	215.67	2.96	437.07	3.23	5.60
TEM 22	287.80	3.45	514.62	3.15	8.90
TEM 23	252.80	3.22	511.95	3.18	9.24
TEM 24	218.23	2.76	489.09	3.12	6.89
TEM 25	243.57	2.73	508.03	3.29	8.43
TEM 26	230.82	3.27	505.65	3.65	7.53
TEM 27	183.66	3.61	494.83	3.63	6.96
TEM 28	134.29	4.97	450.93	4.64	5.52
TEM 29	132.31	4.10	457.20	3.87	5.05
TEM 30	91.59	3.86	479.79	4.03	5.59
TEM 31	293.43	2.80	497.84	3.53	8.26
TEM 32	272.84	3.65	496.04	3.12	9.52
TEM 33	243.74	3.04	510.18	3.43	7.92
TEM 34	19.40	3.98	458.65	4.14	5.67

Table A1. Continued

Regions of Interest	Malignant				
	1	2	3	4	5
Features					
<i>Skewness Texture of Parenchyma</i>					
TEM 1	-11.95	-0.05	17.39	-1.28	-1.74
TEM 2	-9.14	-0.17	16.10	-0.98	-1.64
TEM 3	-2.29	-0.15	16.12	-0.81	-0.67
TEM 4	-1.37	-0.35	13.57	-1.19	-0.79
TEM 5	-12.40	-0.82	17.07	-1.04	-1.67
TEM 6	-11.54	-0.57	17.50	-0.86	-1.38
TEM 7	-5.22	-1.06	15.59	-0.49	-1.13
TEM 8	-11.35	-0.40	17.73	-0.81	-1.08
TEM 9	-5.92	-1.05	16.62	-0.40	-1.13
TEM 10	-4.85	-1.53	16.66	-0.32	-1.29
TEM 11	-13.06	-0.60	18.53	-0.61	-1.66
TEM 12	-11.14	-0.14	17.37	-0.55	-1.46
TEM 13	-11.40	-0.29	17.94	-0.35	-1.42
TEM 14	-12.03	-0.15	17.36	-0.46	-1.28
TEM 15	-12.38	-0.70	16.77	-1.46	-1.51
TEM 16	-12.01	-0.83	17.35	-0.93	-1.45
TEM 17	-9.82	-0.53	17.74	-0.62	-1.15
TEM 18	-3.88	-2.19	16.62	-0.55	-1.09
TEM 19	-13.71	-0.84	17.79	-0.54	-1.58
TEM 20	-13.02	-0.68	17.90	-0.61	-1.22
TEM 21	-11.61	-0.21	16.51	-0.48	-1.04
TEM 22	-13.76	-0.85	18.22	-0.55	-1.85
TEM 23	-13.42	-0.40	18.56	-0.57	-1.69
TEM 24	-12.04	-0.01	18.04	-0.34	-1.22
TEM 25	-13.30	0.09	18.51	-0.54	-1.52
TEM 26	-12.74	-0.18	18.34	-0.65	-1.37
TEM 27	-10.69	-0.79	18.28	-0.26	-1.62
TEM 28	-8.67	-1.28	17.00	-0.57	-1.42
TEM 29	-8.57	-1.05	17.17	-0.46	-1.43
TEM 30	-6.42	-1.07	17.95	-0.50	-1.48
TEM 31	-13.64	-0.81	18.04	-0.80	-1.71
TEM 32	-13.70	-0.82	17.96	-0.60	-1.91
TEM 33	-13.29	-0.14	18.60	-0.47	-1.42
TEM 34	-2.38	-1.11	17.46	-0.95	-1.37

Table A2. The feature values computed during Feature Extraction for the 7 benign regions of interest from NLST.

Regions of Interest	Benign						
	1	2	3	4	5	6	7
Features							
Demographics							
Age	57	62	58	55	63	55	70
Race	2	2	2	2	2	2	2
Ethnicity	5	5	5	5	5	5	5
Gender	2	2	2	2	1	1	2
Years Smoked	32	43	36	35	52	43	50
Pack Years	30	20	30	30	60	40	20
Intensity							
<i>Nodule</i>							
Mean HU	649.32	-308.36	-313.70	-241.63	-293.06	-371.63	-255.31
Variance	787998.39	68688.14	60228.80	64914.60	75879.60	64193.55	52242.44
Maximum HU	2463.00	75.00	124.00	191.00	326.00	148.00	149.00
Minimum HU	-979.00	-893.00	-808.00	-778.00	-774.00	-831.00	-732.00
Median HU	412.00	-314.00	-318.00	-230.00	-312.00	-431.50	-243.00
FWHM	0.00	0.03	0.01	0.01	0.03	0.01	0.01
Entropy	9.40	8.46	8.15	8.50	7.75	7.85	8.06
Kurtosis	1.97	1.71	1.79	1.84	2.04	1.94	1.86
Skewness	0.51	-0.13	0.03	-0.15	0.24	0.39	-0.12
<i>Parenchyma</i>							
Mean HU	-864.63	-939.75	-895.68	-887.46	-894.04	-907.69	-920.24
Variance	15530.92	2257.95	6188.62	5945.84	4500.89	3944.62	7696.01
Maximum HU	105.00	-593.00	-282.00	-297.00	-316.00	-358.00	-348.00
Minimum HU	-1024.00	-1000.00	-1024.00	-1024.00	-1024.00	-1024.00	-1024.00
Median HU	-890.00	-950.00	-908.00	-904.00	-906.00	-915.00	-939.00
FWHM	0.00	0.14	0.12	0.09	0.10	0.12	0.00
Entropy	8.50	7.18	8.03	7.84	7.76	7.80	7.94
Kurtosis	8.46	9.74	7.75	10.36	10.98	7.85	7.29
Skewness	1.92	2.04	1.61	2.16	2.00	1.41	1.72

Table A2. Continued

Regions of Interest	Benign						
	1	2	3	4	5	6	7
Features							
Shape							
Recist	6.94	7.70	5.47	6.15	6.17	5.03	5.49
Sphericity	1.19	1.12	1.22	1.31	1.31	1.16	1.23
Effective Radius	3.59	3.60	2.81	2.89	2.59	2.63	2.53
<i>Differences</i>							
Mean	0.14	0.09	0.14	0.10	0.14	0.24	0.15
Variance	0.01	0.00	0.02	0.01	0.01	0.07	0.01
Kurtosis	3.78	2.60	8.09	3.78	2.60	8.26	3.28
Skewness	0.96	0.57	2.05	1.09	0.59	2.29	0.80
Range	0.54	0.26	0.74	0.41	0.42	1.34	0.50
Border							
Mean of Slopes	-453.02	-196.37	-284.96	-290.37	-117.66	-153.28	-174.20
Variance of Slopes	28.84	13.97	8.03	37.25	12.67	19.76	14.00

Table A2. Continued

Regions of Interest	Benign						
	1	2	3	4	5	6	7
Features							
Texture							
<i>Mean Texture of Nodule</i>							
TEM 1	4.02	5.91	5.32	1.98	4.11	5.84	5.89
TEM 2	3.99	5.91	5.32	2.01	4.04	5.82	5.88
TEM 3	3.94	5.91	5.33	1.91	4.01	5.82	5.88
TEM 4	4.01	5.91	5.33	1.83	4.04	5.81	5.88
TEM 5	4.33	5.91	5.33	2.01	4.17	5.82	5.87
TEM 6	4.37	5.91	5.32	1.98	4.17	5.83	5.88
TEM 7	4.26	5.91	5.32	1.89	4.18	5.82	5.89
TEM 8	4.25	5.91	5.32	2.00	4.15	5.82	5.88
TEM 9	4.13	5.91	5.31	1.94	4.16	5.82	5.88
TEM 10	4.14	5.91	5.30	1.99	4.15	5.82	5.88
TEM 11	4.37	5.91	5.32	1.97	4.17	5.83	5.88
TEM 12	4.31	5.91	5.32	1.90	4.18	5.82	5.88
TEM 13	4.36	5.91	5.31	1.92	4.16	5.83	5.88
TEM 14	4.30	5.91	5.32	1.88	4.20	5.82	5.89
TEM 15	4.15	5.90	5.32	1.99	4.20	5.83	5.88
TEM 16	4.32	5.91	5.33	2.00	4.11	5.82	5.87
TEM 17	4.17	5.91	5.34	2.01	4.14	5.82	5.88
TEM 18	4.12	5.91	5.28	1.98	4.18	5.82	5.87
TEM 19	4.42	5.91	5.34	1.98	4.17	5.82	5.88
TEM 20	4.46	5.91	5.34	2.00	4.19	5.83	5.89
TEM 21	4.32	5.91	5.34	1.88	4.20	5.82	5.89
TEM 22	4.37	5.91	5.33	1.94	4.14	5.82	5.88
TEM 23	4.45	5.91	5.32	1.96	4.14	5.82	5.88
TEM 24	4.34	5.91	5.32	1.89	4.15	5.82	5.88
TEM 25	4.47	5.91	5.30	1.96	4.16	5.82	5.88
TEM 26	4.36	5.91	5.32	1.96	4.18	5.82	5.88
TEM 27	4.34	5.91	5.30	1.99	4.19	5.83	5.88
TEM 28	4.17	5.91	5.31	1.92	4.15	5.82	5.88
TEM 29	4.28	5.91	5.31	1.94	4.14	5.83	5.87
TEM 30	4.29	5.91	5.30	2.04	4.19	5.83	5.87
TEM 31	4.41	5.91	5.31	2.03	4.29	5.82	5.89
TEM 32	4.43	5.91	5.34	1.91	4.12	5.82	5.88
TEM 33	4.43	5.91	5.29	2.01	4.20	5.81	5.88
TEM 34	4.34	5.90	5.28	2.11	4.11	5.84	5.87

Table A2. Continued

Regions of Interest	Benign						
	1	2	3	4	5	6	7
Features							
<i>Variance Texture of Nodule</i>							
TEM 1	0.06	0.16	0.08	0.04	0.14	0.17	0.12
TEM 2	0.05	0.16	0.08	0.03	0.15	0.17	0.12
TEM 3	0.05	0.15	0.08	0.04	0.14	0.17	0.12
TEM 4	0.04	0.15	0.08	0.04	0.15	0.17	0.12
TEM 5	0.06	0.16	0.08	0.03	0.14	0.17	0.13
TEM 6	0.06	0.17	0.08	0.04	0.14	0.17	0.12
TEM 7	0.06	0.16	0.08	0.04	0.15	0.17	0.12
TEM 8	0.06	0.17	0.08	0.03	0.15	0.17	0.12
TEM 9	0.06	0.16	0.08	0.04	0.14	0.17	0.12
TEM 10	0.07	0.17	0.08	0.04	0.15	0.17	0.12
TEM 11	0.06	0.16	0.08	0.04	0.14	0.17	0.12
TEM 12	0.07	0.17	0.08	0.04	0.14	0.17	0.12
TEM 13	0.08	0.17	0.08	0.04	0.14	0.17	0.12
TEM 14	0.07	0.17	0.08	0.04	0.14	0.17	0.12
TEM 15	0.06	0.16	0.08	0.04	0.14	0.17	0.12
TEM 16	0.06	0.16	0.08	0.03	0.15	0.17	0.13
TEM 17	0.06	0.17	0.08	0.03	0.15	0.17	0.12
TEM 18	0.07	0.16	0.08	0.04	0.14	0.17	0.13
TEM 19	0.06	0.16	0.08	0.04	0.14	0.17	0.12
TEM 20	0.06	0.16	0.08	0.04	0.14	0.17	0.12
TEM 21	0.07	0.16	0.08	0.04	0.14	0.17	0.12
TEM 22	0.06	0.17	0.08	0.04	0.15	0.17	0.12
TEM 23	0.07	0.17	0.08	0.04	0.14	0.17	0.12
TEM 24	0.08	0.17	0.08	0.04	0.14	0.17	0.12
TEM 25	0.07	0.17	0.08	0.04	0.14	0.17	0.12
TEM 26	0.06	0.16	0.08	0.04	0.14	0.17	0.12
TEM 27	0.08	0.17	0.08	0.04	0.14	0.17	0.12
TEM 28	0.08	0.17	0.08	0.04	0.14	0.17	0.12
TEM 29	0.08	0.17	0.08	0.04	0.14	0.17	0.12
TEM 30	0.08	0.17	0.08	0.03	0.14	0.17	0.13
TEM 31	0.06	0.16	0.08	0.03	0.13	0.17	0.12
TEM 32	0.07	0.18	0.08	0.04	0.15	0.17	0.12
TEM 33	0.08	0.17	0.08	0.03	0.13	0.17	0.12
TEM 34	0.09	0.18	0.08	0.03	0.14	0.17	0.12

Table A2. Continued

Regions of Interest	Benign						
	1	2	3	4	5	6	7
Features							
<i>Kurtosis Texture of Nodule</i>							
TEM 1	114.23	158.33	348.42	387.74	73.58	146.76	227.25
TEM 2	126.20	156.73	347.23	383.25	70.19	143.86	223.45
TEM 3	141.64	160.00	347.36	397.70	69.61	148.21	234.90
TEM 4	122.19	162.99	348.19	412.06	69.65	144.15	242.08
TEM 5	148.64	156.27	347.75	383.38	75.98	144.35	209.80
TEM 6	146.81	153.00	347.05	387.45	76.68	147.01	221.44
TEM 7	123.99	157.08	346.92	402.94	75.76	141.20	229.38
TEM 8	132.52	152.57	347.07	383.83	73.65	144.80	218.51
TEM 9	110.70	152.21	346.10	394.59	76.03	142.17	221.85
TEM 10	106.45	149.67	345.80	385.60	74.79	141.87	212.36
TEM 11	131.35	156.17	348.14	390.35	75.56	147.91	227.86
TEM 12	106.42	150.60	347.39	401.74	77.64	144.82	230.67
TEM 13	102.26	150.42	345.69	398.18	76.98	146.17	220.08
TEM 14	108.39	150.73	347.07	405.27	79.35	145.16	236.16
TEM 15	121.32	153.68	346.48	386.55	78.79	146.90	220.66
TEM 16	147.85	156.51	347.45	383.91	72.47	142.60	206.89
TEM 17	120.39	149.89	348.16	382.34	73.56	142.06	217.23
TEM 18	102.07	149.64	344.53	388.31	78.07	144.58	205.85
TEM 19	154.69	159.93	349.12	388.22	76.20	145.39	227.56
TEM 20	146.55	158.55	349.81	385.53	77.51	150.92	230.48
TEM 21	115.02	153.51	348.26	405.10	78.48	144.70	237.38
TEM 22	142.38	155.72	348.14	394.92	73.69	145.30	224.43
TEM 23	119.85	152.34	346.86	392.06	74.94	150.09	217.93
TEM 24	102.23	148.15	346.34	403.37	77.21	146.68	226.34
TEM 25	115.56	153.87	346.24	390.92	76.88	147.16	216.37
TEM 26	125.65	156.69	348.73	390.46	76.42	145.57	228.69
TEM 27	100.75	151.39	345.75	385.81	78.36	142.85	218.38
TEM 28	94.63	151.18	346.82	397.57	76.73	144.46	219.38
TEM 29	98.03	150.13	345.06	394.97	76.56	147.88	212.38
TEM 30	99.66	150.87	345.45	376.93	79.88	146.07	208.75
TEM 31	148.56	161.65	346.55	380.13	87.13	146.03	234.84
TEM 32	127.89	151.30	347.64	399.20	73.23	149.76	220.79
TEM 33	108.69	152.55	346.71	382.57	81.20	138.55	217.35
TEM 34	96.64	147.36	344.46	364.71	77.23	151.39	209.31

Table A2. Continued

Regions of Interest	Benign						
	1	2	3	4	5	6	7
Features							
<i>Skewness Texture of Nodule</i>							
TEM 1	-7.15	-11.75	-18.25	15.01	-6.20	-11.00	-13.79
TEM 2	-7.46	-11.76	-18.20	14.71	-6.05	-10.86	-13.64
TEM 3	-7.50	-11.80	-18.21	15.72	-5.92	-11.08	-14.10
TEM 4	-6.44	-11.92	-18.24	16.60	-6.05	-10.91	-14.37
TEM 5	-8.62	-11.70	-18.22	14.71	-6.44	-10.86	-13.09
TEM 6	-8.50	-11.61	-18.19	15.01	-6.46	-11.01	-13.57
TEM 7	-7.60	-11.72	-18.19	16.02	-6.45	-10.73	-13.87
TEM 8	-7.90	-11.57	-18.19	14.77	-6.31	-10.91	-13.44
TEM 9	-6.93	-11.54	-18.15	15.50	-6.46	-10.78	-13.57
TEM 10	-6.83	-11.44	-18.14	14.90	-6.39	-10.78	-13.20
TEM 11	-7.93	-11.71	-18.24	15.20	-6.40	-11.02	-13.81
TEM 12	-7.07	-11.50	-18.21	15.94	-6.55	-10.89	-13.92
TEM 13	-7.08	-11.48	-18.14	15.70	-6.53	-10.96	-13.50
TEM 14	-7.06	-11.51	-18.19	16.17	-6.63	-10.90	-14.14
TEM 15	-7.19	-11.56	-18.17	14.93	-6.60	-11.00	-13.53
TEM 16	-8.52	-11.70	-18.21	14.75	-6.23	-10.79	-12.97
TEM 17	-7.41	-11.46	-18.24	14.68	-6.28	-10.78	-13.40
TEM 18	-6.83	-11.45	-18.08	15.07	-6.60	-10.89	-12.94
TEM 19	-8.74	-11.84	-18.28	15.04	-6.44	-10.90	-13.80
TEM 20	-8.47	-11.81	-18.31	14.86	-6.52	-11.17	-13.92
TEM 21	-7.29	-11.59	-18.25	16.15	-6.60	-10.87	-14.19
TEM 22	-8.28	-11.69	-18.24	15.50	-6.32	-10.89	-13.67
TEM 23	-7.61	-11.56	-18.18	15.30	-6.37	-11.11	-13.42
TEM 24	-6.93	-11.40	-18.17	16.04	-6.52	-10.97	-13.75
TEM 25	-7.56	-11.62	-18.16	15.22	-6.45	-10.99	-13.36
TEM 26	-7.81	-11.73	-18.26	15.20	-6.44	-10.93	-13.84
TEM 27	-7.13	-11.53	-18.14	14.88	-6.62	-10.82	-13.43
TEM 28	-6.65	-11.53	-18.18	15.68	-6.48	-10.88	-13.47
TEM 29	-6.98	-11.46	-18.11	15.51	-6.50	-11.04	-13.19
TEM 30	-7.07	-11.49	-18.13	14.29	-6.68	-10.97	-13.04
TEM 31	-8.37	-11.93	-18.17	14.47	-7.10	-10.95	-14.10
TEM 32	-7.83	-11.54	-18.22	15.77	-6.33	-11.08	-13.53
TEM 33	-7.46	-11.60	-18.17	14.65	-6.65	-10.61	-13.40
TEM 34	-6.92	-11.35	-18.08	13.42	-6.47	-11.19	-13.05

Table A2. Continued

Regions of Interest	Benign						
	1	2	3	4	5	6	7
Features							
<i>Mean Texture of Parenchyma</i>							
TEM 1	4.02	5.99	5.34	1.98	4.17	5.97	5.99
TEM 2	3.99	5.99	5.34	2.01	4.10	5.94	5.98
TEM 3	3.93	5.98	5.34	1.91	4.05	5.89	5.96
TEM 4	4.00	5.94	5.35	1.83	4.05	5.81	5.93
TEM 5	4.33	6.00	5.35	2.01	4.23	5.98	5.99
TEM 6	4.38	6.00	5.34	1.98	4.23	5.98	5.99
TEM 7	4.26	5.99	5.34	1.89	4.24	5.97	5.99
TEM 8	4.25	6.00	5.34	2.00	4.21	5.97	5.99
TEM 9	4.14	5.99	5.33	1.93	4.22	5.97	5.98
TEM 10	4.14	5.98	5.32	1.99	4.20	5.97	5.98
TEM 11	4.38	6.00	5.34	1.96	4.23	5.98	5.99
TEM 12	4.31	5.99	5.34	1.89	4.24	5.98	5.99
TEM 13	4.36	5.99	5.33	1.92	4.22	5.98	5.99
TEM 14	4.30	6.00	5.34	1.87	4.25	5.98	5.99
TEM 15	4.16	6.00	5.34	1.99	4.27	5.99	5.99
TEM 16	4.32	6.00	5.35	2.00	4.18	5.98	5.99
TEM 17	4.17	5.99	5.36	2.01	4.20	5.97	5.99
TEM 18	4.13	5.98	5.30	1.97	4.23	5.96	5.98
TEM 19	4.42	6.00	5.36	1.98	4.23	5.99	6.00
TEM 20	4.46	6.00	5.36	1.99	4.25	5.98	5.99
TEM 21	4.32	6.00	5.36	1.88	4.26	5.98	5.99
TEM 22	4.38	6.00	5.35	1.94	4.20	5.98	5.99
TEM 23	4.46	6.00	5.34	1.96	4.20	5.98	5.99
TEM 24	4.34	6.00	5.34	1.89	4.20	5.98	5.99
TEM 25	4.47	6.00	5.32	1.96	4.22	5.97	5.99
TEM 26	4.36	6.00	5.34	1.96	4.24	5.98	5.99
TEM 27	4.34	5.99	5.32	1.99	4.25	5.98	5.99
TEM 28	4.18	5.99	5.33	1.92	4.21	5.98	5.99
TEM 29	4.29	5.99	5.33	1.93	4.19	5.98	5.99
TEM 30	4.30	5.99	5.32	2.04	4.24	5.98	5.99
TEM 31	4.41	6.00	5.33	2.03	4.35	5.99	6.00
TEM 32	4.44	6.00	5.36	1.91	4.18	5.98	5.99
TEM 33	4.43	6.00	5.31	2.01	4.25	5.97	5.99
TEM 34	4.35	5.99	5.30	2.11	4.16	5.98	5.98

Table A2. Continued

Regions of Interest	Benign						
	1	2	3	4	5	6	7
Features							
<i>Variance Texture of Parenchyma</i>							
TEM 1	1.9E-04	3.3E-06	3.1E-07	1.3E-09	2.6E-06	1.3E-05	3.0E-06
TEM 2	5.3E-04	1.2E-05	4.1E-07	4.5E-09	1.2E-05	4.2E-05	8.6E-06
TEM 3	1.3E-03	2.1E-04	1.6E-06	2.6E-08	1.4E-04	1.5E-04	3.5E-05
TEM 4	2.1E-03	2.5E-03	6.2E-06	2.7E-07	1.3E-03	8.9E-04	2.8E-04
TEM 5	6.4E-04	1.5E-06	1.5E-06	1.9E-09	2.4E-06	2.6E-05	5.3E-06
TEM 6	7.6E-04	7.4E-06	2.0E-06	5.3E-09	8.5E-06	4.1E-05	7.2E-06
TEM 7	1.1E-03	9.2E-05	2.2E-06	3.8E-08	5.2E-05	9.3E-05	3.5E-05
TEM 8	8.2E-04	1.0E-05	1.7E-06	6.9E-09	1.0E-05	3.8E-05	9.0E-06
TEM 9	1.1E-03	1.3E-04	1.6E-06	4.3E-08	4.1E-05	6.2E-05	3.5E-05
TEM 10	8.6E-04	3.5E-04	1.1E-06	8.4E-08	7.2E-05	7.9E-05	7.2E-05
TEM 11	4.5E-04	1.1E-06	1.8E-06	2.5E-09	2.9E-06	5.1E-05	5.6E-06
TEM 12	5.4E-04	1.7E-05	7.6E-07	5.0E-09	3.5E-06	4.0E-05	6.4E-06
TEM 13	4.6E-04	1.6E-05	6.6E-07	4.2E-09	6.6E-06	3.5E-05	1.2E-05
TEM 14	6.0E-04	7.5E-06	1.2E-06	3.7E-09	3.4E-06	4.3E-05	5.3E-06
TEM 15	4.5E-04	1.9E-06	1.2E-06	3.7E-09	2.6E-06	1.2E-05	5.7E-06
TEM 16	8.1E-04	2.4E-06	1.5E-06	2.1E-09	3.9E-06	3.7E-05	5.8E-06
TEM 17	7.6E-04	3.8E-05	1.3E-06	1.7E-08	2.1E-05	4.0E-05	1.9E-05
TEM 18	7.9E-04	7.0E-04	1.1E-06	2.2E-07	2.1E-04	2.2E-04	2.0E-04
TEM 19	5.5E-04	1.2E-06	2.1E-06	2.7E-09	3.9E-06	4.5E-05	6.1E-06
TEM 20	5.1E-04	1.1E-06	1.8E-06	2.3E-09	3.6E-06	4.7E-05	5.5E-06
TEM 21	6.9E-04	5.5E-06	1.4E-06	4.0E-09	4.5E-06	4.7E-05	5.2E-06
TEM 22	5.1E-04	9.3E-07	2.2E-06	2.8E-09	3.2E-06	5.3E-05	5.9E-06
TEM 23	4.5E-04	1.2E-06	1.6E-06	2.9E-09	3.4E-06	5.6E-05	8.0E-06
TEM 24	5.3E-04	9.1E-06	1.0E-06	3.6E-09	5.0E-06	4.0E-05	9.1E-06
TEM 25	3.9E-04	2.4E-06	1.2E-06	2.7E-09	4.0E-06	4.9E-05	8.4E-06
TEM 26	3.9E-04	2.1E-06	1.4E-06	2.6E-09	2.3E-06	5.1E-05	5.6E-06
TEM 27	3.9E-04	2.5E-05	5.1E-07	5.3E-09	9.4E-06	3.4E-05	1.5E-05
TEM 28	6.8E-04	4.1E-05	4.6E-07	1.3E-08	1.2E-05	3.6E-05	1.4E-05
TEM 29	5.4E-04	4.2E-05	4.4E-07	8.2E-09	1.4E-05	2.9E-05	2.2E-05
TEM 30	4.3E-04	4.4E-05	3.9E-07	9.1E-09	1.5E-05	2.6E-05	2.3E-05
TEM 31	5.4E-04	2.8E-06	2.5E-06	5.7E-09	6.4E-06	3.1E-05	6.9E-06
TEM 32	4.9E-04	9.5E-07	2.3E-06	3.7E-09	3.2E-06	6.1E-05	7.8E-06
TEM 33	3.3E-04	5.4E-06	8.4E-07	2.8E-09	5.7E-06	5.1E-05	9.8E-06
TEM 34	4.4E-04	3.1E-05	5.4E-07	1.2E-08	2.1E-05	4.9E-05	4.0E-05

Table A2. Continued

Regions of Interest	Benign						
	1	2	3	4	5	6	7
Features							
<i>Kurtosis Texture of Parenchyma</i>							
TEM 1	257.26	2.27	4.49	2.35	3.03	4.05	3.06
TEM 2	259.27	2.01	4.81	2.51	2.39	3.50	2.77
TEM 3	258.60	1.87	4.32	2.81	2.00	2.78	2.93
TEM 4	263.20	1.79	3.13	3.11	1.86	2.65	2.65
TEM 5	249.24	3.37	3.87	2.32	2.48	4.40	2.82
TEM 6	247.45	5.04	4.18	2.51	3.69	3.78	2.36
TEM 7	249.59	6.01	4.46	2.86	3.65	3.10	2.96
TEM 8	249.20	6.46	4.50	2.56	3.29	4.57	2.77
TEM 9	255.63	8.22	4.55	2.69	3.68	3.40	3.19
TEM 10	254.01	9.83	4.38	2.77	4.07	3.72	3.49
TEM 11	254.19	2.89	4.11	2.10	2.76	2.92	3.02
TEM 12	255.62	10.27	4.47	3.89	4.80	2.74	2.56
TEM 13	267.67	10.09	4.14	3.47	3.29	2.60	2.54
TEM 14	255.98	9.41	4.19	3.68	4.14	3.04	2.59
TEM 15	250.74	2.86	4.09	2.98	2.67	5.11	3.00
TEM 16	250.90	4.92	4.05	2.72	3.24	4.63	2.45
TEM 17	250.89	7.91	4.87	2.39	3.27	3.36	3.20
TEM 18	260.66	10.21	3.05	2.97	5.02	4.61	4.11
TEM 19	251.40	3.47	4.33	2.35	2.43	4.10	3.44
TEM 20	252.88	3.25	4.07	2.17	2.40	4.20	3.74
TEM 21	250.01	8.88	4.06	3.78	3.96	4.03	2.81
TEM 22	252.39	3.40	4.09	2.06	2.44	3.21	3.50
TEM 23	259.80	3.15	4.13	2.11	3.35	2.46	2.52
TEM 24	267.59	10.21	4.11	3.23	3.42	2.49	2.50
TEM 25	260.61	5.66	4.39	2.08	3.04	2.46	2.52
TEM 26	253.15	4.92	4.32	2.28	3.00	2.61	2.55
TEM 27	264.31	9.05	4.22	3.41	3.35	2.86	2.61
TEM 28	261.06	11.42	4.30	3.22	5.89	3.61	4.04
TEM 29	273.80	10.61	4.03	3.36	4.02	3.08	2.83
TEM 30	270.72	9.29	4.27	3.56	4.06	3.04	2.47
TEM 31	254.08	3.45	5.02	2.30	2.92	5.11	2.68
TEM 32	255.90	3.39	3.88	2.10	3.04	2.61	2.76
TEM 33	255.87	7.00	4.46	2.24	2.65	2.58	2.76
TEM 34	279.26	7.25	4.11	3.59	4.20	2.97	2.43

Table A2. Continued

Regions of Interest	Benign						
	1	2	3	4	5	6	7
Features							
<i>Skewness Texture of Parenchyma</i>							
TEM 1	14.20	-0.29	-1.36	-0.40	-0.38	-0.98	-0.72
TEM 2	14.29	-0.24	-1.24	-0.39	-0.20	-0.78	-0.45
TEM 3	14.27	-0.29	-1.15	-0.33	-0.11	-0.52	0.02
TEM 4	14.49	-0.34	-0.65	0.29	-0.29	-0.27	0.13
TEM 5	13.80	-0.65	-1.28	-0.30	-0.38	-1.07	-0.67
TEM 6	13.73	-1.33	-1.37	-0.27	-1.03	-0.89	-0.37
TEM 7	13.83	-1.68	-1.36	-0.64	-1.07	-0.67	-0.72
TEM 8	13.80	-1.85	-1.42	-0.50	-0.92	-1.15	-0.61
TEM 9	14.10	-2.31	-1.40	-0.74	-1.09	-0.84	-0.93
TEM 10	14.06	-2.70	-1.30	-0.93	-1.22	-1.01	-1.18
TEM 11	14.06	-0.80	-1.23	0.18	0.43	-0.48	-0.46
TEM 12	14.16	-2.73	-1.22	-0.97	-0.88	-0.15	0.11
TEM 13	14.70	-2.63	-1.07	-0.82	-0.64	0.22	0.19
TEM 14	14.15	-2.53	-1.18	-0.67	-0.54	-0.18	0.05
TEM 15	13.87	-0.74	-1.32	-0.70	-0.55	-1.13	-0.88
TEM 16	13.88	-1.28	-1.31	-0.52	-0.72	-1.12	-0.51
TEM 17	13.90	-2.29	-1.48	-0.59	-0.95	-0.80	-0.91
TEM 18	14.33	-2.73	-0.91	-1.10	-1.53	-1.49	-1.53
TEM 19	13.93	-1.00	-1.30	-0.53	-0.17	-0.81	-0.95
TEM 20	14.00	-0.87	-1.25	-0.07	0.20	-0.81	-0.96
TEM 21	13.88	-2.40	-1.18	-0.63	-0.62	-0.47	-0.31
TEM 22	13.98	-0.91	-1.24	-0.01	0.18	-0.67	-0.83
TEM 23	14.32	-0.87	-1.17	0.06	0.18	-0.16	0.00
TEM 24	14.68	-2.62	-1.06	-0.65	-0.52	0.16	0.22
TEM 25	14.38	-1.56	-1.21	-0.06	0.01	0.16	0.14
TEM 26	14.05	-1.42	-1.25	0.05	0.56	-0.21	-0.07
TEM 27	14.58	-2.37	-1.07	-0.79	-0.75	0.27	0.29
TEM 28	14.36	-2.94	-1.13	-1.07	-1.62	-0.26	-0.60
TEM 29	14.94	-2.67	-1.02	-0.92	-1.03	-0.24	-0.09
TEM 30	14.84	-2.39	-1.09	-1.00	-1.10	-0.32	0.23
TEM 31	14.04	-1.11	-1.47	-0.65	-0.71	-0.96	-0.70
TEM 32	14.16	-0.83	-1.16	0.04	0.27	-0.43	-0.35
TEM 33	14.22	-1.91	-1.17	-0.01	-0.29	0.29	0.24
TEM 34	15.21	-1.83	-0.84	-0.95	-1.10	-0.51	0.45

Table A3. The feature values computed during Feature Extraction for the 5 malignant regions of interest from COPDGene.

Regions of Interest	Malignant				
	1	2	3	4	5
Features					
Intensity					
<i>Nodule</i>					
Mean HU	-185.93	-470.10	-396.01	-475.10	-265.27
Variance	53665.71	22831.64	40915.75	27654.46	40645.77
Maximum HU	173.00	-26.00	26.00	-65.00	154.00
Minimum HU	-864.00	-830.00	-763.00	-822.00	-735.00
Median HU	-80.00	-491.00	-433.00	-499.50	-231.00
FWHM	0.06	0.06	0.02	0.02	0.03
Entropy	9.26	8.59	8.53	7.99	7.48
Kurtosis	2.56	2.55	1.98	2.35	2.30
Skewness	-0.87	0.47	0.34	0.41	-0.20
<i>Parenchyma</i>					
Mean HU	-815.72	-834.83	-846.01	-884.56	-899.65
Variance	8958.72	4307.72	2711.02	3552.85	18306.52
Maximum HU	-189.00	-481.00	-335.00	-304.00	-44.00
Minimum HU	-1024.00	-1004.00	-933.00	-979.00	-1024.00
Median HU	-821.00	-849.00	-857.00	-899.00	-931.00
FWHM	0.17	0.15	0.12	0.08	0.08
Entropy	8.51	7.87	7.39	7.44	7.92
Kurtosis	5.01	5.04	9.42	13.43	21.72
Skewness	0.80	1.21	1.96	2.50	4.02
Shape					
Recist	17.410485	9.5372085	7.6699022	5.0779499	7.7118502
Sphericity	1.074044	0.9182396	1.1860947	1.1399446	1.1426534
Effective Radius	7.4344159	4.3197343	3.5649466	2.7334185	3.1197049
<i>Differences</i>					
Mean	0.14	0.23	0.14	0.32	0.23
Variance	0.01	0.05	0.02	0.10	0.03
Kurtosis	3.31	3.72	10.26	4.35	3.80
Skewness	0.84	1.24	2.51	1.50	1.00
Range	0.56	0.95	0.72	1.31	0.86
Border					
Mean of Slopes	-56.24	-52.88	-142.34	-157.39	-227.67
Variance of Slopes	5.09	0.92	7.85	10.35	10.35

Table A3. Continued

Regions of Interest	Malignant				
	1	2	3	4	5
Features					
<i>Mean Texture of Nodule</i>					
TEM 1	3.49	2.25	5.33	0.77	1.25
TEM 2	3.64	1.64	5.33	0.86	0.83
TEM 3	3.00	1.67	5.27	1.05	0.57
TEM 4	3.25	1.87	5.31	1.35	0.47
TEM 5	3.39	1.79	5.27	0.96	0.62
TEM 6	3.32	1.86	5.25	1.04	0.49
TEM 7	3.26	1.83	5.30	1.45	0.48
TEM 8	3.44	1.70	5.27	0.94	0.50
TEM 9	3.23	1.75	5.29	1.23	0.48
TEM 10	3.41	1.70	5.28	1.05	0.48
TEM 11	3.44	1.65	5.28	0.80	0.42
TEM 12	3.34	1.65	5.29	0.96	0.47
TEM 13	3.36	1.62	5.31	0.82	0.45
TEM 14	3.26	1.61	5.28	0.98	0.50
TEM 15	3.42	2.08	5.20	0.89	0.83
TEM 16	3.37	1.74	5.28	0.98	0.53
TEM 17	3.62	1.63	5.26	0.81	0.50
TEM 18	3.25	1.76	5.29	1.14	0.47
TEM 19	3.28	1.94	5.28	0.90	0.45
TEM 20	3.35	1.87	5.27	0.90	0.44
TEM 21	3.26	1.72	5.29	1.16	0.50
TEM 22	3.35	1.76	5.27	0.87	0.41
TEM 23	3.46	1.61	5.29	0.67	0.38
TEM 24	3.30	1.59	5.28	0.86	0.49
TEM 25	3.51	1.55	5.31	0.65	0.39
TEM 26	3.49	1.58	5.29	0.74	0.42
TEM 27	3.46	1.68	5.32	0.74	0.40
TEM 28	3.22	1.68	5.29	1.15	0.48
TEM 29	3.22	1.65	5.30	0.94	0.47
TEM 30	3.35	1.79	5.30	0.78	0.43
TEM 31	3.36	2.11	5.25	0.78	0.48
TEM 32	3.37	1.70	5.27	0.78	0.37
TEM 33	3.55	1.53	5.31	0.62	0.36
TEM 34	3.30	1.89	5.24	0.64	0.48

Table A3. Continued

Regions of Interest	Malignant				
	1	2	3	4	5
Features					
<i>Variance Texture of Nodule</i>					
TEM 1	2.2E-03	5.0E-07	4.9E-01	1.0E-05	6.2E-06
TEM 2	2.4E-03	1.0E-06	4.9E-01	7.4E-06	3.2E-06
TEM 3	1.7E-03	7.6E-07	4.8E-01	3.6E-06	1.3E-06
TEM 4	2.0E-03	2.4E-07	3.8E-01	2.4E-06	4.7E-07
TEM 5	2.2E-03	9.8E-07	4.8E-01	7.2E-06	9.4E-07
TEM 6	2.1E-03	6.3E-07	5.2E-01	4.3E-06	5.6E-07
TEM 7	2.0E-03	3.0E-07	4.8E-01	2.2E-06	3.6E-07
TEM 8	2.3E-03	5.2E-07	5.0E-01	4.7E-06	3.8E-07
TEM 9	2.0E-03	2.9E-07	4.8E-01	3.1E-06	2.8E-07
TEM 10	2.2E-03	2.6E-07	4.9E-01	3.3E-06	2.8E-07
TEM 11	2.2E-03	4.6E-07	5.0E-01	3.6E-06	2.6E-07
TEM 12	2.1E-03	2.5E-07	4.9E-01	3.0E-06	2.5E-07
TEM 13	2.1E-03	2.4E-07	4.9E-01	3.4E-06	2.0E-07
TEM 14	2.0E-03	2.9E-07	5.1E-01	2.6E-06	2.6E-07
TEM 15	2.2E-03	9.2E-07	5.3E-01	1.0E-05	1.7E-06
TEM 16	2.2E-03	8.3E-07	4.8E-01	6.3E-06	5.3E-07
TEM 17	2.4E-03	3.8E-07	5.2E-01	4.0E-06	3.3E-07
TEM 18	2.0E-03	1.9E-07	4.7E-01	3.3E-06	2.5E-07
TEM 19	2.1E-03	9.9E-07	4.8E-01	6.6E-06	4.4E-07
TEM 20	2.1E-03	6.2E-07	5.0E-01	3.9E-06	3.4E-07
TEM 21	2.0E-03	3.4E-07	4.9E-01	2.4E-06	2.8E-07
TEM 22	2.2E-03	7.3E-07	5.0E-01	5.5E-06	2.8E-07
TEM 23	2.3E-03	4.2E-07	5.1E-01	3.4E-06	2.0E-07
TEM 24	2.1E-03	3.1E-07	5.2E-01	3.1E-06	2.2E-07
TEM 25	2.3E-03	3.3E-07	4.9E-01	3.3E-06	1.7E-07
TEM 26	2.3E-03	3.4E-07	4.9E-01	3.1E-06	2.4E-07
TEM 27	2.3E-03	2.1E-07	4.9E-01	3.8E-06	1.7E-07
TEM 28	2.0E-03	1.8E-07	5.0E-01	2.8E-06	2.4E-07
TEM 29	2.0E-03	1.5E-07	5.1E-01	3.0E-06	1.9E-07
TEM 30	2.1E-03	1.6E-07	5.1E-01	3.6E-06	1.7E-07
TEM 31	2.2E-03	1.4E-06	5.1E-01	8.0E-06	7.4E-07
TEM 32	2.2E-03	6.1E-07	5.3E-01	4.7E-06	2.2E-07
TEM 33	2.4E-03	2.8E-07	4.9E-01	3.6E-06	1.4E-07
TEM 34	2.0E-03	1.7E-07	5.6E-01	3.6E-06	2.2E-07

Table A3. Continued

Regions of Interest	Malignant				
	1	2	3	4	5
Features					
<i>Kurtosis Texture of Nodule</i>					
TEM 1	5210.84	4.98	18.26	4.85	16.64
TEM 2	5116.82	4.28	18.26	3.42	17.03
TEM 3	4521.32	4.29	18.24	2.74	16.53
TEM 4	4578.10	4.43	17.52	4.10	15.53
TEM 5	4818.79	4.53	17.63	4.47	16.13
TEM 6	4647.00	4.53	16.78	4.86	16.27
TEM 7	4704.67	4.97	18.25	5.14	15.20
TEM 8	4593.27	5.12	17.49	5.07	14.94
TEM 9	4688.56	5.82	18.17	5.37	14.82
TEM 10	4848.70	6.49	17.94	5.35	14.32
TEM 11	4744.45	5.54	17.25	4.92	15.60
TEM 12	4739.36	6.16	17.92	4.99	14.85
TEM 13	4725.50	5.84	17.81	5.10	14.39
TEM 14	4651.90	5.85	17.51	5.08	14.61
TEM 15	4898.93	5.15	15.53	4.61	17.88
TEM 16	4601.23	4.54	17.93	4.76	14.51
TEM 17	4883.82	6.03	17.11	5.05	15.83
TEM 18	4799.68	6.89	18.35	5.49	15.06
TEM 19	4538.08	4.39	17.71	4.47	16.15
TEM 20	4665.35	5.31	17.25	4.74	17.01
TEM 21	4693.70	5.67	17.82	5.04	15.46
TEM 22	4572.38	4.83	17.14	4.72	15.47
TEM 23	4803.15	6.09	17.30	5.05	15.70
TEM 24	4705.43	5.83	17.41	5.06	13.70
TEM 25	4852.19	6.28	17.60	5.00	15.76
TEM 26	4890.71	6.12	17.48	4.85	15.76
TEM 27	4755.79	5.70	17.90	5.02	14.38
TEM 28	4717.64	6.09	17.72	5.14	14.40
TEM 29	4706.65	5.55	17.32	5.24	14.38
TEM 30	4736.94	5.53	17.42	5.24	13.89
TEM 31	4633.01	4.21	16.46	4.61	18.22
TEM 32	4709.38	5.62	17.02	4.91	15.68
TEM 33	4815.73	6.15	17.69	4.89	15.05
TEM 34	4928.99	5.94	16.47	5.27	14.93

Table A3. Continued

Regions of Interest	Malignant				
	1	2	3	4	5
Features					
<i>Skewness Texture of Nodule</i>					
TEM 1	-70.28	-1.33	-3.49	-1.41	-3.10
TEM 2	-69.41	-1.23	-3.49	-0.88	-3.18
TEM 3	-63.78	-1.23	-3.50	-0.72	-3.14
TEM 4	-64.43	-1.25	-3.34	-1.35	-2.97
TEM 5	-66.62	-1.23	-3.39	-1.32	-3.04
TEM 6	-65.06	-1.25	-3.33	-1.46	-3.07
TEM 7	-65.58	-1.38	-3.46	-1.54	-2.99
TEM 8	-64.57	-1.37	-3.40	-1.52	-2.94
TEM 9	-65.42	-1.54	-3.46	-1.60	-2.94
TEM 10	-66.92	-1.65	-3.45	-1.59	-2.87
TEM 11	-65.98	-1.47	-3.35	-1.40	-3.03
TEM 12	-65.89	-1.58	-3.44	-1.44	-2.94
TEM 13	-65.79	-1.52	-3.42	-1.49	-2.91
TEM 14	-65.08	-1.52	-3.40	-1.46	-2.93
TEM 15	-67.36	-1.33	-3.17	-1.35	-3.22
TEM 16	-64.62	-1.25	-3.42	-1.39	-2.89
TEM 17	-67.27	-1.54	-3.37	-1.52	-3.03
TEM 18	-66.44	-1.68	-3.48	-1.62	-2.96
TEM 19	-64.02	-1.19	-3.40	-1.27	-3.08
TEM 20	-65.25	-1.40	-3.36	-1.36	-3.17
TEM 21	-65.49	-1.50	-3.42	-1.46	-3.03
TEM 22	-64.37	-1.30	-3.33	-1.33	-3.01
TEM 23	-66.52	-1.61	-3.36	-1.45	-3.05
TEM 24	-65.60	-1.54	-3.39	-1.46	-2.85
TEM 25	-66.97	-1.61	-3.39	-1.46	-3.06
TEM 26	-67.33	-1.57	-3.38	-1.39	-3.03
TEM 27	-66.07	-1.43	-3.43	-1.50	-2.90
TEM 28	-65.68	-1.53	-3.43	-1.50	-2.92
TEM 29	-65.59	-1.38	-3.39	-1.54	-2.92
TEM 30	-65.88	-1.31	-3.40	-1.56	-2.87
TEM 31	-64.88	-1.15	-3.27	-1.29	-3.26
TEM 32	-65.64	-1.52	-3.32	-1.39	-3.04
TEM 33	-66.63	-1.53	-3.41	-1.46	-2.99
TEM 34	-67.68	-1.37	-3.30	-1.55	-3.01

Table A3. Continued

Regions of Interest	Malignant				
	1	2	3	4	5
Features					
<i>Mean Texture of Parenchyma</i>					
TEM 1	3.49	2.25	5.86	0.78	1.26
TEM 2	3.64	1.64	5.72	0.86	0.83
TEM 3	3.00	1.67	5.25	1.04	0.57
TEM 4	3.26	1.87	4.55	1.35	0.47
TEM 5	3.39	1.79	5.92	0.96	0.63
TEM 6	3.32	1.87	5.88	1.05	0.49
TEM 7	3.26	1.83	5.83	1.45	0.48
TEM 8	3.44	1.70	5.88	0.94	0.50
TEM 9	3.23	1.75	5.83	1.24	0.48
TEM 10	3.42	1.70	5.80	1.05	0.48
TEM 11	3.44	1.65	5.93	0.80	0.42
TEM 12	3.34	1.65	5.91	0.96	0.47
TEM 13	3.36	1.62	5.91	0.82	0.45
TEM 14	3.26	1.61	5.92	0.99	0.50
TEM 15	3.42	2.08	5.94	0.89	0.83
TEM 16	3.37	1.74	5.91	0.98	0.53
TEM 17	3.62	1.63	5.85	0.81	0.50
TEM 18	3.25	1.76	5.73	1.14	0.47
TEM 19	3.28	1.94	5.94	0.90	0.45
TEM 20	3.35	1.87	5.93	0.90	0.44
TEM 21	3.26	1.72	5.92	1.16	0.50
TEM 22	3.35	1.77	5.94	0.87	0.41
TEM 23	3.46	1.61	5.94	0.68	0.38
TEM 24	3.30	1.59	5.91	0.86	0.49
TEM 25	3.52	1.55	5.93	0.65	0.39
TEM 26	3.49	1.58	5.93	0.75	0.42
TEM 27	3.46	1.68	5.90	0.74	0.40
TEM 28	3.22	1.69	5.90	1.15	0.48
TEM 29	3.23	1.65	5.90	0.95	0.47
TEM 30	3.35	1.79	5.89	0.78	0.43
TEM 31	3.36	2.11	5.94	0.79	0.48
TEM 32	3.37	1.71	5.94	0.78	0.37
TEM 33	3.55	1.53	5.92	0.63	0.36
TEM 34	3.30	1.90	5.88	0.64	0.48

Table A3. Continued

Regions of Interest	Malignant				
	1	2	3	4	5
Features					
<i>Variance Texture of Parenchyma</i>					
TEM 1	1.0E-10	4.3E-08	7.2E-04	2.8E-07	1.2E-08
TEM 2	1.5E-10	2.0E-07	2.3E-03	5.2E-07	8.2E-09
TEM 3	3.0E-10	6.4E-07	1.7E-02	1.4E-06	1.4E-08
TEM 4	6.6E-10	1.7E-06	7.8E-02	8.1E-06	2.3E-08
TEM 5	1.1E-10	3.7E-08	1.6E-03	2.5E-07	2.4E-09
TEM 6	1.3E-10	6.1E-08	4.2E-03	6.2E-07	1.6E-09
TEM 7	1.3E-10	1.1E-07	1.3E-02	2.2E-06	1.6E-09
TEM 8	7.5E-11	4.4E-08	4.3E-03	1.1E-06	6.3E-10
TEM 9	5.4E-11	6.5E-08	1.1E-02	3.5E-06	7.5E-10
TEM 10	3.6E-11	7.3E-08	1.7E-02	6.9E-06	6.5E-10
TEM 11	3.9E-11	1.6E-08	9.3E-04	2.0E-07	4.2E-10
TEM 12	1.9E-11	4.0E-09	1.1E-03	3.0E-07	4.0E-10
TEM 13	1.8E-11	5.3E-09	1.1E-03	2.9E-07	3.4E-10
TEM 14	2.2E-11	5.6E-09	1.1E-03	2.0E-07	4.6E-10
TEM 15	1.0E-10	2.9E-08	9.7E-04	1.3E-07	6.0E-09
TEM 16	9.5E-11	3.4E-08	2.2E-03	5.7E-07	9.2E-10
TEM 17	4.8E-11	5.5E-08	7.3E-03	2.1E-06	5.9E-10
TEM 18	4.0E-11	7.3E-08	3.3E-02	1.5E-05	7.1E-10
TEM 19	8.6E-11	2.7E-08	7.0E-04	2.4E-07	9.8E-10
TEM 20	6.1E-11	2.1E-08	9.4E-04	1.6E-07	6.8E-10
TEM 21	3.0E-11	8.6E-09	1.2E-03	1.7E-07	6.0E-10
TEM 22	6.6E-11	2.6E-08	8.1E-04	2.9E-07	5.5E-10
TEM 23	2.5E-11	1.4E-08	1.0E-03	2.3E-07	2.9E-10
TEM 24	1.9E-11	6.0E-09	1.2E-03	2.1E-07	3.9E-10
TEM 25	1.9E-11	9.9E-09	1.0E-03	2.2E-07	2.7E-10
TEM 26	2.6E-11	9.5E-09	9.6E-04	1.9E-07	3.3E-10
TEM 27	1.8E-11	6.3E-09	1.2E-03	3.8E-07	3.1E-10
TEM 28	2.0E-11	2.9E-09	1.5E-03	6.1E-07	6.2E-10
TEM 29	2.1E-11	4.3E-09	1.3E-03	4.7E-07	4.7E-10
TEM 30	2.0E-11	6.4E-09	1.2E-03	5.3E-07	4.4E-10
TEM 31	9.0E-11	2.5E-08	6.4E-04	2.3E-07	2.0E-09
TEM 32	4.1E-11	2.3E-08	9.7E-04	3.5E-07	3.6E-10
TEM 33	1.8E-11	9.2E-09	1.2E-03	2.9E-07	2.8E-10
TEM 34	2.2E-11	9.7E-09	1.8E-03	6.0E-07	8.7E-10

Table A3. Continued

Regions of Interest	Malignant				
	1	2	3	4	5
Features					
<i>Kurtosis Texture of Parenchyma</i>					
TEM 1	99.52	3.21	2.59	2.44	6.60
TEM 2	107.28	2.34	2.79	3.00	2.51
TEM 3	77.52	2.51	2.92	2.81	2.28
TEM 4	106.84	2.89	2.73	2.14	2.48
TEM 5	40.03	3.38	3.70	3.36	10.67
TEM 6	61.51	3.54	3.91	2.36	5.35
TEM 7	119.89	3.11	3.98	2.40	3.02
TEM 8	48.07	2.74	4.15	2.87	3.65
TEM 9	107.88	3.03	3.99	2.57	2.83
TEM 10	101.31	2.81	4.15	2.64	3.39
TEM 11	26.32	6.24	4.02	3.41	6.34
TEM 12	79.14	3.39	6.05	4.75	3.34
TEM 13	74.48	2.36	4.03	4.64	3.04
TEM 14	70.07	5.17	5.34	3.48	5.77
TEM 15	40.56	3.07	4.75	2.83	9.71
TEM 16	30.18	2.65	3.89	3.88	8.34
TEM 17	64.89	2.59	4.04	2.61	3.43
TEM 18	96.83	2.86	4.89	3.49	3.58
TEM 19	12.29	4.75	3.83	2.45	9.48
TEM 20	22.90	6.18	4.52	2.71	7.34
TEM 21	61.89	5.99	6.61	3.02	6.75
TEM 22	13.66	5.49	3.38	3.15	9.02
TEM 23	27.59	6.15	3.43	4.13	4.15
TEM 24	69.05	2.72	3.87	3.93	5.08
TEM 25	44.30	4.90	3.67	4.75	2.95
TEM 26	46.28	5.80	4.51	3.69	3.87
TEM 27	72.90	2.35	4.39	4.86	2.39
TEM 28	122.54	3.54	6.80	7.03	2.16
TEM 29	101.03	2.37	4.56	6.06	2.41
TEM 30	87.03	2.08	4.40	6.15	2.25
TEM 31	10.01	5.20	3.89	1.99	8.23
TEM 32	14.83	5.76	3.01	3.72	5.87
TEM 33	50.95	3.26	3.62	4.89	2.53
TEM 34	112.48	2.05	3.40	6.93	2.54

Table A3. Continued

Regions of Interest	Malignant				
	1	2	3	4	5
Features					
<i>Skewness Texture of Parenchyma</i>					
TEM 1	-7.41	-1.10	-0.63	0.23	-1.73
TEM 2	-7.54	-0.96	-0.60	0.06	-0.61
TEM 3	-6.08	-1.11	-0.73	-0.82	-0.66
TEM 4	-7.29	-1.30	-0.73	-0.78	-0.88
TEM 5	-4.18	-1.00	-0.93	-0.91	-2.40
TEM 6	-5.38	-1.21	-1.04	-0.76	-1.43
TEM 7	-8.24	-1.29	-1.06	-0.79	-0.95
TEM 8	-4.58	-1.04	-1.10	-0.88	-0.86
TEM 9	-7.39	-1.23	-1.04	-0.86	-0.71
TEM 10	-6.98	-1.17	-1.10	-0.90	-0.75
TEM 11	-3.05	-1.89	-0.83	-0.69	-1.18
TEM 12	-5.92	-0.75	-1.18	-1.27	-0.52
TEM 13	-5.51	-0.62	-0.73	-1.25	-0.49
TEM 14	-5.46	-1.39	-1.10	-0.74	-1.19
TEM 15	-4.22	-0.83	-1.17	-0.49	-2.41
TEM 16	-3.58	-0.89	-0.98	-1.14	-1.72
TEM 17	-5.33	-1.04	-1.09	-0.83	-0.83
TEM 18	-6.82	-1.24	-1.30	-1.17	-0.86
TEM 19	-2.17	-1.58	-0.74	-0.47	-2.04
TEM 20	-2.95	-1.84	-0.91	-0.32	-1.54
TEM 21	-5.14	-1.66	-1.39	-0.49	-1.52
TEM 22	-2.22	-1.76	-0.72	-0.76	-1.78
TEM 23	-2.81	-1.86	-0.77	-0.95	-0.66
TEM 24	-5.23	-0.79	-0.76	-0.86	-1.07
TEM 25	-3.65	-1.45	-0.77	-1.13	-0.27
TEM 26	-4.13	-1.70	-0.88	-0.70	-0.63
TEM 27	-5.45	-0.55	-0.75	-1.40	-0.24
TEM 28	-8.01	-0.82	-1.43	-2.05	0.01
TEM 29	-7.00	-0.52	-0.80	-1.81	-0.07
TEM 30	-6.37	-0.37	-0.66	-1.85	0.20
TEM 31	-1.98	-1.59	-0.68	-0.39	-1.99
TEM 32	-2.11	-1.78	-0.70	-1.00	-1.13
TEM 33	-3.90	-0.86	-0.73	-1.30	-0.10
TEM 34	-7.54	-0.31	-0.56	-1.93	0.16

Table A4. The feature values computed during Feature Extraction for the 10 benign regions of interest from COPDGene.

Regions of Interest	Benign									
	1	2	3	4	5	6	7	8	9	10
Features										
Intensity										
<i>Nodule</i>										
Mean HU	-329.9	-167.2	-245.3	-286.4	-476.3	-233.1	-317.1	-396.7	-163.5	-346.5
Variance	4.0E4	5.1E4	3.6E4	6.8E4	5.8E4	5.4E4	7.5E4	4.9E4	4.7E4	5.5E4
Maximum HU	22.0	125.0	49.0	64.0	132.0	74.0	167.0	117.0	139.0	87.0
Minimum HU	-806.0	-830.0	-735.0	-881.0	-937.0	-886.0	-885.0	-934.0	-773.0	-756.0
Median HU	-327.0	-89.0	-206.5	-248.0	-534.0	-162.0	-334.5	-421.0	-77.0	-379.5
FWHM	0.18	0.06	0.04	0.01	0.09	0.03	0.01	0.03	0.03	0.03
Entropy	9.23	9.28	8.77	8.86	9.62	9.01	8.98	9.36	8.95	7.65
Kurtosis	1.93	2.40	2.12	1.79	2.35	2.17	1.83	2.25	2.34	1.81
Skewness	-0.18	-0.76	-0.50	-0.36	0.60	-0.63	0.04	0.26	-0.78	0.12
<i>Parenchyma</i>										
Mean HU	-823.0	-828.2	-828.8	-872.9	-888.6	-895.4	-863.5	-851.3	-841.1	-893.6
Variance	5.2E3	8.3E3	9.3E3	2.8E3	3.2E3	8.7E3	5.8E3	6.1E3	1.6E4	5.9E3
Maximum HU	-41.0	-50.0	-199.0	-420.0	-413.0	-319.0	-276.0	-306.0	195.0	40.0
Minimum HU	-952.0	-986.0	-1.0E3	-1.0E3	-1.0E3	-1.0E3	-1.0E3	-1.0E3	-992.0	-1.0E3
Median HU	-840.0	-855.0	-845.0	-884.0	-900.0	-913.0	-882.0	-871.0	-885.0	-915.0
FWHM	0.09	0.08	0.16	0.08	0.10	0.17	0.11	0.11	0.05	0.04
Entropy	7.72	8.06	8.43	7.32	7.58	8.27	7.86	7.96	8.03	7.48
Kurtosis	24.17	10.77	5.55	11.75	8.09	5.87	8.96	7.82	17.52	36.27
Skewness	3.26	2.26	1.21	2.33	1.75	1.41	2.03	1.87	3.27	4.19
Shape										
Recist	11.02	15.97	8.46	8.96	17.69	9.48	10.73	12.70	10.01	5.14
Sphericity	0.82	0.97	1.16	1.18	0.76	1.19	1.14	0.79	1.17	1.34
Effective Radius	5.44	7.70	4.30	4.42	6.99	5.09	3.99	5.77	5.11	2.55
<i>Differences</i>										
Mean	0.42	0.17	0.16	0.14	0.26	0.13	0.16	0.49	0.17	0.17
Variance	0.11	0.01	0.01	0.02	0.04	0.01	0.01	0.18	0.02	0.02
Kurtosis	3.50	3.13	2.69	7.62	3.23	3.72	2.43	3.00	3.68	7.42
Skewness	1.03	0.65	0.64	2.06	0.85	0.94	0.48	1.03	1.08	1.86
Range	1.55	0.56	0.47	0.73	0.96	0.46	0.51	1.75	0.64	0.78
Border										
Mean of Slopes	-99.51	-133.2	-183.4	-259.5	-45.1	-334.6	-129.5	-17.5	16.7	-224.4
Variance of Slopes	6.20	7.39	20.15	12.53	5.88	24.55	4.24	9.94	7.88	12.28

Table A4. Continued

Regions of Interest	Benign									
	1	2	3	4	5	6	7	8	9	10
Features										
<i>Mean of Nodule</i>										
TEM 1	0.66	2.58	5.58	0.25	3.98	4.02	0.75	3.24	3.27	0.14
TEM 2	0.68	2.38	5.65	0.23	4.17	4.14	0.87	2.92	2.59	0.14
TEM 3	0.83	2.30	5.55	0.26	4.18	4.14	1.12	3.37	2.94	0.13
TEM 4	0.94	2.44	5.62	0.25	4.20	4.06	1.48	3.45	3.34	0.18
TEM 5	0.77	2.44	5.58	0.24	4.07	4.00	0.84	3.07	3.19	0.14
TEM 6	0.88	2.38	5.62	0.25	4.12	4.02	1.09	3.43	3.36	0.14
TEM 7	0.90	2.45	5.63	0.26	4.22	4.02	1.27	3.55	3.49	0.17
TEM 8	0.90	2.32	5.63	0.24	4.23	4.12	1.06	3.58	3.53	0.15
TEM 9	0.95	2.32	5.65	0.26	4.21	4.03	1.19	3.65	3.66	0.16
TEM 10	0.97	2.17	5.67	0.26	4.16	4.09	1.07	3.60	3.78	0.17
TEM 11	0.90	2.42	5.65	0.21	4.03	4.02	1.12	3.52	3.28	0.16
TEM 12	0.92	2.41	5.66	0.22	4.09	3.96	1.11	3.54	3.67	0.17
TEM 13	0.97	2.46	5.67	0.23	4.12	3.99	1.15	3.38	3.73	0.18
TEM 14	0.96	2.47	5.65	0.24	4.05	3.99	1.17	3.54	3.59	0.17
TEM 15	0.67	2.32	5.54	0.24	3.93	3.74	0.64	2.78	3.46	0.14
TEM 16	0.85	2.38	5.59	0.24	4.24	4.07	1.00	3.35	3.33	0.15
TEM 17	0.97	2.16	5.65	0.24	4.23	4.11	1.07	3.60	3.70	0.14
TEM 18	0.92	2.20	5.70	0.26	4.03	4.14	1.00	3.55	3.81	0.19
TEM 19	0.80	2.24	5.62	0.22	3.90	4.12	0.92	3.17	3.11	0.16
TEM 20	0.89	2.38	5.65	0.21	4.01	4.05	1.10	3.52	3.23	0.15
TEM 21	0.93	2.37	5.64	0.24	4.10	4.06	1.21	3.62	3.48	0.16
TEM 22	0.86	2.30	5.63	0.22	3.88	4.16	1.09	3.38	3.11	0.16
TEM 23	0.97	2.42	5.64	0.22	4.03	3.97	1.22	3.52	3.38	0.17
TEM 24	1.00	2.54	5.66	0.24	4.10	3.94	1.17	3.42	3.66	0.17
TEM 25	1.01	2.45	5.65	0.21	4.13	3.96	1.23	3.46	3.52	0.17
TEM 26	0.91	2.44	5.66	0.21	4.11	3.99	1.10	3.52	3.42	0.16
TEM 27	0.98	2.44	5.68	0.22	4.07	4.17	1.20	3.38	3.79	0.19
TEM 28	0.89	2.40	5.67	0.23	4.13	4.02	1.11	3.62	3.93	0.18
TEM 29	0.91	2.36	5.70	0.24	4.13	4.10	1.21	3.52	4.02	0.19
TEM 30	0.89	2.35	5.70	0.23	4.01	4.27	1.28	3.53	4.07	0.20
TEM 31	0.71	2.10	5.61	0.23	4.02	4.06	0.67	2.76	3.20	0.15
TEM 32	0.96	2.31	5.63	0.22	3.80	4.15	1.22	3.50	3.12	0.17
TEM 33	1.07	2.52	5.67	0.21	4.14	4.02	1.29	3.38	3.59	0.19
TEM 34	0.79	2.42	5.72	0.24	3.87	4.14	1.45	3.68	4.12	0.20

Table A4. Continued

Regions of Interest	Benign									
	1	2	3	4	5	6	7	8	9	10
Features										
<i>Variance</i>										
<i>Texture of Nodule</i>										
TEM 1	2.4E-6	6.2E-3	2.8E-1	4.1E-2	7.1E-3	1.5E-2	5.4E-3	5.3E-3	6.5E-3	2.5E-6
TEM 2	6.1E-7	5.6E-3	2.4E-1	4.0E-2	6.9E-3	1.5E-2	7.7E-3	3.5E-3	8.9E-3	2.6E-6
TEM 3	1.7E-7	5.1E-3	2.9E-1	4.2E-2	6.0E-3	1.6E-2	6.6E-3	1.5E-3	7.7E-3	2.4E-6
TEM 4	8.0E-8	4.4E-3	2.4E-1	4.0E-2	6.5E-3	1.5E-2	2.7E-3	3.5E-4	5.3E-3	1.5E-6
TEM 5	3.3E-7	8.3E-3	2.8E-1	4.1E-2	7.5E-3	1.5E-2	3.4E-3	1.7E-3	6.0E-3	1.4E-6
TEM 6	1.2E-7	8.0E-3	2.5E-1	4.1E-2	7.0E-3	1.5E-2	4.1E-3	9.2E-4	5.6E-3	1.3E-6
TEM 7	5.3E-8	7.0E-3	2.5E-1	4.1E-2	6.7E-3	1.5E-2	1.9E-3	3.1E-4	4.9E-3	1.1E-6
TEM 8	8.3E-8	7.7E-3	2.6E-1	4.1E-2	6.9E-3	1.5E-2	2.6E-3	5.8E-4	4.4E-3	1.3E-6
TEM 9	4.6E-8	8.1E-3	2.5E-1	4.0E-2	7.0E-3	1.4E-2	1.5E-3	1.9E-4	4.0E-3	1.3E-6
TEM 10	3.8E-8	8.9E-3	2.3E-1	4.0E-2	7.2E-3	1.4E-2	1.3E-3	1.2E-4	3.5E-3	1.5E-6
TEM 11	8.4E-8	8.0E-3	2.4E-1	4.0E-2	8.3E-3	1.5E-2	1.5E-3	3.1E-4	5.3E-3	9.3E-7
TEM 12	3.6E-8	8.9E-3	2.4E-1	4.0E-2	7.5E-3	1.4E-2	1.3E-3	1.1E-4	4.1E-3	1.1E-6
TEM 13	4.2E-8	8.8E-3	2.3E-1	4.0E-2	8.0E-3	1.4E-2	1.0E-3	8.8E-5	3.9E-3	1.1E-6
TEM 14	4.7E-8	8.8E-3	2.5E-1	4.0E-2	7.5E-3	1.4E-2	1.3E-3	1.7E-4	4.5E-3	1.0E-6
TEM 15	1.3E-6	7.8E-3	2.9E-1	4.1E-2	7.3E-3	1.4E-2	1.9E-3	3.1E-3	4.9E-3	1.7E-6
TEM 16	1.6E-7	7.9E-3	2.9E-1	4.1E-2	7.2E-3	1.5E-2	3.2E-3	1.1E-3	5.1E-3	1.2E-6
TEM 17	5.7E-8	7.9E-3	2.5E-1	4.0E-2	6.6E-3	1.5E-2	2.0E-3	3.4E-4	3.6E-3	1.4E-6
TEM 18	3.2E-8	9.5E-3	2.3E-1	4.0E-2	7.5E-3	1.5E-2	8.2E-4	6.4E-5	3.4E-3	1.4E-6
TEM 19	2.8E-7	8.1E-3	2.6E-1	4.0E-2	9.3E-3	1.6E-2	1.3E-3	9.8E-4	5.8E-3	1.1E-6
TEM 20	1.1E-7	7.9E-3	2.4E-1	4.1E-2	8.5E-3	1.5E-2	2.1E-3	5.1E-4	5.7E-3	1.1E-6
TEM 21	5.4E-8	8.7E-3	2.5E-1	4.1E-2	7.2E-3	1.5E-2	1.6E-3	2.5E-4	5.0E-3	1.1E-6
TEM 22	1.7E-7	8.1E-3	2.6E-1	4.1E-2	9.0E-3	1.5E-2	1.3E-3	5.4E-4	5.8E-3	8.9E-7
TEM 23	8.2E-8	8.1E-3	2.5E-1	4.0E-2	8.5E-3	1.4E-2	1.2E-3	1.8E-4	5.0E-3	7.4E-7
TEM 24	4.8E-8	8.7E-3	2.4E-1	4.0E-2	8.1E-3	1.4E-2	1.0E-3	1.2E-4	4.1E-3	9.9E-7
TEM 25	6.2E-8	8.7E-3	2.4E-1	4.0E-2	7.9E-3	1.4E-2	1.2E-3	1.3E-4	4.5E-3	8.0E-7
TEM 26	5.4E-8	8.4E-3	2.3E-1	4.0E-2	7.6E-3	1.5E-2	1.4E-3	1.9E-4	4.8E-3	9.6E-7
TEM 27	4.3E-8	8.5E-3	2.3E-1	4.0E-2	7.9E-3	1.4E-2	1.0E-3	8.0E-5	3.8E-3	1.2E-6
TEM 28	2.6E-8	8.9E-3	2.4E-1	4.0E-2	7.9E-3	1.5E-2	1.0E-3	7.6E-5	3.3E-3	1.2E-6
TEM 29	2.9E-8	8.4E-3	2.2E-1	4.0E-2	8.0E-3	1.4E-2	9.5E-4	7.0E-5	3.0E-3	1.2E-6
TEM 30	3.2E-8	8.2E-3	2.2E-1	4.0E-2	8.1E-3	1.5E-2	8.9E-4	7.2E-5	3.1E-3	1.3E-6
TEM 31	7.2E-7	8.3E-3	2.8E-1	4.0E-2	9.2E-3	1.6E-2	9.2E-4	2.0E-3	5.5E-3	1.3E-6
TEM 32	1.4E-7	7.9E-3	2.6E-1	4.0E-2	9.5E-3	1.5E-2	1.0E-3	2.9E-4	5.7E-3	6.7E-7
TEM 33	5.8E-8	9.1E-3	2.3E-1	4.0E-2	8.0E-3	1.4E-2	1.2E-3	9.6E-5	4.5E-3	9.0E-7
TEM 34	2.9E-8	8.1E-3	2.1E-1	4.0E-2	8.6E-3	1.4E-2	7.5E-4	6.5E-5	3.4E-3	1.4E-6

Table A4. Continued

Regions of Interest	Benign									
	1	2	3	4	5	6	7	8	9	10
Features										
<i>Kurtosis Texture of Nodule</i>										
TEM 1	6.98	688.27	26.20	706.35	1.0E+3	710.04	690.33	1.5E+3	9.1E+2	103.31
TEM 2	6.70	541.41	35.57	747.70	1.2E+3	742.43	693.59	1.5E+3	9.9E+2	109.04
TEM 3	6.37	549.05	26.46	689.02	1.5E+3	692.71	712.06	1.5E+3	8.7E+2	109.43
TEM 4	5.19	560.12	32.29	732.57	1.4E+3	692.99	712.24	1.5E+3	9.7E+2	120.17
TEM 5	6.52	576.85	26.86	730.32	1.0E+3	685.86	702.55	1.5E+3	9.8E+2	117.60
TEM 6	5.79	610.20	30.66	718.98	1.2E+3	681.40	714.65	1.5E+3	9.2E+2	120.92
TEM 7	5.58	616.02	30.47	719.88	1.3E+3	691.95	703.93	1.5E+3	9.7E+2	116.09
TEM 8	5.65	684.67	30.53	727.14	1.3E+3	749.31	701.47	1.5E+3	1.0E+3	121.85
TEM 9	5.44	645.95	31.46	727.66	1.3E+3	736.56	691.07	1.5E+3	1.0E+3	115.46
TEM 10	5.77	650.13	34.40	744.55	1.2E+3	761.04	688.91	1.5E+3	1.1E+3	115.91
TEM 11	5.26	621.83	33.83	752.29	9.4E+2	699.07	682.69	1.5E+3	1.0E+3	130.29
TEM 12	5.96	572.45	33.79	751.86	1.1E+3	688.82	693.89	1.5E+3	1.0E+3	124.06
TEM 13	6.33	589.74	34.81	752.53	1.0E+3	733.15	683.25	1.5E+3	9.9E+2	123.55
TEM 14	5.46	573.60	31.58	739.28	1.0E+3	710.85	688.22	1.5E+3	9.8E+2	123.19
TEM 15	6.67	664.13	24.62	731.39	9.9E+2	588.15	698.77	1.5E+3	9.8E+2	116.66
TEM 16	5.92	594.16	26.87	721.94	1.2E+3	722.10	690.35	1.5E+3	1.0E+3	121.93
TEM 17	5.80	737.72	32.46	743.47	1.4E+3	753.39	703.26	1.5E+3	1.1E+3	121.06
TEM 18	6.00	609.47	36.14	746.89	1.0E+3	765.38	689.18	1.5E+3	1.1E+3	118.44
TEM 19	5.79	667.23	29.89	746.27	8.5E+2	682.66	676.40	1.5E+3	1.1E+3	128.66
TEM 20	5.33	606.32	33.63	747.42	9.2E+2	680.65	688.22	1.5E+3	1.0E+3	127.58
TEM 21	5.26	568.58	31.44	729.90	1.1E+3	712.72	692.06	1.5E+3	9.6E+2	120.42
TEM 22	5.30	655.52	31.69	745.04	8.5E+2	734.91	675.75	1.5E+3	1.1E+3	132.06
TEM 23	5.44	599.34	31.74	751.58	9.3E+2	724.17	678.29	1.5E+3	1.0E+3	133.06
TEM 24	5.73	568.78	32.56	739.18	1.0E+3	722.12	684.00	1.5E+3	9.9E+2	124.18
TEM 25	6.03	563.09	33.34	756.24	1.0E+3	722.72	679.15	1.5E+3	1.0E+3	131.16
TEM 26	5.64	580.72	34.71	759.32	1.1E+3	695.24	685.68	1.5E+3	1.0E+3	129.69
TEM 27	6.84	611.00	36.90	765.37	9.9E+2	821.47	683.39	1.5E+3	9.7E+2	122.66
TEM 28	6.25	594.93	34.61	743.55	1.0E+3	693.82	688.04	1.5E+3	1.0E+3	124.09
TEM 29	6.47	651.73	38.37	745.34	1.0E+3	762.51	672.51	1.5E+3	9.8E+2	123.20
TEM 30	6.78	682.20	39.55	761.32	9.6E+2	867.68	670.02	1.5E+3	9.3E+2	124.22
TEM 31	6.21	867.11	27.00	747.96	9.2E+2	637.90	668.58	1.5E+3	1.1E+3	131.37
TEM 32	5.14	649.23	30.93	748.66	8.5E+2	790.06	674.68	1.5E+3	1.1E+3	135.49
TEM 33	6.85	549.59	35.21	764.03	9.9E+2	759.51	683.04	1.4E+3	9.5E+2	128.94
TEM 34	7.47	674.38	42.22	766.58	8.6E+2	788.36	662.84	1.5E+3	8.8E+2	130.95

Table A4. Continued

Regions of Interest	Benign									
	1	2	3	4	5	6	7	8	9	10
Features										
<i>Skewness</i>										
<i>Texture of Nodule</i>										
TEM 1	-1.88	6.02	-3.94	25.42	-16.51	-16.14	24.37	-35.83	7.64	7.13
TEM 2	-1.84	2.99	-4.70	26.36	-19.90	-17.88	24.48	-36.42	14.68	7.48
TEM 3	-1.70	6.00	-3.99	25.07	-23.59	-17.32	25.07	-36.28	13.17	7.52
TEM 4	-1.46	6.01	-4.37	25.97	-21.84	-17.15	25.09	-36.25	16.76	8.15
TEM 5	-1.79	8.28	-4.01	25.98	-17.35	-15.44	24.78	-36.31	16.34	7.83
TEM 6	-1.66	9.22	-4.27	25.73	-19.55	-15.60	25.15	-36.46	13.74	8.14
TEM 7	-1.65	10.08	-4.30	25.71	-21.34	-16.28	24.79	-36.76	13.65	7.78
TEM 8	-1.66	11.11	-4.30	25.90	-22.18	-17.98	24.75	-36.38	19.12	8.12
TEM 9	-1.65	11.28	-4.38	25.88	-21.02	-17.41	24.38	-36.49	18.11	7.69
TEM 10	-1.72	12.40	-4.60	26.27	-19.70	-18.39	24.30	-36.45	18.85	7.76
TEM 11	-1.57	9.85	-4.55	26.46	-16.54	-16.14	24.15	-36.10	18.86	8.49
TEM 12	-1.75	9.95	-4.56	26.44	-18.00	-15.95	24.47	-35.76	15.31	8.19
TEM 13	-1.83	10.10	-4.64	26.45	-18.04	-17.21	24.09	-35.82	15.28	8.12
TEM 14	-1.64	9.63	-4.39	26.15	-17.66	-16.42	24.27	-36.04	14.33	8.12
TEM 15	-1.85	10.77	-3.80	26.01	-16.24	-10.78	24.65	-36.55	15.87	7.92
TEM 16	-1.69	8.70	-4.05	25.79	-20.73	-16.93	24.38	-36.74	19.20	8.06
TEM 17	-1.70	13.16	-4.46	26.26	-22.90	-18.27	24.82	-36.52	21.31	8.13
TEM 18	-1.79	11.84	-4.73	26.31	-17.88	-18.82	24.33	-35.77	18.48	7.91
TEM 19	-1.64	11.83	-4.27	26.34	-14.74	-15.93	23.96	-36.56	20.43	8.42
TEM 20	-1.57	9.74	-4.52	26.36	-16.13	-15.99	24.33	-36.18	17.24	8.38
TEM 21	-1.59	9.81	-4.36	25.94	-18.84	-16.99	24.40	-36.17	13.31	7.91
TEM 22	-1.56	10.88	-4.42	26.31	-14.83	-17.54	23.93	-36.64	21.72	8.59
TEM 23	-1.61	9.51	-4.42	26.44	-16.50	-16.28	24.00	-36.04	18.60	8.60
TEM 24	-1.70	9.08	-4.47	26.14	-17.89	-16.25	24.12	-36.15	15.07	8.17
TEM 25	-1.74	9.14	-4.53	26.54	-17.74	-16.50	24.01	-35.55	17.53	8.45
TEM 26	-1.66	9.14	-4.61	26.61	-18.13	-16.09	24.25	-35.50	18.34	8.43
TEM 27	-1.92	10.64	-4.79	26.74	-17.13	-20.42	24.09	-35.72	14.80	8.08
TEM 28	-1.82	10.46	-4.63	26.25	-17.83	-16.68	24.29	-35.85	13.82	8.26
TEM 29	-1.86	11.65	-4.87	26.28	-18.18	-18.73	23.73	-35.90	14.10	8.16
TEM 30	-1.91	12.29	-4.97	26.64	-16.80	-22.05	23.63	-35.78	11.03	8.24
TEM 31	-1.75	17.11	-4.06	26.36	-16.52	-14.21	23.71	-36.32	20.32	8.79
TEM 32	-1.54	10.48	-4.40	26.39	-14.68	-18.74	23.90	-36.61	21.48	8.80
TEM 33	-1.90	9.03	-4.66	26.71	-16.99	-18.12	24.11	-34.90	15.53	8.32
TEM 34	-2.02	11.64	-5.13	26.75	-14.31	-19.80	23.41	-35.91	3.69	8.75

Table A4. Continued

Regions of Interest	Benign									
	1	2	3	4	5	6	7	8	9	10
Features										
<i>Mean Texture of Parenchyma</i>										
TEM 1	0.66	2.58	5.91	0.24	3.98	4.02	0.75	3.24	3.27	0.14
TEM 2	0.68	2.38	5.89	0.23	4.17	4.14	0.87	2.92	2.59	0.14
TEM 3	0.83	2.30	5.73	0.25	4.18	4.14	1.12	3.37	2.94	0.13
TEM 4	0.94	2.43	5.68	0.24	4.19	4.06	1.48	3.44	3.34	0.18
TEM 5	0.77	2.44	5.95	0.23	4.07	4.00	0.84	3.07	3.19	0.14
TEM 6	0.88	2.38	5.94	0.24	4.12	4.02	1.09	3.43	3.36	0.15
TEM 7	0.90	2.45	5.92	0.25	4.22	4.02	1.27	3.55	3.49	0.17
TEM 8	0.90	2.32	5.94	0.24	4.24	4.12	1.06	3.58	3.53	0.15
TEM 9	0.95	2.32	5.93	0.25	4.22	4.03	1.19	3.65	3.66	0.16
TEM 10	0.97	2.17	5.94	0.25	4.16	4.09	1.07	3.59	3.78	0.17
TEM 11	0.90	2.42	5.95	0.20	4.04	4.02	1.12	3.52	3.28	0.16
TEM 12	0.92	2.41	5.95	0.22	4.09	3.96	1.11	3.54	3.67	0.17
TEM 13	0.97	2.46	5.95	0.22	4.13	3.99	1.15	3.38	3.73	0.18
TEM 14	0.96	2.47	5.95	0.23	4.06	3.99	1.17	3.54	3.59	0.17
TEM 15	0.67	2.32	5.95	0.23	3.94	3.74	0.64	2.78	3.46	0.14
TEM 16	0.85	2.38	5.94	0.23	4.25	4.07	1.00	3.35	3.33	0.15
TEM 17	0.97	2.15	5.94	0.24	4.23	4.11	1.07	3.60	3.70	0.14
TEM 18	0.92	2.20	5.94	0.25	4.03	4.14	1.00	3.55	3.81	0.19
TEM 19	0.80	2.24	5.96	0.21	3.90	4.12	0.91	3.17	3.10	0.16
TEM 20	0.89	2.38	5.96	0.21	4.01	4.06	1.09	3.52	3.23	0.15
TEM 21	0.93	2.37	5.95	0.23	4.11	4.06	1.21	3.62	3.48	0.16
TEM 22	0.86	2.30	5.95	0.21	3.89	4.16	1.09	3.38	3.10	0.17
TEM 23	0.97	2.41	5.95	0.21	4.03	3.97	1.22	3.52	3.37	0.17
TEM 24	1.00	2.54	5.95	0.23	4.11	3.94	1.17	3.42	3.66	0.17
TEM 25	1.01	2.45	5.95	0.20	4.13	3.96	1.23	3.46	3.52	0.17
TEM 26	0.91	2.44	5.95	0.20	4.12	3.99	1.10	3.52	3.42	0.16
TEM 27	0.98	2.43	5.95	0.21	4.07	4.17	1.20	3.38	3.79	0.19
TEM 28	0.89	2.40	5.95	0.22	4.13	4.02	1.11	3.62	3.93	0.18
TEM 29	0.91	2.36	5.95	0.23	4.13	4.10	1.21	3.52	4.02	0.19
TEM 30	0.89	2.35	5.96	0.22	4.01	4.27	1.27	3.53	4.07	0.20
TEM 31	0.71	2.10	5.96	0.22	4.02	4.06	0.67	2.76	3.20	0.15
TEM 32	0.96	2.31	5.95	0.21	3.80	4.15	1.22	3.50	3.12	0.17
TEM 33	1.07	2.52	5.95	0.20	4.14	4.02	1.29	3.38	3.59	0.19
TEM 34	0.78	2.42	5.96	0.23	3.87	4.14	1.45	3.68	4.12	0.21

Table A4. Continued

Regions of Interest	Benign									
	1	2	3	4	5	6	7	8	9	10
Features										
<i>Variance Texture of Parenchyma</i>										
TEM 1	5.9E-5	3.0E-9	3.1E-4	5.6E-9	6.0E-7	3.7E-8	5.2E-6	9.8E-3	5.8E-7	2.2E-9
TEM 2	6.2E-5	8.1E-9	2.1E-4	1.4E-8	7.4E-7	1.9E-8	4.3E-6	4.2E-3	8.7E-7	6.1E-9
TEM 3	8.6E-5	2.4E-8	9.5E-4	1.1E-7	2.6E-6	4.3E-8	7.0E-6	2.7E-3	2.7E-6	2.9E-8
TEM 4	1.0E-4	1.2E-7	4.3E-3	4.4E-7	1.7E-5	1.0E-7	6.3E-6	1.5E-3	6.6E-6	2.1E-7
TEM 5	8.4E-5	1.5E-8	4.5E-4	2.1E-8	2.0E-6	5.9E-8	3.6E-6	4.8E-3	1.1E-6	1.4E-9
TEM 6	9.3E-5	1.5E-8	6.3E-4	3.5E-8	2.2E-6	6.5E-8	4.5E-6	3.2E-3	1.7E-6	2.2E-9
TEM 7	9.8E-5	2.1E-8	1.2E-3	6.8E-8	3.9E-6	7.3E-8	4.1E-6	1.7E-3	2.5E-6	1.1E-8
TEM 8	1.0E-4	1.5E-8	2.6E-4	3.9E-8	3.0E-6	4.0E-8	2.8E-6	2.7E-3	8.1E-7	1.7E-9
TEM 9	1.2E-4	2.4E-8	3.7E-4	5.3E-8	4.7E-6	3.4E-8	2.4E-6	1.4E-3	7.9E-7	8.2E-9
TEM 10	1.2E-4	2.6E-8	3.6E-4	4.4E-8	4.7E-6	2.3E-8	2.3E-6	1.2E-3	4.0E-7	1.4E-8
TEM 11	1.1E-4	6.8E-9	2.0E-4	2.6E-8	1.2E-6	5.9E-8	2.5E-6	1.9E-3	7.6E-7	4.4E-10
TEM 12	1.1E-4	2.6E-9	1.5E-4	1.1E-8	9.3E-7	3.2E-8	2.3E-6	1.4E-3	4.4E-7	6.7E-10
TEM 13	1.3E-4	2.0E-9	1.8E-4	8.3E-9	8.1E-7	3.3E-8	2.5E-6	1.5E-3	3.5E-7	4.1E-10
TEM 14	1.2E-4	4.0E-9	1.7E-4	1.8E-8	1.2E-6	5.0E-8	2.2E-6	1.6E-3	6.9E-7	6.8E-10
TEM 15	7.2E-5	1.2E-8	4.1E-4	1.9E-8	1.2E-6	9.2E-8	3.3E-6	7.3E-3	8.8E-7	1.9E-9
TEM 16	1.0E-4	1.8E-8	3.0E-4	2.7E-8	2.9E-6	5.0E-8	2.8E-6	3.9E-3	8.4E-7	1.0E-9
TEM 17	1.1E-4	1.6E-8	2.5E-4	4.1E-8	2.8E-6	2.6E-8	2.8E-6	1.9E-3	4.9E-7	3.6E-9
TEM 18	1.3E-4	4.0E-8	5.1E-4	5.4E-8	6.9E-6	2.6E-8	2.0E-6	1.1E-3	2.9E-7	2.9E-8
TEM 19	8.6E-5	1.5E-8	2.4E-4	2.7E-8	1.9E-6	9.2E-8	2.4E-6	2.9E-3	8.8E-7	7.5E-10
TEM 20	9.4E-5	9.3E-9	1.9E-4	3.0E-8	1.4E-6	7.1E-8	2.8E-6	2.2E-3	1.1E-6	7.1E-10
TEM 21	1.1E-4	7.0E-9	1.8E-4	2.8E-8	1.4E-6	7.5E-8	2.7E-6	1.7E-3	1.3E-6	1.3E-9
TEM 22	1.1E-4	1.3E-8	2.4E-4	2.9E-8	1.7E-6	8.4E-8	2.3E-6	2.1E-3	7.9E-7	4.9E-10
TEM 23	1.2E-4	4.6E-9	2.5E-4	2.4E-8	1.0E-6	5.6E-8	2.8E-6	1.7E-3	5.6E-7	3.2E-10
TEM 24	1.3E-4	2.7E-9	1.8E-4	1.3E-8	9.8E-7	4.6E-8	2.5E-6	1.6E-3	4.6E-7	3.6E-10
TEM 25	1.2E-4	3.0E-9	2.3E-4	1.6E-8	7.6E-7	4.0E-8	3.1E-6	1.7E-3	4.2E-7	3.1E-10
TEM 26	1.0E-4	4.0E-9	1.8E-4	1.8E-8	9.4E-7	4.0E-8	2.7E-6	1.8E-3	5.3E-7	4.3E-10
TEM 27	1.4E-4	1.7E-9	2.1E-4	6.2E-9	7.9E-7	2.4E-8	2.6E-6	1.7E-3	2.9E-7	4.7E-10
TEM 28	1.2E-4	2.4E-9	1.9E-4	7.2E-9	8.5E-7	2.8E-8	2.1E-6	1.3E-3	3.1E-7	1.2E-9
TEM 29	1.3E-4	1.8E-9	1.8E-4	6.6E-9	7.6E-7	2.6E-8	2.3E-6	1.4E-3	2.7E-7	5.8E-10
TEM 30	1.4E-4	1.6E-9	2.0E-4	5.2E-9	7.9E-7	2.0E-8	2.3E-6	1.8E-3	2.3E-7	5.9E-10
TEM 31	7.2E-5	1.4E-8	3.3E-4	2.9E-8	1.7E-6	1.2E-7	2.2E-6	4.4E-3	9.0E-7	1.0E-9
TEM 32	1.3E-4	8.8E-9	3.0E-4	3.2E-8	1.5E-6	7.9E-8	2.4E-6	1.7E-3	6.8E-7	3.6E-10
TEM 33	1.3E-4	2.4E-9	2.5E-4	1.3E-8	6.9E-7	2.9E-8	3.4E-6	1.8E-3	3.6E-7	3.4E-10
TEM 34	1.4E-4	1.9E-9	1.8E-4	7.7E-9	7.5E-7	2.0E-8	2.1E-6	1.7E-3	2.1E-7	7.4E-10

Table A4. Continued

Regions of Interest	Benign									
	1	2	3	4	5	6	7	8	9	10
Features										
<i>Kurtosis Texture of Parenchyma</i>										
TEM 1	49.78	12.08	4.67	9.29	66.08	32.60	51.88	296.99	84.78	2.87
TEM 2	48.58	10.04	2.92	8.15	66.23	13.95	47.46	186.77	85.98	1.58
TEM 3	48.78	3.80	2.71	8.24	42.84	13.33	42.90	176.17	81.84	1.54
TEM 4	47.75	2.79	2.57	4.84	24.55	7.88	42.48	151.11	78.95	1.50
TEM 5	47.71	10.56	2.87	5.66	56.07	17.45	45.09	191.02	81.70	5.74
TEM 6	45.96	6.51	3.70	5.31	52.69	16.34	42.52	182.24	78.17	2.69
TEM 7	44.49	3.93	4.28	4.90	45.32	23.92	47.01	147.05	74.44	2.46
TEM 8	44.70	6.49	3.60	5.76	54.49	17.29	45.22	174.25	81.18	3.10
TEM 9	44.04	7.96	4.14	5.07	54.38	25.20	49.88	148.83	75.12	2.67
TEM 10	42.50	8.33	5.45	4.70	43.21	22.04	55.31	151.25	72.68	3.38
TEM 11	43.59	7.32	2.91	5.06	47.48	25.17	45.78	163.68	79.91	8.77
TEM 12	43.11	7.44	3.47	5.08	49.21	34.80	51.63	156.63	75.21	4.39
TEM 13	43.86	6.77	3.37	4.58	50.31	40.40	49.81	162.61	77.61	5.36
TEM 14	42.61	6.76	3.38	5.48	55.34	34.77	49.33	156.97	75.56	6.05
TEM 15	50.73	11.91	3.17	5.57	59.22	32.19	48.87	211.85	83.01	5.39
TEM 16	47.20	8.37	2.84	5.76	58.08	16.69	43.80	194.26	82.01	5.56
TEM 17	43.61	6.27	4.25	5.10	47.61	17.39	49.81	163.74	80.64	3.79
TEM 18	41.65	9.40	5.75	6.50	35.76	26.39	59.61	163.72	66.41	3.83
TEM 19	43.04	10.19	5.21	4.98	52.72	23.11	48.84	173.55	80.43	6.78
TEM 20	42.83	8.62	2.90	5.43	52.73	22.17	44.86	163.74	78.39	6.28
TEM 21	42.93	6.78	3.68	6.67	59.98	31.92	49.08	149.98	76.07	7.80
TEM 22	43.13	9.03	4.48	4.89	49.45	24.88	46.79	172.37	80.45	9.60
TEM 23	45.51	5.73	2.73	4.36	44.75	29.35	45.89	167.93	82.43	11.55
TEM 24	44.19	6.36	3.34	4.81	53.14	40.39	49.33	160.64	75.68	7.06
TEM 25	44.26	4.94	2.96	4.37	42.47	31.05	47.44	166.33	82.57	9.59
TEM 26	44.22	6.09	2.94	5.04	44.05	26.58	47.09	159.99	78.94	7.61
TEM 27	44.50	6.54	2.77	4.05	52.57	37.09	50.24	167.18	80.23	4.23
TEM 28	42.54	6.45	4.10	4.65	49.07	46.61	54.83	160.85	73.51	3.99
TEM 29	43.36	6.15	3.63	4.00	54.35	43.92	49.50	161.90	75.35	4.55
TEM 30	46.71	5.96	3.16	3.60	55.27	34.02	46.67	165.27	78.63	4.82
TEM 31	44.71	11.06	6.16	4.68	56.76	31.19	51.53	178.83	81.92	4.61
TEM 32	46.89	7.44	3.57	4.38	48.65	27.92	45.80	171.50	82.25	12.01
TEM 33	44.72	4.95	2.59	4.24	42.20	31.99	50.51	167.65	84.04	5.45
TEM 34	60.73	4.80	3.31	2.92	51.03	28.88	42.26	164.92	80.28	4.37

Table A4. Continued

Regions of Interest	Benign									
	1	2	3	4	5	6	7	8	9	10
Features										
<i>Skewness</i>										
<i>Texture of Parenchyma</i>										
TEM 1	0.63	-2.29	-1.26	-2.02	-7.14	-4.46	4.13	-13.55	4.96	-0.46
TEM 2	1.14	-1.92	-0.26	-1.80	-7.03	-2.77	3.91	-8.29	5.44	0.06
TEM 3	1.01	-1.02	-0.37	-1.75	-5.13	-2.60	3.52	-7.26	4.96	-0.16
TEM 4	1.18	-1.08	-0.62	-1.25	-3.47	-1.77	2.72	-5.18	4.49	-0.38
TEM 5	0.41	-2.32	-0.49	-1.40	-6.54	-3.17	3.60	-8.37	4.58	-1.39
TEM 6	0.04	-1.58	-0.93	-1.25	-6.18	-3.02	3.18	-7.63	4.03	-0.56
TEM 7	0.14	-1.04	-1.17	-1.20	-5.42	-3.64	3.16	-4.86	2.85	-0.67
TEM 8	0.04	-1.67	-0.70	-1.43	-6.36	-3.15	3.91	-7.59	4.59	-0.71
TEM 9	0.16	-1.82	-1.02	-1.28	-6.17	-3.73	4.33	-4.74	3.25	-0.71
TEM 10	-0.35	-1.84	-1.35	-1.16	-5.35	-3.47	4.81	-4.77	3.38	-0.99
TEM 11	-0.47	-1.83	0.07	-1.48	-5.80	-3.89	4.00	-5.78	3.86	-1.87
TEM 12	-0.54	-1.50	-0.40	-1.35	-5.77	-4.66	4.49	-3.53	2.13	-1.11
TEM 13	-0.18	-1.28	-0.40	-1.11	-5.86	-5.05	4.46	-4.05	3.57	-1.04
TEM 14	-0.71	-1.66	-0.31	-1.54	-6.21	-4.57	4.21	-4.46	2.28	-1.48
TEM 15	1.36	-2.49	-0.60	-1.39	-6.69	-4.41	3.87	-9.86	4.76	-1.54
TEM 16	0.62	-2.07	-0.37	-1.49	-6.67	-3.10	3.78	-9.12	4.54	-1.30
TEM 17	-0.70	-1.49	-1.09	-1.19	-5.79	-3.18	4.30	-6.22	4.79	-0.98
TEM 18	-0.25	-2.08	-1.42	-1.56	-4.76	-3.63	5.07	-1.79	2.68	-1.19
TEM 19	-0.41	-2.32	-1.03	-1.37	-6.27	-3.68	4.02	-7.11	3.94	-1.59
TEM 20	-0.81	-2.04	-0.04	-1.52	-6.17	-3.62	3.63	-6.04	3.47	-1.50
TEM 21	-0.77	-1.82	-0.31	-1.78	-6.52	-4.33	3.76	-3.86	1.89	-1.78
TEM 22	-0.17	-2.18	-0.66	-1.42	-6.04	-3.83	3.95	-7.24	3.91	-2.05
TEM 23	0.18	-1.47	0.09	-1.34	-5.53	-4.23	4.20	-5.93	4.48	-2.24
TEM 24	0.02	-1.37	-0.27	-1.32	-6.03	-4.99	4.36	-4.67	3.07	-1.41
TEM 25	-0.58	-1.08	-0.08	-1.27	-5.33	-4.41	4.40	-5.41	4.69	-1.90
TEM 26	-0.66	-1.44	0.14	-1.46	-5.47	-4.07	4.20	-5.05	3.82	-1.61
TEM 27	-0.19	-1.22	-0.44	-0.86	-6.09	-4.87	4.51	-4.03	4.26	-0.80
TEM 28	0.01	-1.22	-0.84	-1.04	-5.75	-5.42	4.67	-2.12	1.77	-1.12
TEM 29	0.42	-1.16	-0.70	-0.79	-6.10	-5.24	4.34	-3.20	3.28	-1.10
TEM 30	1.05	-1.19	-0.74	-0.64	-6.27	-4.55	4.11	-3.87	4.05	-1.16
TEM 31	0.20	-2.42	-1.39	-1.25	-6.50	-4.31	4.25	-7.74	4.48	-1.25
TEM 32	0.87	-1.92	-0.34	-1.34	-5.88	-4.09	4.01	-6.82	4.29	-2.37
TEM 33	-1.16	-0.85	-0.24	-1.05	-5.29	-4.52	4.63	-5.02	5.07	-1.11
TEM 34	3.57	-0.86	-0.86	-0.69	-5.88	-4.08	3.55	-4.36	4.32	-1.06

REFERENCES

1. West. *Lung Cancer Screening, Part 1: The Arguments FOR CT Screening*. 2007 [cited 2013; Available from: <http://cancergrace.org/lung/2007/01/23/ct-screening-for-lung-ca-advantages/>].
2. Park, S.H., J.M. Goo, and C.-H. Jo, *Receiver Operating Characteristic (ROC) Curve: Practical Review for Radiologists*. Korean J Radiol, 2004. **5**(1): p. 11-18.
3. Howlader, N., et al., *SEER Cancer Statistics Review, 1975-2009 (Vintage 2009 Populations)*. National Cancer Institute, 2012.
4. Howlader, N., et al., *SEER Cancer Statistics Review, 1975-2009 (Vintage 2009 Populations)*. National Cancer Institute, 2012.
5. Parham, P., *Cancer and Its Interactions with the Immune System*, in *The Immune System*, Garland Science, Taylor & Francis Group, LLC: London and New York. p. 488-506.
6. Kumar, V., et al., *Robbins and Cotran Pathologic Basis of Disease*, E. Saunders, Editor 2010.
7. *The Health Consequences of Smoking. A Report of the U.S. Surgeon General*, 2004, U.S. Department of Health and Human Services.
8. Group, U.S.C.S.W. *United States Cancer Statistics: 1999-2009 Incidence and Mortality Web-based Report*. 2013 3/5/2013]; Available from: <http://apps.nccd.cdc.gov/uscs/toptencancers.aspx>.
9. *Lung Cancer (Small Cell)*, 2013, American Cancer Society.
10. Bach, P.B., et al., *Screening for Lung Cancer: A review of the current literature*. Chest, 2003. **123**(1): p. 72S-82S.
11. Prince, J.L. and J.M. Links, *Medical Imaging Signals and Systems* 2006, New Jersey: Pearson Education, Inc.
12. The Prostate, L., Colorectal, and Ovarian (PLCO) Randomized Trial., et al., *Screening by chest radiograph and lung cancer mortality: the Prostate, Lung, Colorectal, and Ovarian (PLCO) randomized trial*. JAMA, 2011. **306**(17): p. 1865-73.
13. Aberle, D.R., et al., *The National Lung Screening Trial: overview and study design*. Radiology, 2011. **248**(1): p. 243-53.
14. The National Lung Screening Trial Research Team, *The National Lung Screening Trial: overview and study design*. Radiology, 2011. **258**: p. 243-253.
15. Doi, K., *Computer-Aided Diagnosis in Medical Imaging: Historical Review, Current Status and Future Potential*. Computerized Medical Imaging and Graphics, 2007. **31**(4-5): p. 198-211.

16. Brandman, S. and J.P. Ko, *Pulmonary Nodule Detection, Characterization, and Management With Multidetector Computed Tomography*. J Thorac Imaging, 2011. **26**(2): p. 90-105.
17. Jarvis, S., *Data mining with learner corpora*, in *A Taste for Corpora*, F. Meunier, et al., Editors. 2011, John Benjamins Publishing Company: Philadelphia, PA.
18. McNitt-Gray, M.F., et al., *A pattern classification approach to characterizing solitary pulmonary nodes imaged on high resolution CT: Preliminary results*. Medical Physics, 1998. **26**(6): p. 881-888.
19. Armato, S.G., et al., *Automated lung nodule classification following automated nodule detection on CT: A serial approach*. Medical Physics, 2003. **30**(6): p. 1188-1197.
20. Chen Hui, W.X.-h., MA Da-ying and MA Bin-rong, *Neural network-based computer-aided diagnosis in distinguishing malignant from benign solitary pulmonary nodules by computed tomography*. Chinese Medical Journal, 2007. **120**(12): p. 1211-1215.
21. Way, T.W., et al., *Computer-aided diagnosis of pulmonary nodules on CT scans: Improvement of classification performance with nodule surface features*. Medical Physics, 2009. **36**(7): p. 3086.
22. Aoyama, M., et al., *Computerized scheme for determination of the likelihood measure of malignancy for pulmonary nodules on low-dose CT images*. Medical Physics, 2003. **30**(3): p. 387.
23. Xu, Y., et al., *Sensitivity and specificity of 3-D texture analysis of lung parenchyma is better than 2-D for discrimination of lung pathology in stage 0 COPD*. 2005. **5746**: p. 474-485.
24. Weisstein, E.W. *Full Width at Half Maximum*. MathWorld--A Wolfram Web Resource; Available from: <http://mathworld.wolfram.com/FullWidthatHalfMaximum.html>.
25. Sonka, M., V. Hlavac, and R. Boyle, *Image Processing, Analysis, and Machine Vision*. 3rd Edition ed2008: Thomson Engineering.
26. NIST/SEMATECH, *e-Handbook of Statistical Methods*, 2003.
27. Eisenhauer, E.A., et al., *New response evaluation criteria in solid tumours: revised RECIST guideline (version 1.1)*. European Journal of Cancer, 2009. **45**(2): p. 228-47.
28. Wadell, H., *Volume, Shape and Roundness of Quartz Particles*. Journal of Geology, 1935. **43**(3): p. 250-280.
29. Way, T.W., et al., *Computer-aided diagnosis of pulmonary nodules on CT scans: Segmentation and classification using 3D active contours*. Medical Physics, 2006. **33**(7): p. 2323.

30. Laws, K.I., *Rapid texture identification*, in *Image Processing for Missile Guidance*, T.F. Wiener, Editor 1980, The Society of Photo-Optical Instrumentation Engineers: Bellingham, Washington. p. 376-280.
31. Suzuki, M.T. and Y. Yaginuma, *A Solid Texture Analysis Based on Three Dimensional Convolution Kernels*. International Society for Optics and Photonics Electronic Imaging, 2007. **6491**: p. 1-8.
32. COPDGene, *COPDGene COPD Genetic Epidemiology*.
33. Longanathan, R.S., et al., *Prevalence of COPD in Women Compared to Men Around the Time of Diagnosis of Primary Lung Cancer*. *Chest*, 2006. **129**(5): p. 1305-1312.
34. COPDGene, *Clinical Center Manual of Procedures*, 2009.
35. Pao, W. and V.A. Miller, *Epidermal growth factor receptor mutations, small-molecule kinase inhibitors, and non-small-cell lung cancer: current knowledge and future directions*. *Journal of Clinical Oncology*, 2005. **23**(11): p. 2556-68.
36. Gierada, D.S., et al., *Quantitative CT Assessment of Emphysema and Airways in Relation to Lung Cancer Risk*. *Radiology*, 2011.
37. Lee, H.-J., et al., *Epidermal Growth Factor Receptor Mutation in Lung Adenocarcinomas: Relationship with CT Characteristics and Histologic Subtypes*. *Radiology*, 2013.